The Immunomodulatory Properties of Mesenchymal Stem Cells

Lead Guest Editor: Junji Xu
Guest Editors: Dunfang Zhang, Peter Zanvit, and Dandan Wang
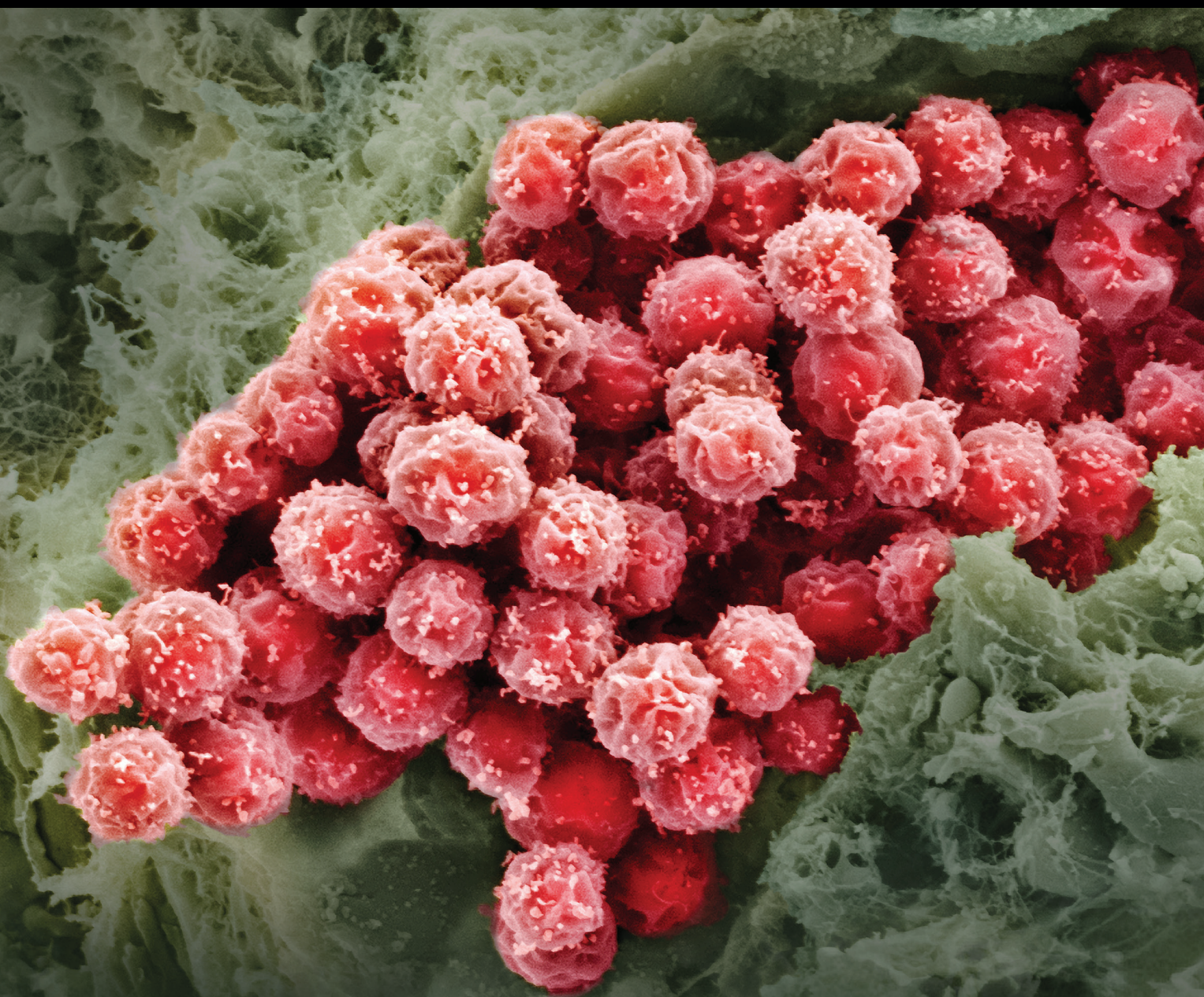
The Immunomodulatory Properties of Mesenchymal Stem Cells

The Immunomodulatory Properties of Mesenchymal Stem Cells

Lead Guest Editor: Junji Xu
Guest Editors: Dunfang Zhang, Peter Zanvit, and Dandan Wang

Wasco Wruck, Germany
Qingzhong Xiao, UK
Takao Yasuhara, Japan
Zhaohui Ye, USA

Holm Zaehres, Germany
Elias T. Zambidis, USA
Ludovic Zimmerlin, USA
Ewa K. Zuba-Surma, Poland

Eder Zucconi, Brazil
Maurizio Zuccotti, Italy
Nicole Isolde zur Nieden, USA

Contents

Editorial

The Immunomodulatory Properties of Mesenchymal Stem Cells

Junji Xu [ID],[1,2] **Dunfang Zhang** [ID],[2,3] **Peter Zanvit,**[2] **and Dandan Wang** [ID][4]

[1]*Molecular Laboratory for Gene Therapy and Tooth Regeneration, Beijing Key Laboratory of Tooth Regeneration and Function Reconstruction, Capital Medical University School of Stomatology, Beijing, China*
[2]*National Institute of Dental and Craniofacial Research, National Institutes of Health, Bethesda, Maryland, USA*
[3]*Sichuan University, Chengdu, China*
[4]*Department of Rheumatology and Immunology, The Affiliated Drum Tower Hospital of Nanjing University Medical School, Nanjing, China*

Correspondence should be addressed to Junji Xu; uujkl@163.com

Mesenchymal stem cells (MSCs) were initially described as a group of multipotent, self-renewal cells derived from bone marrow, adipose tissue, umbilical cord, dental pulps, and other tissues. Although there are different voices recently about the name or concept of MSCs, studies in the latest decades showed that these groups of cells could mediate a variety of immunomodulatory properties, which may affect both innate and adaptive immune responses. Moreover, dysfunction of the immunoregulatory function of MSCs has been suggested to play a role in the pathogenesis of autoimmune and inflammatory diseases. Therapeutic effects of MSCs on experimental and clinical autoimmune diseases and inflammation including Sjogren's syndrome, Crohn's disease, systemic lupus erythematosus, and rheumatoid arthritis have also been reported. However, the mechanisms mediating the immunosuppressive effects of MSCs remain incompletely understood.

Here, we highlight some of the critical ongoing challenges published in this special issue. Y. Su et al. found that the impairment of immunoregulatory function in MSCs from Sjogren's syndrome was because of the higher expression of BMP6. Their result showed that BMP6 could downregulate PGE2 secretion from MSCs via Id1 (inhibitor of DNA-binding protein 1); neutralizing BMP6 and knockdown of Id1 could restore the BMMSC immunosuppressive function both in vitro and in vivo. L. Guo et al. found that D-mannose could affect the immunomodulation of tooth MSCs. Their results showed that MSCs pretreated by D-mannose have stronger inhibition function on T cell proliferation and induce more T cells to differentiate into regulatory T cell by decreasing IL-6 production. F. Yan and O. Liu found that MSCs from the dental pulp can regulate natural killer cell function. Their results showed that MSCs could impair proliferation and promote apoptosis of activated NK cells and decrease cytotoxicity of activated NK cells via CD73 and adenosine. H. K. Lee et al. showed that prednisone or mycophenolate mofetil combined with MSCs has a better therapeutic effect than single therapy in lupus-prone MRL.Fas^{lpr} mice. Their result showed that this combination could synergistically inhibit T cell proliferation.

In this special issue, we present eight papers that address the issue about the multiple functions of postnatal MSCs, focusing on the investigation of immunomodulatory properties in these cells.

Conflicts of Interest

The editors do not have any possible conflict of interest or private agreements with companies.

Junji Xu
Dunfang Zhang
Peter Zanvit
Dandan Wang

Research Article

Guanylate-Binding Protein 1 Promotes Migration and Invasion of Human Periodontal Ligament Stem Cells

Shi Bai [iD],[1,2,3] **Tao Chen,**[1,2,3] **and Xia Deng** [iD][4]

[1]*Stomatological Hospital of Chongqing Medical University, Chongqing 400065, China*
[2]*Chongqing Key Laboratory of Oral Diseases and Biomedical Sciences, Chongqing 400044, China*
[3]*Chongqing Municipal Key Laboratory of Oral Biomedical Engineering of Higher Education, 401147 Chongqing, China*
[4]*Department of Stomatology, Nuclear of Industry 416 Hospital, Chengdu, Sichuan 610051, China*

Correspondence should be addressed to Shi Bai; baishi1980713@163.com

Mesenchymal stem/stromal cells (MSCs) are capable of migrating to sites of injury and inflammation in response to various cytokines to improve tissue repair. Previous studies have shown interferon-gamma (IFN-γ) promoted migration of the V54/2 cell line and dental pulp stem cells (DPSCs), but the underlying mechanisms remain largely unknown. In this study, we found IFN-γ induced migration and invasion of periodontal ligament stem cells (PDLSCs) in a dose-dependent manner *in vitro*. While knockdown of guanylate-binding protein 1 (GBP1) suppressed IFN-γ-induced migration and invasion, ectopic expression of GBP1 potentiated IFN-γ-induced migration and invasion of PDLSCs. Furthermore, we demonstrated GBP1 was required for IFN-γ-induced processing of matrix metallopeptidase 2 (MMP2) in PDLSCs. Our findings indicate that GBP1 promotes IFN-γ-induced migration and invasion of PDLSCs by MMP2, and GBP1 may serve as a new target to facilitate MSC homing and migration.

1. Introduction

Mesenchymal stem/stromal cells (MSCs) are a heterogeneous population of cells that are capable of self-renewal and differentiation into specific sublineages, including osteoblasts, adipocytes, and chondrocytes [1, 2]. In addition to their promising potentials in bone and cartilage regeneration, MSCs are currently being investigated in various studies and clinical trials of immunological disorders, such as graft-versus-host disease (GVHD), Crohn's disease, and rheumatoid arthritis [3, 4]. Although administration of exogenous MSCs can be delivered locally and systemically, the migration activity of MSCs to the sites of injury is critical for the therapeutic effects [5, 6]. MSCs are classically isolated from bone marrow, and they can be found in multiple fetal and adult tissues, including umbilical cord blood, fetal lung, and adipose tissue, as well as dental tissues [7, 8]. In dental tissues, MSCs have been found in dental pulp, periodontal ligament, and apical papilla [9–11]. Periodontal ligament stem cells (PDLSCs), a kind of dental stem cells, possess

comparable proliferation rate with bone marrow-derived MSCs (BM-MSCs) [10, 12]. In regard to differentiation capacity, PDLSCs can also give rise to osteoblasts, chondrocytes, and adipocytes [10, 12].

Interferon-gamma (IFN-γ) plays an important role in innate and adaptive immune responses against infections of various viruses and bacteria [13]. IFN-γ also showed critical regulatory effects on multiple biological behaviors of MSC, including proliferation, migration, and osteogenic differentiation. He et al. reported that treatment with low concentration of IFN-γ at 0.05 ng/ml can significantly promote the proliferation but inhibit osteogenic differentiation of dental pulp stem cells (DPSCs) *in vitro* [14]. Treatment with IFN-γ at 100 IU/ml (approximately 5 ng/ml) inhibited both proliferation and osteogenic differentiation potential of human BM-MSCs [15]. In regard to MSC migration, IFN-γ promoted migration of the V54/2 cell line and DPSCs, although the underlying mechanism is still not fully understood [14, 16]. In addition to the continuous exposure to IFN-γ, IFN-γ was also used for pretreatment of MSCs.

TABLE 1: Primer sequence.

Gene	Forward primer (5′-3′)	Reverse primer (5′-3′)
GAPDH	GGAGCGAGATCCCTCCAAAAT	GGCTGTTGTCATACTTCTCATG
GBP1	GAAGTGCTAGAAGCCAGTGC	CCACCACCATAGGCTGTGTA
MMP1	ATGAAGCAGCCCAGATGTGGAG	TGGTCCACATCTGCTCTTGGCA
MMP2	AGCGAGTGGATGCCGCCTTTAA	CATTCCAGGCATCTGCGATGAG
MMP9	TGTACCGCTATGGTTACACTCG	GGCAGGGACAGTTGCTTCT
MMP14	CCTTGGACTGTCAGGAATGAGG	TTCTCCGTGTCCATCCACTGGT
CEACAM1	AGCTCATGGACCTTTCCAGAC	GTTTCCTGCGCTGTCGTTTG
ICAM1	ATGCCCAGACATCTGTGTCC	GGGGTCTCTATGCCCAACAA

Interestingly, IFN-γ prestimulation of MSCs increased their migration potential to the inflamed sites and reduced mucosal damage in experimental colitis [17].

Guanylate-binding protein 1 (GBP1) is a type of cytokine-induced guanosine triphosphatase and is an IFN-γ response factor [18–20]. GBP1 plays an essential role in mediating the antibacterial and antiviral activities of IFN-γ [21, 22]. We have previously shown GBP1 is of highest expression level in all the 7 GBPs in human BM-MSCs, and GBP1 is required for IFN-γ-induced processing of indoleamine 2,3 dioxygenase (IDO), Interleukin 6 (IL-6), and IL-8 [23]. Given the critical role of GBP1 in IFN-γ signaling, we hypothesized GBP1 may also play an important role in migration of MSCs in response to IFN-γ treatment. To address this, we investigated the migration and invasion capacity in GBP1-depleted and GBP1-overexpressed PDLSCs in response to IFN-γ treatment, respectively. We further found GBP1 was required for IFN-γ-induced upregulation of matrix metalloproteinase 2 (MMP2) expression in PDLSCs.

2. Methods and Materials

2.1. Subjects and Cell Culture.
Disease-free impacted third molars that were indicated for extraction were collected from patients, aged 20–28 years, at Stomatological Hospital of Chongqing Medical University. Written informed consent was obtained from each patient. PDLSCs were isolated as previously described [10]. All procedures were conducted in accordance with the guidelines and regulations approved by Chongqing Medical University. PDLSCs were maintained in DMEM, containing 15% heat-inactivated fetal bovine serum, 100 U/ml of K-Penicillin G and 100 mg/ml of streptomycin sulfate (all from Thermo Fisher Scientific) at 37°C in a humidified atmosphere of 5% CO_2. PDLSCs within passages 4–10 from up to 4 donors were used in this study. Recombinant human IFN-γ (R&D systems) was used to treat PDLSCs as indicated.

2.2. siRNA Silencing and Overexpression of GBP1.
A pool of 3 target-specific 19–25 nt siRNAs targeting human GBP1 and scrambled siRNAs (siSCR) were purchased from Santa Cruz Biotechnology. PDLSCs were overnight plated, and siRNA transfection was performed using Lipofectamine RNAiMAX reagent (Thermo Fisher Scientific) according to the manufacturer's instructions. For ectopic expression of

GBP1, lentiviruses expressing human GBP1 gene were purchased from Fulengen Inc. (Guangzhou, China). PDLSCs were infected in the presence of 8 μg/ml of polybrene (Sigma) for 2 days and then selected with 2 μg/ml puromycin for 3 days. PDLSCs transfected by empty vector were used as control.

2.3. Monolayer Cell Wound Healing Assay.
The 100% confluent monolayer PDLSCs were scraped with sterile 200 μl pipette tips. The cells were then washed to remove cellular debris and allowed to migrate for 24 hours. Representative images at the initial time point (0 h) and after incubation (24 h) were acquired using an inverted microscope (Olympus) to evaluate the migration distance as previously described [24].

2.4. Transwell Assay.
1×10^5 PDLSCs in 200 μl of DMEM without FBS were seeded into Matrigel invasion chambers (Corning, NY). Transwell lower chamber is filled with 500 μl of complete growth medium. After 48 hours, the invaded cells were stained with the HEMA-3 kit (Fisher) and counted under optical microscope (Olympus).

2.5. RNA Isolation and RT-qPCR.
Total RNA was extracted from the cells using the TRIzol reagent according to the manufacturer's instructions (Thermo Fisher Scientific) and treated with RQ1 DNase (Promega). 2 μg aliquots of total RNA was used to generate the first-strand complementary DNA. Quantitative polymerase chain reaction (qPCR) was performed using SYBR Premix Ex Taq kit (TAKARA) using various specific primer sets (Table 1).

2.6. Western Blot.
Protein was isolated using RIPA buffer (Santa Cruz Biotechnology) containing 1% protease inhibitor cocktail (Roche) according to the manufacturer's instructions. 25–40 μg aliquots of the lysates were separated on a 10% sodium dodecyl sulfate-polyacrylamide gel. The resolved proteins were transferred onto nitrocellulose membrane (Bio-Rad) and incubated with antibodies overnight at 4°C. Protein bands were detected using an enhanced chemiluminescence Western blotting detection kit (Thermo Fisher Scientific). Antibodies used in this study includes rabbit polyclonal anti-human GBP1 antibody (Invitrogen) and rabbit polyclonal anti-human MMP2 antibody (Cell Signaling Technology).

(a)

(b)

(c)

(d)

(e)
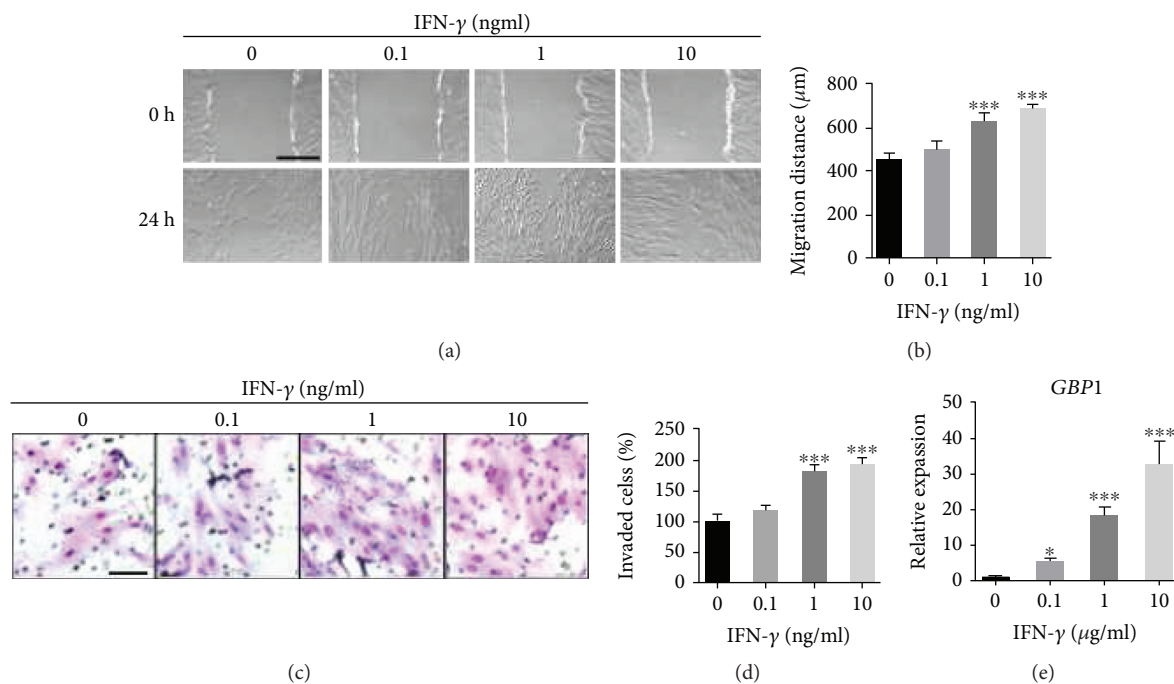
FIGURE 1: IFN-γ promoted migration and invasion and expression of GBP1 in PDLSCs. Results of wound healing assay revealed an increase in migration distance of PDLSCs in response to IFN-γ treatment at 1 and 10 ng/ml (a and b). Bar indicates 500 μm in (a). Results of transwell assay showed an increase in invade cell number of PDLSCs in response to IFN-γ treatment at 1 and 10 ng/ml (c and d). Bar indicates 100 μm in (c). GBP1 expression was upregulated in IFN-γ-treated PDLSCs as determined by RT-qPCR (e). $^{*}p < 0.05$; $^{***}p < 0.001$.

2.7. Statistical Analysis. Student's *t*-test were used for single comparisons. One-way analysis of variance (ANOVA) and two-way ANOVA with post-hoc Tukey's tests were performed for multiple comparisons using GraphPad Prism 6 software. Data was expressed as mean ± SD from at least three independent experiments. $p < 0.05$ was considered as significant. $^{*}p < 0.05$; $^{**}p < 0.01$; $^{***}p < 0.001$.

3. Results

3.1. IFN-γ Treatment Promoted Migration and Invasion and Expression of GBP1 in a Dose-Dependent Manner in PDLSCs. To investigate the effect of IFN-γ on migration of PDLSCSs, monolayer cell wound healing assay was performed. As shown in Figures 1(a) and 1(b), the migration distance of PDLSCs was significantly increased in response to IFN-γ treatment at 1 and 10 ng/ml but not at 0.1 ng/ml. Consistently, the invasion capacity of PDLSCs was also enhanced by IFN-γ treatment at 1 and 10 ng/ml but not at 0.1 ng/ml (Figures 1(c) and 1(d)). We further confirmed that the expression level of GBP1, a well-established IFN-γ response gene, was induced by IFN-γ treatment in a dose-dependent manner in PDLSCs (Figure 1(e)). As 10 ng/ml was the optimal concentration for IFN-γ-induced migration and invasion and expression of *GBP1* in PDLSCs, this concentration was selected for the rest of the study.

3.2. siRNA-Mediated Depletion of GBP1 Suppressed IFN-γ-Induced Migration and Invasion of PDLSCs. Next, we sought to investigate whether GBP1 is required for IFN-γ-induced migration and invasion. A pool of siRNAs targeting

GBP1 was used to knockdown GBP1 expression, and the knockdown efficiency was confirmed by RT-qPCR analysis and Western blot (Figures 2(a) and 2(b)). The transfected cells were then seeded into six-well plates and allowed to grow confluent. Interestingly, depletion of GBP1 significantly inhibited the IFN-γ-induced upregulation of migration activity, while it did not affect the migration of PDLSCs in absence of IFN-γ (Figures 2(c) and 2(d)). Depletion of GBP1 also suppressed the increase in invaded cell number induced by IFN-γ treatment at a concentration of 10 ng/ml (Figures 2(e) and 2(f)).

3.3. Overexpression of GBP1 Potentiated IFN-γ-Induced Migration and Invasion of PDLSCs. Next, PDLSCs were infected by lentiviruses expressing GBP1, and the overexpression of GBP1 was confirmed by RT-qPCR analysis and Western blot (Figures 3(a) and 3(b)). As shown in Figures 3(c) and 3(d), ectopic expression of GBP1 did not promote the migration of PDLSCs, but it further enhanced the migration activity of PDLSCs in presence of IFN-γ at a concentration of 10 ng/ml. The invasion capacity of IFN-γ-treated PDLSCs was also promoted by ectopic expression of GBP1 (Figures 3(e) and 3(f)). Above all, these findings indicated GBP1 is essential for the upregulation of migration and invasion of PDLSCs induced by IFN-γ treatment.

3.4. GBP1 Was Required for IFN-γ-Induced Processing of MMP2 in PDLSCs. Previous studies have reported that MMPs play an important role in regulating the migratory activity of MSCs [25, 26]. We screened the expression levels of several MMPs by RT-qPCR in PDLSCs in response

(a)

(b)

(c)

(d)

(e)

(f)
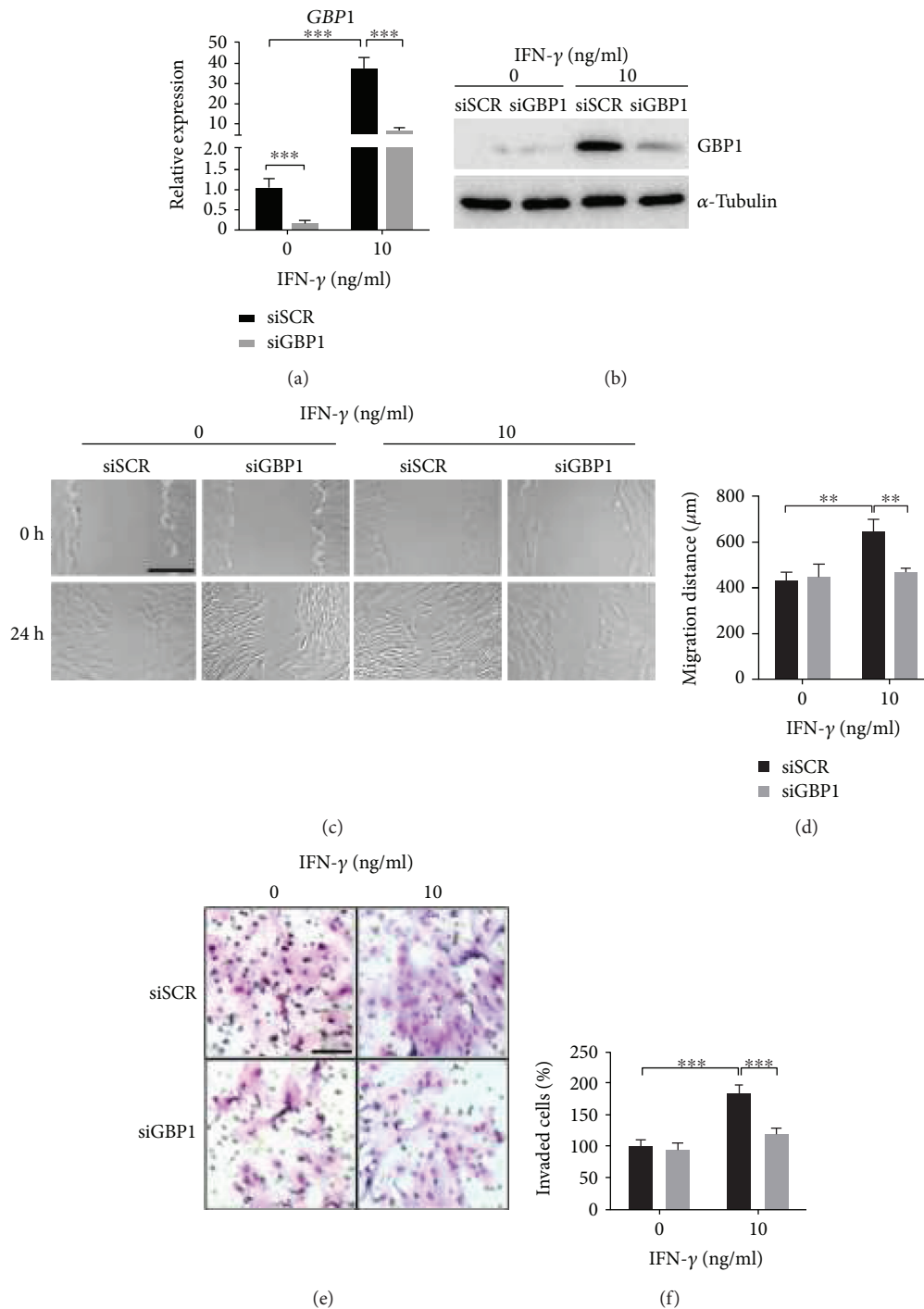
Figure 2: Depletion of GBP1 suppressed IFN-γ-induced migration and invasion of PDLSCs. The knockdown efficiency was confirmed by RT-qPCR and Western blot (a and b). To examine the effect of GBP1 knockdown on migration of PDLSCs, wound healing assay was performed using GBP1-depleted PDLSCs (siGBP1) and scrambled siRNA-transfected cells (siSCR). Representative images were acquired at the initial time point (0 h) and after 24-hour migration (24 h), respectively. The upregulation of migration induced by IFN-γ treatment was inhibited by GBP1 knockdown (c and d). Bar indicates 500 μm in (c). The upregulation of invasion induced by IFN-γ treatment was also inhibited by GBP1 knockdown as revealed by transwell invasion assay (e and f). Bar indicates 100 μm in (e). $^{**}p < 0.01$; $^{***}p < 0.001$.

to IFN-γ treatment for 48 hours. Interestingly, IFN-γ treatment specifically induced *MMP2* expression in PDLSCs, instead of *MMP1*, *MMP9*, and *MMP14* (Figures 4(a)–4(d)). We also investigated the effect of IFN-γ treatment on

expression of carcinoembryonic antigen-related cell adhesion molecule 1 (CEACAM1) and intercellular adhesion molecule 1 (ICAM1), and we found IFN-γ treatment did not affect the mRNA expression of *CEACAM1* or *ICAM1*
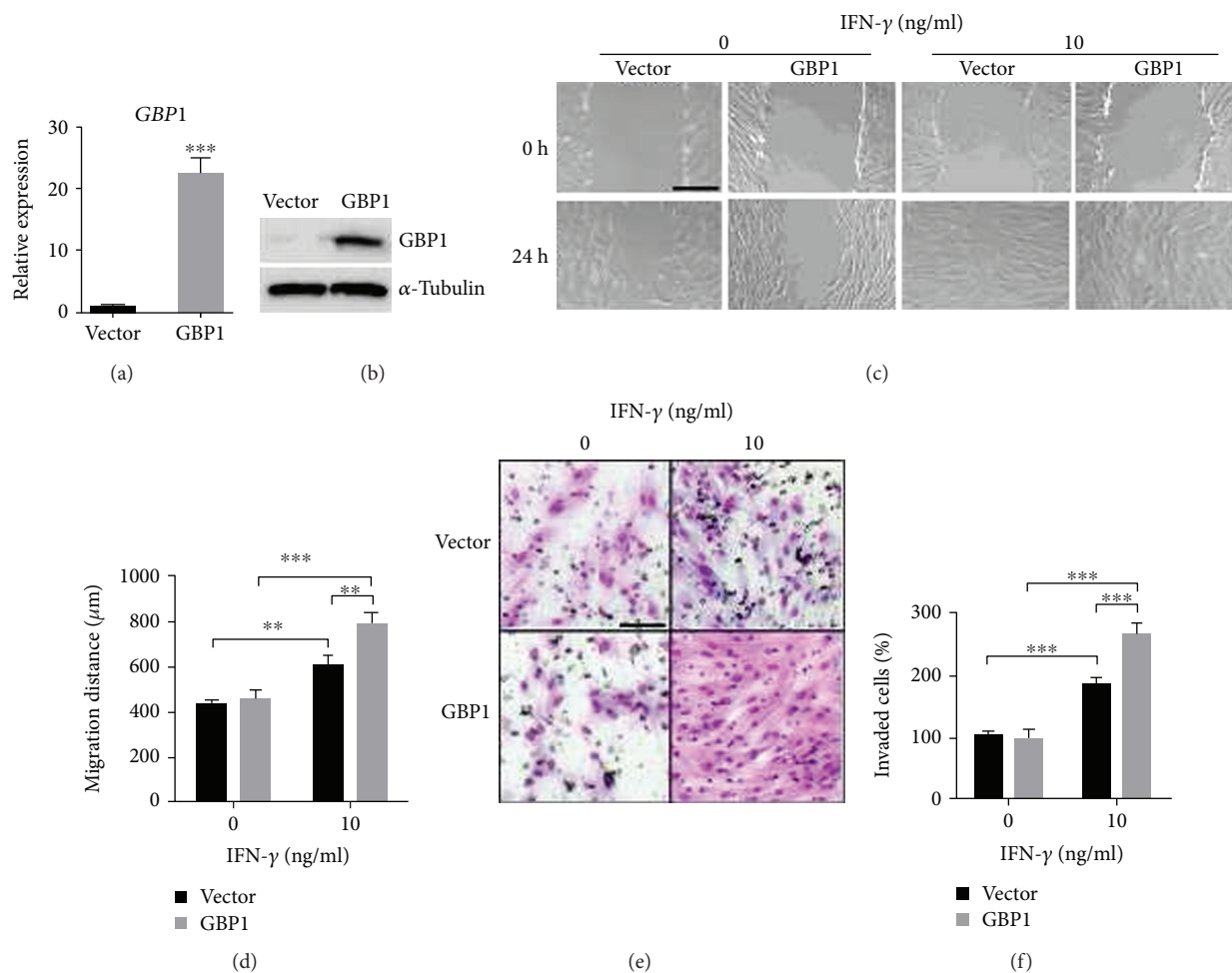
FIGURE 3: Overexpression of GBP1 potentiated IFN-γ-induced migration and invasion of PDLSCs. The overexpression of GBP1 in PDLSCs was confirmed by RT-qPCR and Western blot (a and b). Wound healing assay was performed using GBP1-overexpressed PDLSCs and control cells (vector). Representative images were acquired at the initial time point (0 h) and after 24-hour migration (24 h), respectively. Overexpression of GBP1 further enhanced the migration as well as invasion of PDLSCs induced by IFN-γ treatment (c–f). Bars indicate 500 μm in (c) and 100 μm in (e), respectively. ***$p < 0.001$.

in PDLSCs (Supplementary Figure 1 (a and b)). We then confirmed the upregulation of MMP2 by IFN-γ treatment in PDLSCs by Western blot (Figure 4(e)). Furthermore, we found depletion of GBP1 significantly suppressed IFN-γ-induced processing of MMP2 (Figures 4(f) and 4(g)). Taken together, our findings suggested GBP1 is required for IFN-γ-induced processing of MMP2 thereby promoting migration and invasion of PDLSCs induced by IFN-γ treatment.

4. Discussion

In this study, we found treatment with IFN-γ promoted migration and invasion of PDLSCs, and enhanced expression levels of MMP2. Although depletion of GBP1 did not affect the migration and invasion capacity of PDLSCs, it significantly suppressed the upregulation of migration and invasion induced by IFN-γ treatment. In addition, ectopic expression of GBP1 in PDLSCs further enhanced the IFN-γ-induced migration and invasion of PDLSCs. Finally, we showed GBP1 was required for the processing of MMP2 induced by

IFN-γ, by which it may promote the IFN-γ-induced migration and invasion of PDLSCs.

The migration activity of MSCs to the sites of injury is critical for their function to facilitate tissue repair. Previous studies have shown IFN-γ may promote migration of MSCs, depending on the treatment concentration and the source of MSCs. Treatments with IFN-γ at 0.05, 0.5, and 5 ng/ml enhanced migration activity of DPSCs [14], and treatments with IFN-γ at 1000 U/mL (approximately 50 ng/ml) promoted migration activity in V54/2 cell line. However, treatment with IFN-γ at 1000 IU/ml (approximately 50 ng/ml) only slightly increased the migration of BM-MSCs, but only one concentration level of IFN-γ was tested in that study [16]. In this study, we found the migration and invasion of PDLSCs was significantly increased in response to IFN-γ treatment at 1 and 10 ng/ml. More importantly, our findings indicate GBP1 is a pivotal mediator in IFN-γ-induced migration of PDLSCs. Since the optimal concentration of IFN-γ might vary across individuals, it is possible that targeting GBP1 is more practicable for clinical applications.
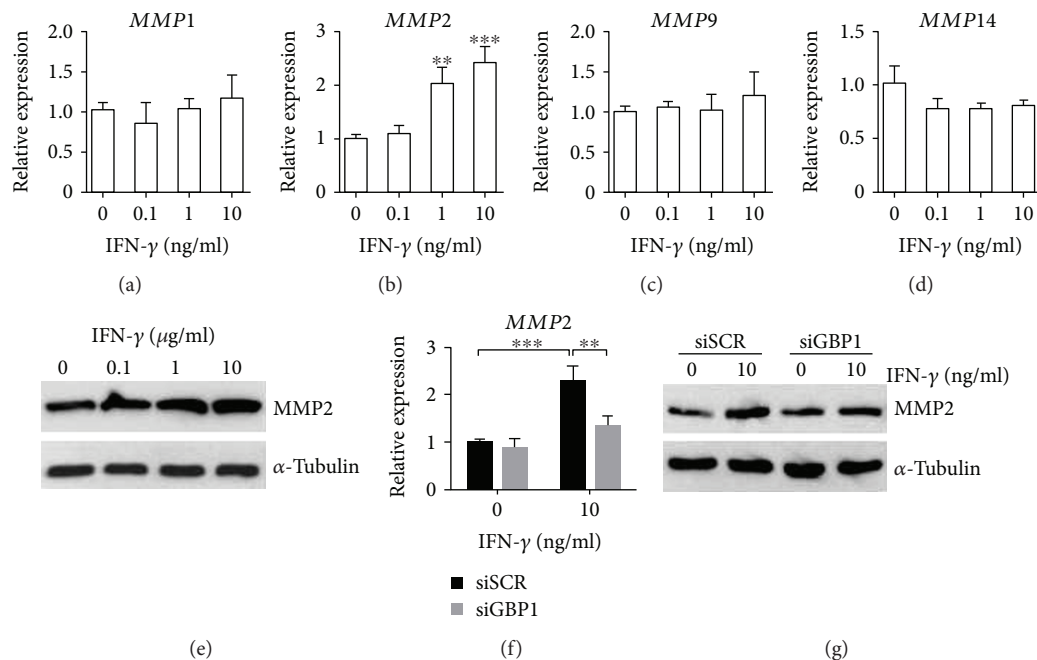
Figure 4: GBP1 is required for upregulation of MMP2 by IFN-γ treatment in PDLSCs. RT-qPCR analysis of matrix metalloproteinase gene expression after 48 hours of IFN-γ treatment in PDLSCs and control cells (a–d). MMP2 expression was upregulated by IFN-γ treatment in a dose-dependent manner (b and e). The IFN-γ-induced upregulation of MMP2 was inhibited by depletion of GBP1 as determined by RT-qPCR analysis and Western blot (f and g). $^{**}p < 0.01$; $^{***}p < 0.001$.

Furthermore, the immune properties of MSCs after homing to the injured sites are also important for tissue repair. Although recent studies suggest resting MSCs may not have significant immunomodulatory activity, but treatment with IFN-γ are capable of enhancing the immunosuppressive properties of MSCs. For instance, MSCs primed with IFN-γ was found to prevent the development of GVHD more efficiently, compared to unstimulated MSCs [27, 28]. Since GBP1 is essential for IFN-γ signaling, GBP1 may also play a role in IFN-γ-induced cytokine production and immunomodulatory activity of MSCs [16, 23].

MMPs are a family of zinc-dependent proteolytic enzymes that are involved in the degradation of extracellular matrix (ECM). Previous studies have highlighted the role of MMP1, MMP2, MMP9, and MMP14 in regulation of MSC migration [25, 26, 29]. Expression of MMP2 and MMP9 was elevated by IFN-γ treatment in a human salivary gland cell line (HSG), but IFN-γ inhibits constitutive MMP-2 expression in human astroglioma cells [30, 31]. In this study, we found IFN-γ treatment specifically induced expression of *MMP2*, instead of *MMP1*, *MMP9*, and *MMP14* in PDLSCs, and GBP1 was required for IFN-γ-induced processing of MMP2 as evidenced by RT-qPCR and Western blot. In addition, He et al. reported IFN-γ regulates cell behavior of DPSCs via NF-κB and MAPK signaling. More efforts are still needed to investigate how GBP1 is incorporated into the downstream signaling in IFN-γ-treated MSCs. Duijvestein et al. have showed *CEACAM1* expression was upregulated after 6 days of treatment with IFN-γ in human BM-MSCs [17]. However, in this study, we found 2 days of IFN-γ treatment did not affect the mRNA expression of *CEACAM1* or *ICAM1* in PDLSCs. It is possible that *CEACAM1* is not direct

target of IFN-γ signaling, but it can be induced by activation of NF-κB and/or MAPK signaling.

In conclusion, our findings indicate GBP1 mediates IFN-γ-induced migration of PDLSCs via MMP2. And GBP1 may be a new therapeutic target to promote MSC migration that can facilitate treatment with IFN-γ-primed MSCs.

Data Availability

The data used to support the findings of this study are included within the article.

Conflicts of Interest

The authors declare no conflicts of interest.

Acknowledgments

Supplementary Materials

The effect of IFN-γ treatment on expression of *CEACAM1* or *ICAM1* in PDLSCs. Supplementary Figure 1: IFN-γ treatment did not affect the expression of CEACAM1 or ICAM1 in PDLSCs. RT-qPCR analysis of *CEACAM1* expression after 48 hours of IFN-γ treatment in PDLSCs and control cells (a). RT-qPCR analysis of *ICAM1* expression after 48 hours of IFN-γ treatment in PDLSCs and control cells (b). *(Supplementary Materials)*

References

[1] P. Bianco, P. G. Robey, and P. J. Simmons, "Mesenchymal stem cells: revisiting history, concepts, and assays," *Cell Stem Cell*, vol. 2, no. 4, pp. 313–319, 2008.

[2] D. J. Prockop, "Marrow stromal cells as stem cells for nonhematopoietic tissues," *Science*, vol. 276, no. 5309, pp. 71–74, 1997.

[3] T. Squillaro, G. Peluso, and U. Galderisi, "Clinical trials with mesenchymal stem cells: an update," *Cell Transplantation*, vol. 25, no. 5, pp. 829–848, 2016.

[4] A. Augello, R. Tasso, S. M. Negrini, R. Cancedda, and G. Pennesi, "Cell therapy using allogeneic bone marrow mesenchymal stem cells prevents tissue damage in collagen-induced arthritis," *Arthritis & Rheumatism*, vol. 56, no. 4, pp. 1175–1186, 2007.

[5] S. K. Kang, I. S. Shin, M. S. Ko, J. Y. Jo, and J. C. Ra, "Journey of mesenchymal stem cells for homing: strategies to enhance efficacy and safety of stem cell therapy," *Stem Cells International*, vol. 2012, Article ID 342968, 11 pages, 2012.

[6] A. Sohni and C. M. Verfaillie, "Mesenchymal stem cells migration homing and tracking," *Stem Cells International*, vol. 2013, Article ID 130763, 8 pages, 2013.

[7] X. Zhang, M. Hirai, S. Cantero et al., "Isolation and characterization of mesenchymal stem cells from human umbilical cord blood: reevaluation of critical factors for successful isolation and high ability to proliferate and differentiate to chondrocytes as compared to mesenchymal stem cells from bone marrow and adipose tissue," *Journal of Cellular Biochemistry*, vol. 112, no. 4, pp. 1206–1218, 2011.

[8] B. Bunnell, M. Flaat, C. Gagliardi, B. Patel, and C. Ripoll, "Adipose-derived stem cells: isolation, expansion and differentiation," *Methods*, vol. 45, no. 2, pp. 115–120, 2008.

[9] B. C. Perry, D. Zhou, X. Wu et al., "Collection, cryopreservation, and characterization of human dental pulp–derived mesenchymal stem cells for banking and clinical use," *Tissue Engineering Part C: Methods*, vol. 14, no. 2, pp. 149–156, 2008.

[10] I. C. Gay, S. Chen, and M. MacDougall, "Isolation and characterization of multipotent human periodontal ligament stem cells," *Orthodontics & Craniofacial Research*, vol. 10, no. 3, pp. 149–160, 2007.

[11] W. Sonoyama, Y. Liu, T. Yamaza et al., "Characterization of the apical papilla and its residing stem cells from human immature permanent teeth: a pilot study," *Journal of Endodontics*, vol. 34, no. 2, pp. 166–171, 2008.

[12] R. H. Kim, S. Mehrazarin, and M. K. Kang, "Therapeutic potential of mesenchymal stem cells for oral and systemic diseases," *Dental Clinics of North America*, vol. 56, no. 3, pp. 651–675, 2012.

[13] J. R. Schoenborn and C. B. Wilson, "Regulation of Interferon-γ during innate and adaptive immune responses," *Advances in Immunology*, vol. 96, pp. 41–101, 2007.

[14] X. He, W. Jiang, Z. Luo et al., "IFN-γ regulates human dental pulp stem cells behavior via NF-κB and MAPK signaling," *Scientific Reports*, vol. 7, no. 1, p. 40681, 2017.

[15] J. Croitoru-Lamoury, F. M. J. Lamoury, M. Caristo et al., "Interferon-γ regulates the proliferation and differentiation of mesenchymal stem cells via activation of indoleamine 2,3 dioxygenase (IDO)," *PLoS One*, vol. 6, no. 2, article e14698, 2011.

[16] H. Hemeda, M. Jakob, A.-K. Ludwig, B. Giebel, S. Lang, and S. Brandau, "Interferon-γ and tumor necrosis factor-α differentially affect cytokine expression and migration properties of mesenchymal stem cells," *Stem Cells and Development*, vol. 19, no. 5, pp. 693–706, 2010.

[17] M. Duijvestein, M. E. Wildenberg, M. M. Welling et al., "Pretreatment with interferon-γ enhances the therapeutic activity of mesenchymal stromal cells in animal models of colitis," *Stem Cells*, vol. 29, no. 10, pp. 1549–1558, 2011.

[18] D. J. Vestal and J. A. Jeyaratnam, "The guanylate-binding proteins: emerging insights into the biochemical properties and functions of this family of large interferon-induced guanosine triphosphatase," *Journal of Interferon & Cytokine Research*, vol. 31, no. 1, pp. 89–97, 2011.

[19] M. A. Olszewski, J. Gray, and D. J. Vestal, "*In silico* genomic analysis of the human and murine guanylate-binding protein (GBP) gene clusters," *Journal of Interferon & Cytokine Research*, vol. 26, no. 5, pp. 328–352, 2006.

[20] B. Prakash, G. J. K. Praefcke, L. Renault, A. Wittinghofer, and C. Herrmann, "Structure of human guanylate-binding protein 1 representing a unique class of GTP-binding proteins," *Nature*, vol. 403, no. 6769, pp. 567–571, 2000.

[21] E. M. Selleck, S. J. Fentress, W. L. Beatty et al., "Guanylate-binding protein 1 (Gbp1) contributes to cell-autonomous immunity against toxoplasma gondii," *PLoS Pathogens*, vol. 9, no. 4, article e1003320, 2013.

[22] B.-H. Kim, A. R. Shenoy, P. Kumar, R. Das, S. Tiwari, and J. D. MacMicking, "A family of IFN-γ–inducible 65-kD GTPases protects against bacterial infection," *Science*, vol. 332, no. 6030, pp. 717–721, 2011.

[23] S. Bai, Z. Mu, Y. Huang, and P. Ji, "Guanylate binding protein 1 inhibits osteogenic differentiation of human mesenchymal stromal cells derived from bone marrow," *Scientific Reports*, vol. 8, no. 1, p. 1048, 2018.

[24] P. Deng, J. Wang, X. Zhang et al., "AFF4 promotes tumorigenesis and tumor-initiation capacity of head and neck squamous cell carcinoma cells by regulating SOX2," *Carcinogenesis*, vol. 39, no. 7, pp. 937–947, 2018.

[25] S. G. Almalki and D. K. Agrawal, "Effects of matrix metalloproteinases on the fate of mesenchymal stem cells," *Stem Cell Research & Therapy*, vol. 7, no. 1, p. 129, 2016.

[26] B.-R. Son, L. A. Marquez-Curtis, M. Kucia et al., "Migration of bone marrow and cord blood mesenchymal stem cells in vitro is regulated by stromal-derived factor-1-CXCR4 and hepatocyte growth factor-c-met axes and involves matrix metalloproteinases," *Stem Cells*, vol. 24, no. 5, pp. 1254–1264, 2006.

[27] D. S. Kim, I. K. Jang, M. W. Lee et al., "Enhanced immunosuppressive properties of human mesenchymal stem cells primed by interferon-γ," *eBioMedicine*, vol. 28, pp. 261–273, 2018.

[28] D. Polchert, J. Sobinsky, G. W. Douglas et al., "IFN-γ activation of mesenchymal stem cells for treatment and prevention of graft versus host disease," *European Journal of Immunology*, vol. 38, no. 6, pp. 1745–1755, 2008.

[29] P. Bhoopathi, C. Chetty, V. R. Gogineni et al., "MMP-2 mediates mesenchymal stem cell tropism towards medulloblastoma tumors," *Gene Therapy*, vol. 18, no. 7, pp. 692–701, 2011.

[30] A. J. Wu, R. M. Lafrenie, C. Park et al., "Modulation of MMP-2 (gelatinase A) and MMP-9 (gelatinase B) by interferon-γ in a human salivary gland cell line," *Journal of Cellular Physiology*, vol. 171, no. 2, pp. 117–124, 1997.

[31] H. Qin, J. D. Moellinger, A. Wells, L. J. Windsor, Y. Sun, and E. N. Benveniste, "Transcriptional suppression of matrix metalloproteinase-2 gene expression in human astroglioma cells by TNF-α and IFN-γ," *The Journal of Immunology*, vol. 161, no. 12, pp. 6664–6673, 1998.

Research Article

Azithromycin Promotes the Osteogenic Differentiation of Human Periodontal Ligament Stem Cells after Stimulation with TNF-α

Tingting Meng,[1] Ying Zhou,[1] Jingkun Li,[1] Meilin Hu,[1] Xiaomeng Li,[2] Pingting Wang,[1] Zhi Jia,[1] Liyu Li ![ORCID],[3] and Dayong Liu ![ORCID][1]

[1]*Department of Endodontics & Laboratory of Stem Cells and Endocrine Immunology, Tianjin Medical University School of Stomatology, Tianjin 300070, China*
[2]*Department of Prosthodontics, Tianjin Medical University School of Stomatology, Tianjin 300070, China*
[3]*Department of Intensive Care Unit, The Second Hospital of Tianjin Medical University, Tianjin 300211, China*

Correspondence should be addressed to Liyu Li; tjydlly@126.com and Dayong Liu; dyliuperio@tmu.edu.cn

Background and Objective. This study investigated the effects and underlying mechanisms of azithromycin (AZM) treatment on the osteogenic differentiation of human periodontal ligament stem cells (PDLSCs) after their stimulation with TNF-α *in vitro*. *Methods*. PDLSCs were isolated from periodontal ligaments from extracted teeth, and MTS assay was used to evaluate whether AZM and TNF-α had toxic effects on PDLSCs viability and proliferation. After stimulating PDLSCs with TNF-α and AZM, we analyzed alkaline phosphatase staining, alkaline phosphatase activity, and alizarin red staining to detect osteogenic differentiation. Real-time quantitative polymerase chain reaction (RT-qPCR) analysis was performed to detect the mRNA expression of osteogenic-related genes, including *RUNX2*, *OCN*, and *BSP*. Western blotting was used to measure the NF-κB signaling pathway proteins p65, phosphorylated p65, IκB-α, phosphorylated IκB-α, and β-catenin as well as the apoptosis-related proteins caspase-8 and caspase-3. Annexin V assay was used to detect PDLSCs apoptosis. *Results*. TNF-α stimulation of PDLSCs decreased alkaline phosphatase and alizarin red staining, alkaline phosphatase activity, and mRNA expression of *RUNX2*, *OCN*, and *BSP* in osteogenic-conditioned medium. AZM enhanced the osteogenic differentiation of PDLSCs that were stimulated with TNF-α. Western blot analysis showed that β-catenin, phosphorated p65, and phosphorylated IκB-α protein expression decreased in PDLSCs treated with AZM. In addition, pretreatment of PDLSCs with AZM (10 μg/ml, 20 μg/ml) prevented TNF-α-induced apoptosis by decreasing caspase-8 and caspase-3 expression. *Conclusions*. Our results showed that AZM promotes PDLSCs osteogenic differentiation in an inflammatory microenvironment by inhibiting the WNT and NF-κB signaling pathways and by suppressing TNF-α-induced apoptosis. This suggests that AZM has potential as a clinical therapeutic for periodontitis.

1. Introduction

Periodontitis is a chronic infectious disease of the periodontal supportive tissues, and it is the main cause of tooth loss in adults. Its pathological manifestations include gingival and periodontal ligament inflammatory infiltration, periodontal pocket formation, progressive attachment loss, and alveolar bone destruction [1]. Growing evidence demonstrates the correlation between periodontitis and systemic disorders such as diabetes, cardiovascular diseases, preterm birth, and low birth weight [2, 3]. A recent report identified periodontal disease as a risk factor for non-Hodgkin lymphoma and

colorectal cancer [4]. Etiological evidence shows that periodontal pathogens in the dental biofilm under the gingival epithelium are necessary but insufficient for periodontitis development. Accumulating evidence shows that host susceptibility rather than bacterial plaque leads to periodontal destruction. Indeed, the host inflammatory response plays an essential role in the pathogenesis of periodontitis [5, 6].

Mesenchymal stem cells (MSCs) were first isolated from bone marrow and possess self-renewal, colony-forming unit, and immunomodulation properties. Notably, MSCs can differentiate into osteoblasts, adipocytes, chondrocytes, and neural cells [7]. MSCs play important roles in tissue

hemostasis and in maintaining the balance between effective and regulative immune cells [8], and impaired MSCs in bone marrow or in local tissue may cause disease. We demonstrated previously that MSCs derived from the periodontal ligament tissues of patients with periodontitis showed impaired differentiation and immunomodulation that contributed to the development of periodontal tissue destruction [9–11]. Recent reports indicate the close relationship between impaired MSCs and autoimmune or inflammatory diseases [12]. Indeed, MSC transplantation is a successful therapeutic strategy for treating autoimmune diseases such as SLE [13]; Sjögren syndrome, autoimmune diabetes, and airway inflammation [14]; systemic sclerosis [15]; and periodontitis [16–18]. However, the mechanisms underlying MSC deficiency in periodontitis remain poorly defined and it is unclear how to restore MSC function and achieve periodontal tissue regeneration in an inflammatory microenvironment.

Azithromycin (AZM) is a clinically available macrolide antibiotic like erythromycin A and clarithromycin [19]. In addition to their antimicrobial activity, macrolides can modulate the immune response and inflammation with no effects on homeostatic immunity [20]. In epithelial and immune cells, low-dose macrolides inhibit the secretion of proinflammatory cytokines and chemokines, including IL-6, IL-8, and TNF-α [21, 22]. They also suppress interferon gamma production by memory T cells [23]. CSY0073, an AZM derivative that lacks antibiotic activity, improves the clinical scores of dextran sulfate sodium- (DSS-) induced experimental colitis and collagen-induced arthritis [24]. AZM is reported to be transported into inflamed tissues in the periodontium. After 3 days of daily administration of a single dose of AZM (500 mg), AZM can be detected for up to 6.5 days in the plasma, saliva, and inflamed periodontal tissues of human subjects [25]. Although there are no definitive, controlled clinical studies on the effects of AZM on periodontitis, AZM elicits clinical and microbiological improvement when used in conjunction with nonsurgical periodontal therapy [26–30]. Moreover, one study reported that AZM suppresses human osteoclast differentiation and bone resorption [31]. However, it remains unclear whether AZM affects osteoblasts or the osteogenesis of MSCs in an inflammatory microenvironment.

This study isolated human periodontal ligament stem cells (PDLSCs) and stimulated them with the proinflammatory cytokine TNF-α in vitro. Osteogenic differentiation and cell viability were determined in order to investigate the effects and underlying mechanisms of AZM on the osteogenic differentiation of PDLSCs in an inflammatory microenvironment. Our results showed that AZM promoted PDLSCs osteogenic differentiation after TNF-α stimulation by inhibiting the WNT and NF-κB signaling pathways and by attenuating TNF-α-induced apoptosis.

2. Materials and Methods

2.1. Cell Culture.
All researches involving human stem cells complied with the ISSCR "Guidelines for the Conduct of Human Embryonic Stem Cell Research." PDLSCs were isolated from healthy volunteers who had no history of periodontal diseases and who had relatively healthy periodontiums. All of the experiments followed the guidelines of the Tianjin Medical University School of Stomatology. We obtained written informed consent from all volunteers prior to collecting their cells. PDLSCs were isolated, cultured, and identified as described previously [32]. Generally, the middle one-third of the periodontal ligament was extracted from the surface of the tooth root and then subjected to a gradient wash. Next, the chopped tissues were digested in a solution of 3 mg/ml collagenase type I plus 4 mg/ml dispase (Sigma-Aldrich, St. Louis, MO, USA) for 1 h at 37°C.

The PDLSCs from all of the volunteers were pooled. A single-cell suspension was prepared by passing the cells through a 70 μm strainer (Falcon, BD Labware, Franklin Lakes, NJ, USA), and PDLCSs were plated in complete α-MEM (HyClone, Logan, UT, USA) plus 20% FBS (Gibco, Carlsbad, CA, USA), 100 U/ml penicillin, and 100 μg/ml streptomycin (Invitrogen, Carlsbad, CA, USA). The cells were cultured at 37°C in 5% carbon dioxide, and the culture medium was changed every 3 days. Passages 3–6 were used for the experiments. A total of 15 volunteers, aged 18 to 23 years old, provided informed written consent. PDLSCs were identified by flow cytometry using antibodies against STRO-1, CD90, CD45, and CD146. The details are described in the Supplementary Materials and Methods (available here).

2.2. MTS Assay.
Cell viability was measured using an MTS assay (Promega, Madison, WI, USA). PDLSCs were seeded in 96-well plates at a density of 3×10^3 cells/well and cultured to approximately 80% confluence. TNF-α (20 ng/ml, 100 ng/ml) and AZM (1 μg/ml, 10 μg/ml, and 20 μg/ml) were added. The cells were cultured in osteogenic medium for 48 h at 37°C and then incubated for 3 h with MTS. The OD_{490} was measured using a microplate reader. The experiments, which had 7 replicates, were repeated at least 3 times.

2.3. Alizarin Red Staining and Quantitative Calcium Analysis.
PDLSCs were fixed in 70% ethanol for 1 h and washed with deionized water. We added 40 mM alizarin red staining solution (pH 4.2) into the 6-well plates, incubated the cells at room temperature for 10 min, washed the cells with deionized water 5 times, viewed them under a microscope, and captured the images. For quantitative calcium analysis, the cells were treated with 10% cetylpyridinium chloride solution (Sigma-Aldrich) for 30 min at room temperature. The OD_{562} was used to quantify the degree of mineralization and calcium quantitative analysis for alizarin red staining was normalized to the total protein content before calculation. The experiments were repeated at least 3 times.

2.4. Alkaline Phosphatase Staining.
PDLSCs were seeded in 6-well plates. In addition to the control conditions, there were 3 experimental conditions: 100 ng/ml TNF-α, 100 ng/ml TNF-α plus 10 μg/ml AZM, and 100 ng/ml TNF-α plus 20 μg/ml AZM. We examined osteogenesis at 7 days and acquired images. The alkaline phosphatase (ALP) activity assay is described in the Supplementary Materials and Methods.

2.5. Quantitative Real-Time PCR. Total RNA was isolated from PDLSCs using TRIzol reagent (Life Technologies, Carlsbad, CA, USA). We used oligo (dT) primers and reverse transcriptase to amplify cDNA according to the manufacturer's protocol (Invitrogen). RT-qPCR was performed using the SYBR Green PCR kit (Qiagen, Düsseldorf, Germany). Each reaction was repeated at least three times. Supplementary Table 1 shows the primers for specific genes.

2.6. Western Blot Analysis. Total proteins were extracted from PDLSCs by lysing the cells in RIPA buffer (10 mM Tris-HCl, 1 mM EDTA, 1% sodium dodecyl sulfate (SDS), 1% NP-40, 1 : 100 proteinase inhibitor cocktail, 50 mM β-glycerophosphate, and 50 mM sodium fluoride) and 1% PMSF. The proteins were separated on 10% and 12% SDS polyacrylamide gels and then electrotransferred to polyvinylidene fluoride (PVDF) membranes for 2 h at 300 mA. The membranes were incubated overnight with primary antibodies at 4°C. Primary monoclonal antibodies directed against the following were used in this study: phosphorylated p65, p65, phosphorylated IκB-α, IκB-α, the housekeeping protein glyceraldehyde phosphate dehydrogenase (GAPDH, Abcam, Cambridge, MA, USA), caspase-3, and caspase-8 (Cell Signaling Technology Inc.) Blots were then incubated with the secondary antibody (peroxidase-conjugated goat anti-rabbit; 1 : 1000, Abcam) for 2 h at room temperature. GAPDH was used as the internal control. Each experiment had three replicates and was repeated at least three times.

2.7. Cell Apoptosis Assay. Cells were seeded at a density of $2 \times 10^{3}/\text{cm}^{2}$. After treatment with 100 ng/ml TNF-α or 10 μg/ml AZM plus 20 μg/ml AZM for 24 h, PDLSCs were stained with annexin V-fluorescein isothiocyanate (FITC) and counterstained with propidium iodide (PI). The eBioscience™ annexin V-FITC Apoptosis Detection Kit (Life Technologies) was used. Briefly, cells were washed twice with phosphate-buffered saline (PBS) and then stained with 200 μl binding buffer (1x) and 5 μl annexin V-FITC for 10 min at room temperature in the dark. Finally, 10 μl of PI in 1x binding buffer was added to the cells for 5 minutes. The cells were analyzed using a fluorescence microscope.

2.8. Annexin V Apoptosis Assay. We washed 1×10^{5} cells twice with PBS followed by centrifugation at 4°C at 2000 rpm for 5 minutes to collect cell pellets. The cell pellets were resuspended in 200 μl binding buffer (1x) and stained with 5 μl of annexin V-FITC for 10 min at room temperature in the dark, and then 10 μl PI in 1x binding buffer was added to the cell suspension. The cells were analyzed by fluorescence-activated cell sorting (FACs). Each experiment was performed in triplicate.

2.9. Statistical Analysis. The data are reported as means ± SD. We used one-way ANOVA for statistical analysis, and a P value < 0.05 was considered significant.

3. Results

3.1. TNF-α and AZM at Experimental Levels Had No Toxic Effects on PDLSC Viability or Proliferation. PDLSCs have an elongated spindle morphology (Figure S1). Flow cytometry results for biomarkers are shown in Figure S2. To investigate whether different concentrations of TNF-α and AZM affected cell proliferation and viability, we used MTS assay to compare the viability of PDLSCs cultured in osteogenic conditions versus PDLSCs treated with TNF-α and AZM (Figure S3). TNF-α was used at two concentrations (20 ng/ml, 100 ng/ml) and AZM at three concentrations (1 μg/ml, 10 μg/ml, and 20 μg/ml). TNF-α treatment alone tended to reduce the number of viable cells, although this reduction was not significant. Based on these results, we chose to use 20 ng/ml and 100 ng/ml TNF-α and 10 μg/ml and 20 μg/ml AZM as working concentrations for the subsequent experiments.

3.2. Effects of AZM on the Osteogenic Differentiation of PDLSCs. To investigate the effects of AZM on the osteogenic differentiation of PDLSCs, cells were cultured in osteogenic medium for 7 days. Experimental PDLSCs were treated with TNF-α (100 ng/ml) and AZM (10 μg/ml, 20 μg/ml). The ALP staining results (Figure 1) and alizarin red staining results (Figure 2) showed that AZM can restore the ability of PDLSCs to undergo osteogenic differentiation after the cells are impaired by TNF-α (100 ng/ml). Compared to control cells that underwent osteogenic induction, TNF-α treatment decreased staining and calcium nodule formation (Figure 2). Notably, TNF-α is a proinflammatory cytokine that contributes to bone loss in many different diseases. Until now, the mechanisms by which TNF-α inhibits osteogenic differentiation have been unclear and have been thought to be complex. In accordance with previous results, TNF-α reduced osteogenic differentiation and our data suggested that it decreased the number of calcium nodules that were formed as well (Figure 2(e)). Cotreatment of PDLSCs with TNF-α (100 ng/ml) and AZM (20 μg/ml) rescued the cells' ability to undergo osteogenesis compared with the TNF-α group, even though osteogenesis was lower than that for control cells. The higher the AZM concentration, the deeper the blue or red staining is. This suggests that AZM has a positive role in human PDLSC osteogenic differentiation, since cells underwent osteogenesis when they were cultured in the absence or presence of TNF-α and AZM for 0, 3, or 7 days.

Similar to the ALP staining and alizarin red staining results, analysis of ALP activity demonstrated that AZM caused PDLSCs to regain their osteogenic ability (Figure 1(g)). Remarkably, the cells that were treated with TNF-α alone clearly had fewer cells (Figures 1(b) and 2(b)). As the AZM concentration increased, the number of cells increased as well.

We speculated that AZM could promote osteogenesis and could partially restore PDLSC osteogenic capacity in an inflammatory microenvironment. To verify this, we assessed the mRNA expression of the osteogenic differentiation markers *OCN*, *BSP*, and *RUNX2* by real-time PCR (Figure 3). We found that AZM treatment promoted PDLSCs osteogenic differentiation and the mRNA expression of these genes in a dose-dependent manner (Figure 3(a)–3(f)). When cells were exposed to an inflammatory microenvironment (i.e., treated with TNF-α), the mRNA levels of *OCN*, *BSP*, and *RUNX2* were lower than those in control

(a)

(b)

(c)

(d)

(e)

(f)

(g)
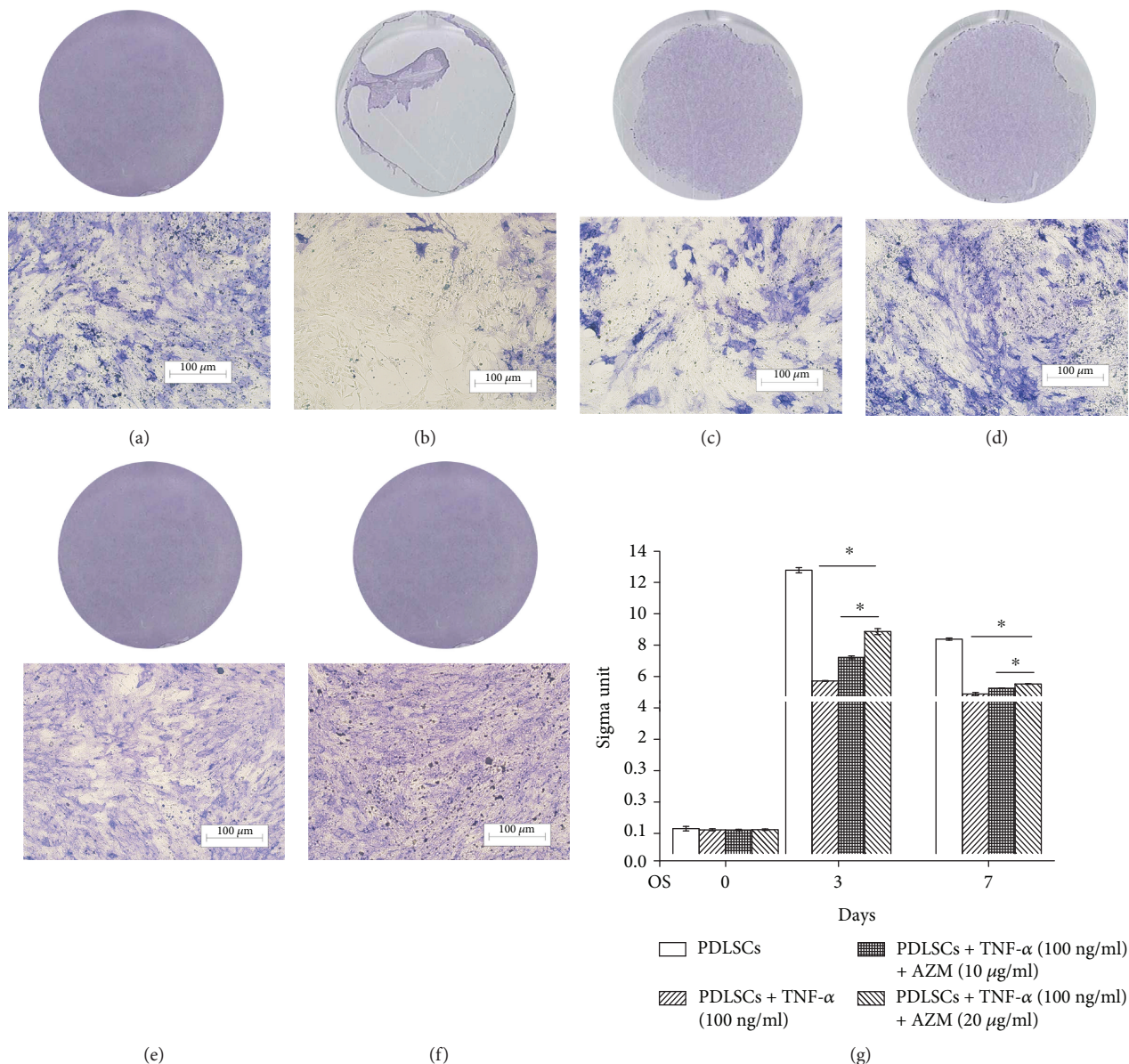
FIGURE 1: Analysis of alkaline phosphatase staining and alkaline phosphatase activity in human PDLSCs after treatment with AZM. (a–f) PDLSCs were cultured in osteogenic medium for 7 days. (a) Control PDLSCs cultured without any additions. (b) PDLSCs treated with TNF-α (100 ng/ml). (c) PDLSCs treated with TNF-α (100 ng/ml) and AZM (10 μg/ml). (d) PDLSCs treated with TNF-α (100 ng/ml) and AZM (20 μg/ml). (e) PDLSCs treated with AZM (10 μg/ml). (f) PDLSCs treated with AZM (20 μg/ml). (g) Alkaline phosphatase activity analysis. PDLSCs were induced to form osteoblasts for 0, 3, or 7 days. The results showed that AZM promoted the ability of PDLSCs to undergo osteogenesis differentiation. $^*P < 0.05$ indicates significant differences. Data are presented as means ± SD.

($P < 0.05$). However, cotreatment with AZM restored the mRNA expression levels (Figure 3(a)–3(f)). The mRNA expression levels of *KDM2A*, *KDM2B*, and *EZH2* were higher in TNF-α-treated cells compared to control cells, and AZM mitigated this effect (Figure 3(g)–3(i)).

3.3. AZM Rescued the Osteogenic Potential of PDLSCs through the WNT and NF-κB Signaling Pathways. In an inflammatory environment, NF-κB plays a vital role in the osteogenic differentiation of PDLSCs [33]. We next asked whether TNF-α-induced osteogenic inhibition could be partially reversed in the presence of AZM through the

suppression of NF-κB signaling. Accordingly, we used Western blotting to analyze the expression of p65, phosphorylated p65, IκB-α, and phosphorylated IκB-α (Figure 4). After 7 days of osteogenic differentiation, TNF-α promoted the expression of phosphorylated p65 and phosphorylated IκB-α in PDLSCs compared with control. However, when PDLSCs were treated with both 100 ng/ml TNF-α and 20 μg/ml AZM, the levels of phosphorylated p65 and phosphorylated IκB-α were lower than those in cells treated with TNF-α alone. We also detected the levels of p65 and IκBα. The protein level is shown in Figure 4.

(a)   (b)   (c)   (d)

(e)
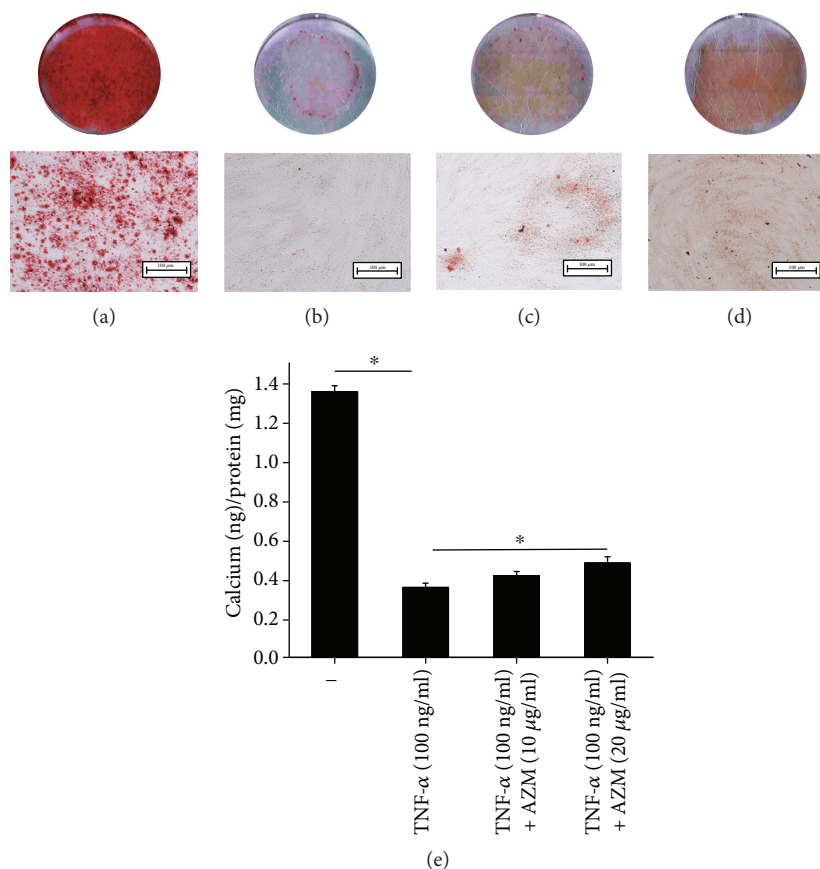
FIGURE 2: Alizarin red staining of human PDLSCs cultured in osteogenic media for 7 days. (a–d) PDLSCs cultured in osteogenic medium for 7 days. (a) Control PDLSCs cultured without any additions. (b) PDLSCs treated with TNF-α (100 ng/ml). (c) PDLSCs treated with TNF-α (100 ng/ml) and AZM (10 μg/ml). (d) PDLSCs treated with TNF-α (100 ng/ml) and AZM (20 μg/ml). (e) Detection of the calcium ion concentration and the calcium quantitative analysis for alizarin red staining were normalized to the total protein content before calculation. Increasing the AZM concentration significantly changed the number of calcium nodules. The results showed that AZM promoted the osteogenic differentiation of PDLSCs. $^{*}P < 0.05$ indicates significant differences. Data are presented as means ± SD.

Consistent with the ALP and alizarin staining results, TNF-α inhibited PDLSC osteogenic differentiation, while AZM partially reversed this effect and promoted PDLSC osteogenic differentiation. Phosphorylated p65 reflects the activation of the NF-κB signaling pathway. Thus, the results showed that AZM promoted osteogenic differentiation by suppressing the NF-κB signaling pathway. We then investigated whether WNT signaling plays a role in this process. We found that β-catenin expression increased after cells were treated with TNF-α. These results suggested that AZM promoted the osteogenic differentiation of PDLSCs in an inflammatory microenvironment by inhibiting the activation of the WNT and NF-κB signaling pathways.

3.4. AZM Promotes PDLSC Osteogenic Differentiation by Suppressing TNF-α-Induced Apoptosis. TNF-α is a strong apoptosis-promoting factor. There were some indications that AZM might repress the TNF-α-induced apoptosis of PDLSCs, since ALP staining showed that TNF-α treatment alone reduced the number of viable cells and that cotreatment with TNF-α plus AZM mitigated this effect (Figures 1 and 2). To investigate the mechanism underlying this phenomenon, we tested whether AZM rescued PDLSC osteogenesis by

suppressing TNF-α-induced apoptosis. PDLSCs were seeded at a density of $2 \times 10^{3}/cm^{2}$ in 6-well plates with or without TNF-α (100 ng/ml) and AZM (10 μg/ml, 20 μg/ml) for 24 hours. Notably, 100 ng/ml TNF-α promoted PDLSCs apoptosis and AZM mitigated this process. In addition, AZM did not promote PDLSCs apoptosis. PI staining and FITC staining were used to follow apoptosis in PDLSCs undergoing osteogenic differentiation and showed that 10 μg/ml or 20 μg/ml AZM had no effect on apoptosis (Figure 5(a)).

In the caspase activation process, the caspase prodomain is cleaved and caspase proteins form a heterotetrameric enzyme in response to proteolytic activation. Next, protein downstream of caspase is activated, resulting in apoptosis [34, 35]. Caspase-8 is an initiator caspase, and caspase-3 is an effector caspase. To further investigate the mechanisms underlying the effects of AZM, we determined the protein levels of caspase-3, caspase-8, cleaved caspase-3, and cleaved caspase-8. The results demonstrated that after PDLSCs underwent osteogenic differentiation for 7 days, the protein levels of caspase-8 and cleaved caspase 3 were high in cells treated with TNF-α alone and lower when AZM was added (Figures 5(b) and 5(c)). PDLSCs treated with 10 μg/ml or
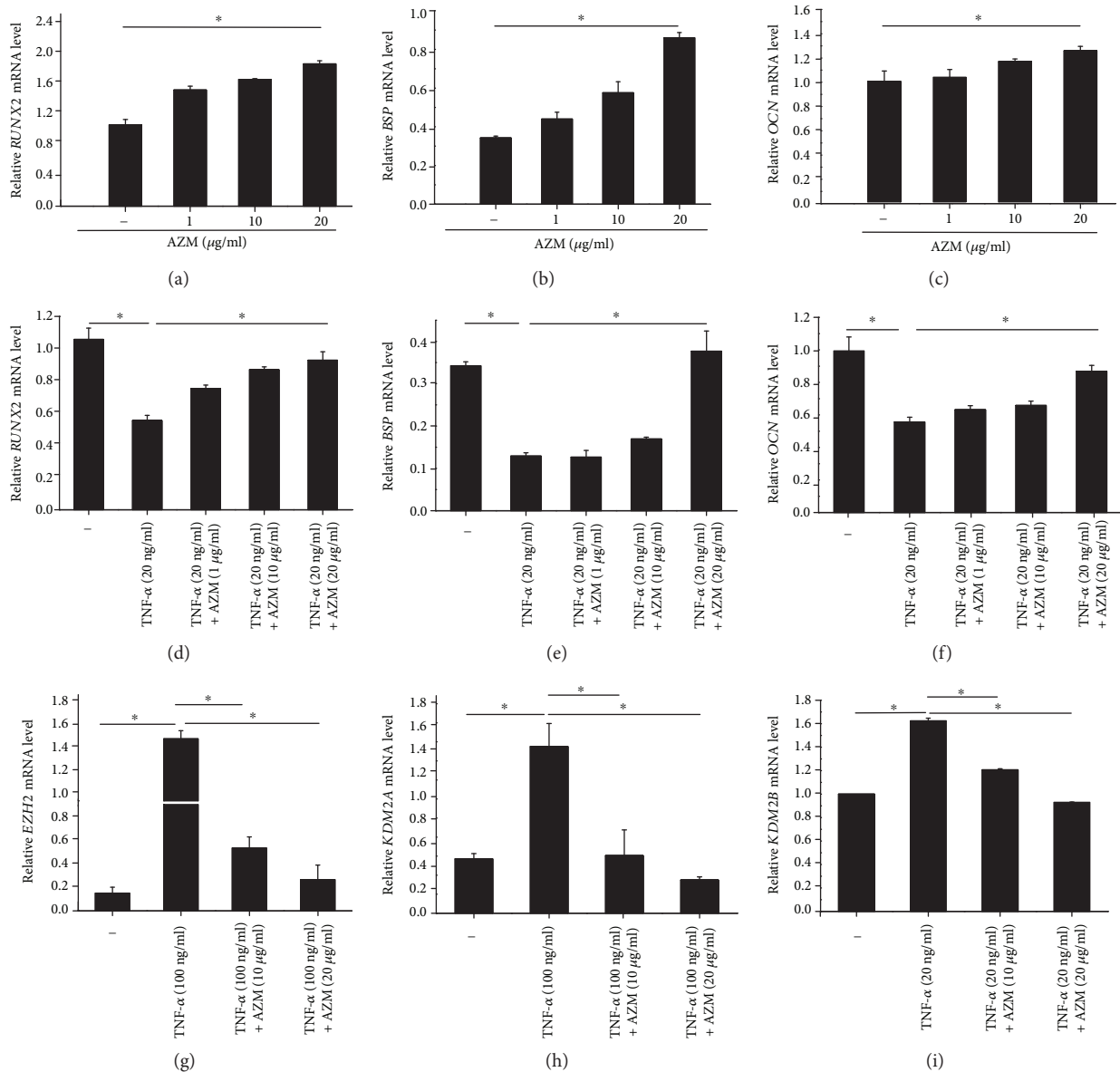
FIGURE 3: RT-qPCR analysis showed that AZM promotes the osteogenic differentiation of human PDLSCs and impacts the mRNA levels of epigenetic-related genes. Quantitative real-time PCR analysis of *RUNX2*, *BSP*, *OCN*, *KDM2A*, *KDM2B*, and *EZH2*. PDLSCs were treated with TNF-α and AZM as indicated. The top three images show the mRNA levels of (a) *RUNX2*, (b) *BSP*, and (c) *OCN* in cells treated with 1 μg/ml, 10 μg/ml, and 20 μg/ml AZM, respectively. The middle three images show the mRNA levels of (d) *RUNX2*, (e) *BSP*, and (f) *OCN* treated with 20 ng/ml TNF-α and 1 μg/ml, 10 μg/ml, or 20 μg/ml AZM. The mRNA levels of (g) *EZH2*, (h) *KDM2A*, and (i) *KDM2B* are shown in the bottom three images. PDLSCs were treated with 20 ng/ml TNF-α and 10 μg/ml AZM or with 20 ng/ml TNF-α and 20 μg/ml AZM. *$P < 0.05$ indicates significant differences. The data are presented as means $\pm$ SD.

20 μg/ml AZM (Figure 5(d)) showed no differences in the protein levels of caspase-3 and caspase-8.

Compared with levels in cells treated with 10 μg/ml AZM, the levels of cleaved caspase-3 and cleaved caspase-8 were higher in cells treated with 20 μg/ml AZM. It is possible that AZM promotes PDLSC differentiation. A more favorable cellular state can increase cell proliferation, although the MTS results showed no statistically significant differences in the proliferation of cells treated with AZM (Figure S3). Compared with cells treated with 10 μg/ml AZM, cells treated with 20 μg/ml AZM showed a slightly increased cell number. The level of apoptosis in cells treated with AZM

was lower than in that cells treated with TNF-α and control cells (Figures 5(b) and 5(d)). AZM inhibited apoptosis in a dose-dependent manner (Figures 5(b) and 5(d)). To confirm if AZM promotes human PDLSC osteogenesis differentiation associated with the suppression of TNF-α-induced apoptosis, PDLSCs were cultured in basal medium and then cultured with or without TNF-α (100 ng/ml) and AZM (10 μg/ml, 20 μg/ml) for 24 hours. Annexin V-positive cells were detected by flow cytometry analysis. Moderate levels of TNF-α can promote apoptosis in PDLSCs, but AZM mitigated this effect. Compared with PDLSCs treated with TNF-α alone (Figure 6), the
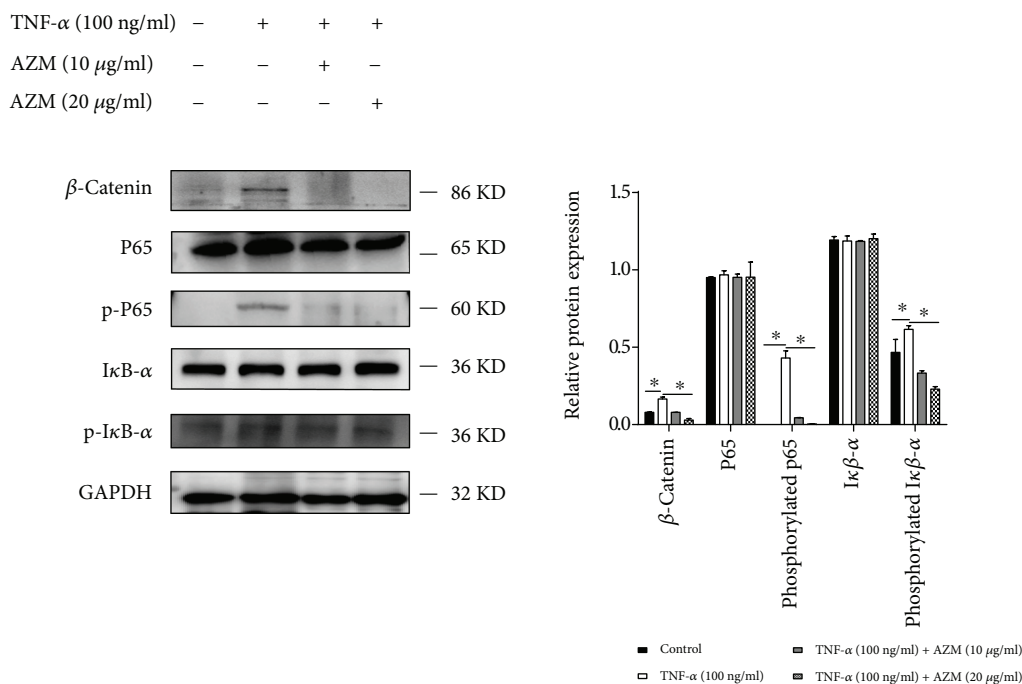
FIGURE 4: AZM restored the osteogenic potential of human PDLSCs through the WNT and NF-κB signaling pathways. PDLSCs were cultured in osteogenic medium and treated with 100 ng/ml TNF-α and AZM (10 μg/ml, 20 μg/ml) for 7 days. The protein levels of p65, phosphorylated p65, β-catenin, IκB-α, and phosphorylated IκB-α were detected by Western blot analysis. $^*P < 0.05$ indicates significant differences. Data are presented as means $\pm$ SD.

apoptosis level decreased in the presence of AZM. Our data thus showed that AZM can block TNF-α-induced apoptosis.

Taken together, these data demonstrate that AZM promotes the osteogenic differentiation of PDLSCs by suppressing TNF-α-induced apoptosis.

4. Discussion

Periodontitis is a complex progressive inflammatory disease that is more prevalent in adults but also occurs in children and adolescents. Notably, periodontitis can lead to alveolar bone loss and systemic inflammation. Dysbiosis of the dental plaque, which interacts with the host immune defense, initiates periodontitis. Because the underlying mechanism is complex, it is challenging to repair bone loss and improve the deep periodontal pocket to achieve a satisfactory end result [9]. Bartold et al. demonstrated that dental plaque is essential but insufficient for periodontitis [4, 5, 36, 37]. AZM has anti-inflammatory properties and it is reported by several groups [38, 39]. Here, we found that AZM can reverse bone loss and suppress PDLSC apoptosis. PDLSCs that can differentiate into osteoblasts show great potential for treating patients with periodontitis.

TNF-α is a strong apoptosis inducer and a proinflammatory cytokine that contributes to bone loss in local and systemic inflammatory bone diseases [40]. TNF-α inhibits the expression of the osteogenic-related gene Runx2 in two ways. First, it suppresses Runx2 gene expression. Second, it promotes Runx2 degradation [41]. Our data provide

evidence that AZM promotes PDLSCs osteogenic differentiation in an inflammatory microenvironment.

This study had four major findings. First, PDLSCs osteogenesis was strikingly inhibited by TNF-α and clearly enhanced by AZM. Second, Western blot analysis showed that TNF-α increased the expression of phosphorylated p65, phosphorylated IκB-α, and β-catenin. In contrast, the levels of these proteins were inhibited by AZM in a concentration-dependent manner. Third, stimulation with TNF-α activated the cleaved caspase-3 protein and AZM reversed the TNF-α-induced apoptosis of PDLSCs. Fourth, flow cytometry analysis showed that moderate concentrations of TNF-α promoted PDLSC apoptosis and that AZM mitigated this process. Our finding that AZM can inhibit the apoptosis of PDLSCs is consistent with the work of Mizunoe et al. [42] and Stamatiou et al. [43].

Our data shed light on the mechanisms by which AZM promotes osteogenesis. When trimeric TNF-α binds to TNFR1, the TNFR1-associated death domain protein (TRADD) is recruited to TNFR1. TRADD then acts as a bridge to recruit other apoptosis-related proteins, such as receptor-interacting protein (RIP), TNF receptor-associated factor 2 (TRAF2), and the Fas-associated death domain protein (FADD). Next, the integration of TRAF2 and RIP leads to the recruitment of the IKK complex. Intriguingly, phosphorylated-IκBα is then degraded and this activates the NF-κB signaling pathway and mediates cell apoptosis. TNF-α can trigger cell apoptosis in another way, that is, via the caspase pathway. This pathway involves FADD, caspase-8, and caspase-3. Caspase-3 activation allows it to cleave related proteins and results in
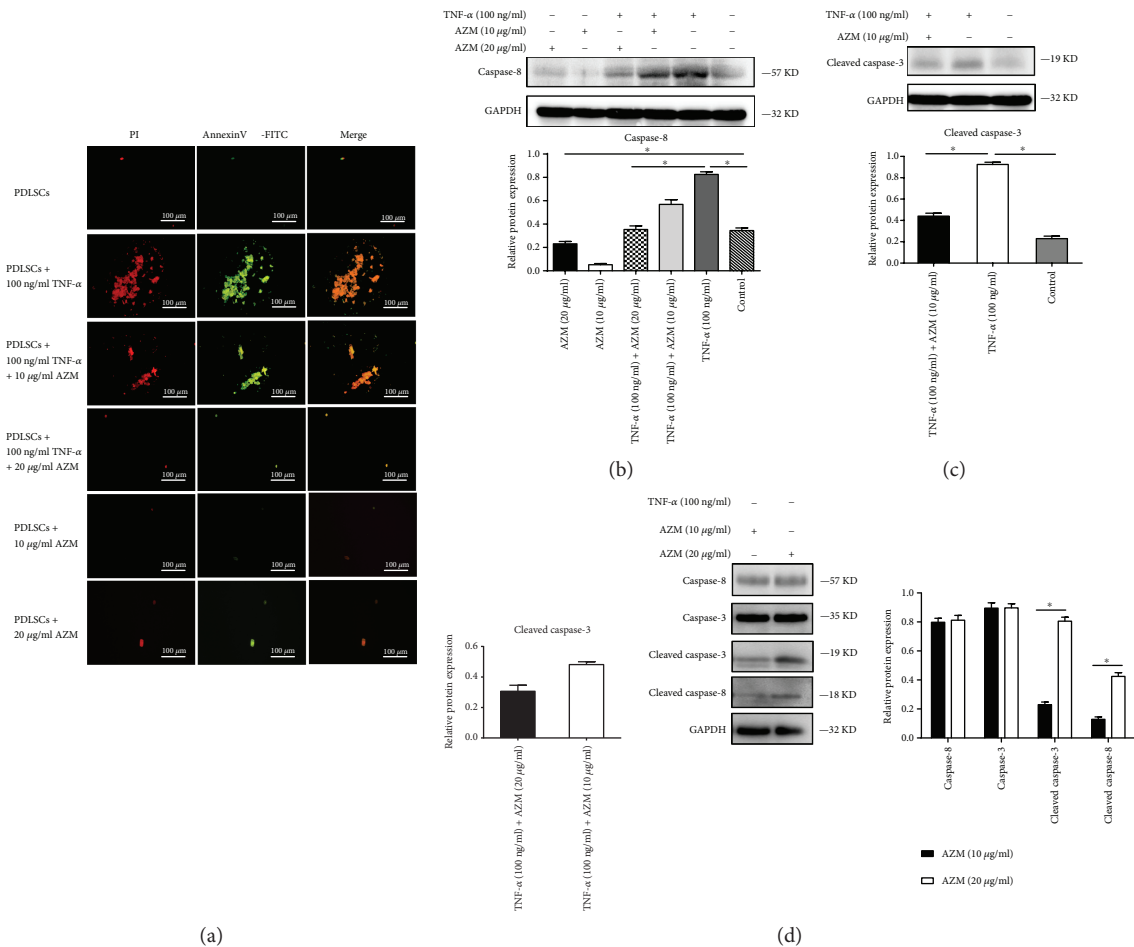
FIGURE 5: Immunocytochemical staining and the expression levels of the apoptosis proteins caspase-3 and caspase-8 in human PDLSCs. (a) Immunofluorescence staining. PDLSCs were incubated in osteogenic medium with or without TNF-α and AZM as indicated for 24 h. (b–d) The expression levels of caspase-3, caspase-8, cleaved caspase-3, and cleaved caspase-8 were detected by Western blot analysis. The results showed that TNF-α induced cell apoptosis and that AZM treatment prevented PDLSCs from undergoing TNF-α-induced apoptosis. AZM alone at 10 or 20 μg/ml had no effect on apoptosis. $^*P < 0.05$ indicates significant differences. Data are presented as means ± SD.

cell death [34]. AZM blocks bone loss induced by TNF-α in two ways. First, it suppresses the activation of NF-κB signaling, and second, it inhibits the cleavage of caspase family proteins.

Increasing evidence shows that the WNT pathway plays an important role in bone metabolism. There are two WNT signaling pathways: the canonical pathway, termed the WNT/β-catenin pathway, and the noncanonical WNT/Ca^{2+} pathway. The activation state of β-catenin is central in the WNT/β-catenin pathway. When WNT proteins bind to Frizzled receptors, β-catenin is activated and accumulates in the cytoplasm. Stable β-catenin is transported into the nucleus and mediates the transcription of downstream genes ([44], Huang, and [45–47]). Notably, high expression of β-catenin decreased the mRNA expression of Runx2, COL1, and OCN in PDLSCs extracted from an inflammatory microenvironment. Some researchers asserted that high β-catenin expression decreases osteogenesis via the noncanonical pathway, while others considered this to occur via the canonical pathway [47, 48]. Because we examined the protein expression of β-catenin, we do not know which

pathway AZM inhibits and additional experiments are needed to determine the precise mechanism.

Epigenetic regulation of gene expression is heritable and reversible. The DNA sequence is not altered in epigenetics; rather, there is methylation of lysine or arginine residues in the histone tails. The methylated lysine residues are considered epigenetic signals that may be related to gene activation, as for methylation at H3K4 and H3K36, or to gene repression, as for methylation at H3K9 and H3K27 [49, 50]. The histone lysine demethylases (KDMs) KDM2A and KDM2B demethylate H3K4me3 and H3K36me1/2 [50]. KDM2B plays an important role in BCOR mutation-associated diseases [51]. Moreover, the interactions between KDM2A and BCOR can inhibit osteogenesis by suppressing epiregulin (EREG) gene transcription, which is required for the expression of osterix (OSX) and distal-less homeobox 5 (DLX5) [52]. Our results are consistent with these reports.

KDM2B is a component of the noncanonical PRC1 (polycomb repressive complex 1), and it recruits Ring1B and Nspc1 to promote H2AK119 monoubiquitylation [53].
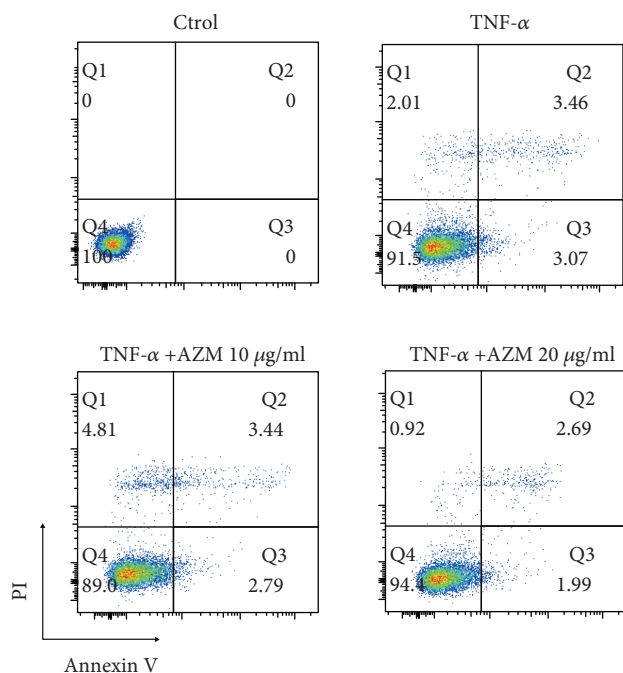
FIGURE 6: Detection of apoptosis in human PDLSCs by flow cytometry. PDLSCs were cultured in standard medium and treated with 100 ng/ml TNF-α and 10 μg/ml or 20 μg/ml AZM as indicated for 24 h. Apoptosis was detected using annexin V apoptosis assay.

The recruited Ring1B may interact with RNA polymerase II (RNAPII), leading to a bivalent state [54]. KDM2B localizes to regions where H3K36me2 levels are low. TNF-α stimulation promotes the removal of the dimethyl markers at H3K36 and inhibits osteogenic-related gene transcription. EZH2, a member of PRC2 (polycomb repressive complex 2), is a type of histone lysine methyltransferase (KMT). EZH2 mainly catalyzes H3K27 trimethyl markers. The canonical PRC1 complex is recruited to the appropriate locations by PRC2, which can recognize H3K27me3 [55]. EZH2 has been known for decades to be a negative mediator of MSC osteogenesis, which is in accordance with our findings. AZM may promote osteogenesis through three ways. First, it can block PRC1 binding to the H2AK119ub promoter and then decrease the level of H2AK119ub. Second, it can increase the level of H3K36me2 and then promote gene transcription. Third, it can decrease the level of H3K27me3 and reduce the recruitment of PRC2, which can inhibit transcription inhibition and promote the expression of downstream genes.

Periodontal diseases contribute to the formation of a complex inflammatory microenvironment. This study showed that AZM has potential as a new drug for treating periodontal diseases. Although AZM cannot completely reverse bone loss, it is likely to be helpful to have some insights into the putative effects of AZM on periodontal diseases. There may be additional mechanisms involved that we did not explore here. In a TNF-α-induced inflammatory microenvironment, we detected the expression of osteoblast-specific genes and cell apoptosis in vitro, and we concluded that AZM promotes the osteogenic differentiation of PDLSCs in an inflammatory microenvironment by inhibiting the WNT and NF-κB signaling pathways and the process associated with suppression of TNF-α-induced apoptosis. This study has some limitations. In particular, this was an in vitro study; animal studies were not conducted. Further experiments focusing on tissue regeneration are needed to better model the environment in humans.

In summary, our study suggested that AZM has potential as a new drug to treat periodontitis diseases and offered some insights into AZM and epigenetics. Further experiments are needed to investigate AZM as a therapeutic drug for periodontitis and bone tissue regeneration.

5. Conclusion

Our results showed that AZM promotes PDLSCs osteogenic differentiation in response to TNF-α stimulation by inhibiting the WNT and NF-κB signaling pathways and by attenuating TNF-α-induced apoptosis.

Abbreviations

BSP:	Bone sialoprotein
EZH2:	Enhancer of zeste homolog 2
FBS:	Fetal bovine serum
FITC:	Fluorescein isothiocyanate
KDM2A:	Lysine-specific demethylase 2A
KDM2B:	Lysine-specific demethylase 2B
OCN:	Osteocalcin
PI:	Propidium iodide
Runx2:	Runt-related transcription factor 2.

Data Availability

The data used to support the findings of this study are available from the corresponding author upon request.

Conflicts of Interest

The authors declare that they have no conflicts of interest.

Authors' Contributions

Acknowledgments

Supplementary Materials

The experimental section of alkaline phosphatase (ALP) activity assay and flow cytometric analysis were in the supplementary materials, and primers for specific genes sequences and the supplementary figures were also included. Supplementary Table 1: primers for gene sequences. Fig. S1: the image of PDLSCs under a 10x microscope. PDLSCs have the elongated spindle morphology. Fig. S2: PDLSCs cultured in normal medium. Flow cytometric analysis of PDLSCs showed positive expression of cell markers STRO-1, CD90, and CD146 and negative results for CD45. Fig. S3: appropriate TNF-α and azithromycin have no overt toxic effect on cell viability and proliferation of PDLSCs. Cell viability was measured using MTS assay; there are no significant difference between the 12 groups. (Supplementary Materials)

References

[1] G. C. Armitage, "Learned and unlearned concepts in periodontal diagnostics: a 50-year perspective," *Periodontology 2000*, vol. 62, no. 1, pp. 20–36, 2013.

[2] A. Khocht and J. M. Albandar, "Aggressive forms of periodontitis secondary to systemic disorders," *Periodontology 2000*, vol. 65, no. 1, pp. 134–148, 2014.

[3] D. F. Kinane and P. Mark Bartold, "Clinical relevance of the host responses of periodontitis," *Periodontology 2000*, vol. 43, no. 1, pp. 278–293, 2007.

[4] M. K. Barton, "Evidence accumulates indicating periodontal disease as a risk factor for colorectal cancer or lymphoma," *CA: A Cancer Journal for Clinicians*, vol. 67, no. 3, pp. 173-174, 2017.

[5] P. M. Bartold and T. E. Van Dyke, "Periodontitis: a host-mediated disruption of microbial homeostasis. Unlearning learned concepts," *Periodontology*, vol. 62, no. 1, pp. 203–217, 2013.

[6] R. C. Page and H. E. Schroeder, "Pathogenesis of inflammatory periodontal disease. A summary of current work," *Laboratory Investigation*, vol. 34, no. 3, pp. 235–249, 1976.

[7] A. J. Friedenstein, R. K. Chailakhjan, and K. S. Lalykina, "The development of fibroblast colonies in monolayer cultures of guinea-pig bone marrow and spleen cells," *Cell and Tissue Kinetics*, vol. 3, no. 4, pp. 393–403, 1970.

[8] Y. Wang, X. Chen, W. Cao, and Y. Shi, "Plasticity of mesenchymal stem cells in immunomodulation: pathological and therapeutic implications," *Nature Immunology*, vol. 15, no. 11, pp. 1009–1016, 2014.

[9] Z. Jia, Y. Wang, Y. Xu et al., "Aberrant gene expression profiles and related pathways in chronic periodontitis," *International Journal of Clinical & Experimental Medicine*, vol. 9, no. 11, 2016.

[10] D. Liu, Y. Wang, Z. Jia et al., "Demethylation of *IGFBP5* by histone demethylase KDM6B promotes mesenchymal stem cell-mediated periodontal tissue regeneration by enhancing osteogenic differentiation and anti-inflammation potentials," *Stem Cells*, vol. 33, no. 8, pp. 2523–2536, 2015.

[11] D. Liu, J. Xu, O. Liu et al., "Mesenchymal stem cells derived from inflamed periodontal ligaments exhibit impaired immunomodulation," *Journal of Clinical Periodontology*, vol. 39, no. 12, pp. 1174–1182, 2012.

[12] J. Xu, D. Wang, D. Liu et al., "Allogeneic mesenchymal stem cell treatment alleviates experimental and clinical Sjogren syndrome," *Blood*, vol. 120, no. 15, pp. 3142–3151, 2012.

[13] L. Sun, K. Akiyama, H. Zhang et al., "Mesenchymal stem cell transplantation reverses multiorgan dysfunction in systemic lupus erythematosus mice and humans," *Stem Cells*, vol. 27, no. 6, pp. 1421–1432, 2009.

[14] D. Zhang, C. Chia, X. Jiao et al., "D-mannose induces regulatory T cells and suppresses immunopathology," *Nature Medicine*, vol. 23, no. 9, pp. 1036–1045, 2017.

[15] K. Akiyama, C. Chen, D. Wang et al., "Mesenchymal-stem-cell-induced immunoregulation involves FAS-ligand-/FAS-mediated T cell apoptosis," *Cell Stem Cell*, vol. 10, no. 5, pp. 544–555, 2012.

[16] G. Ding, Y. Liu, W. Wang et al., "Allogeneic periodontal ligament stem cell therapy for periodontitis in swine," *Stem Cells*, vol. 28, no. 10, pp. 1829–1838, 2010.

[17] O. Liu, J. Xu, G. Ding et al., "Periodontal ligament stem cells regulate B lymphocyte function via programmed cell death protein 1," *Stem Cells*, vol. 31, no. 7, pp. 1371–1382, 2013.

[18] Y. Liu, Y. Zheng, G. Ding et al., "Periodontal ligament stem cell-mediated treatment for periodontitis in miniature swine," *Stem Cells*, vol. 26, no. 4, pp. 1065–1073, 2008.

[19] D. J. Payne, M. N. Gwynn, D. J. Holmes, and D. L. Pompliano, "Drugs for bad bugs: confronting the challenges of antibacterial discovery," *Nature Reviews Drug Discovery*, vol. 6, no. 1, pp. 29–40, 2007.

[20] M. Shinkai, M. O. Henke, and B. K. Rubin, "Macrolide antibiotics as immunomodulatory medications: proposed mechanisms of action," *Pharmacology & Therapeutics*, vol. 117, no. 3, pp. 393–405, 2008.

[21] M. Bosnar, B. Bosnjak, S. Cuzic et al., "Azithromycin and clarithromycin inhibit lipopolysaccharide-induced murine pulmonary neutrophilia mainly through effects on macrophage-derived granulocyte-macrophage colony-stimulating factor and interleukin-1β," *The Journal of Pharmacology and Experimental Therapeutics*, vol. 331, no. 1, pp. 104–113, 2009.

[22] M. Yasutomi, Y. Ohshima, N. Omata et al., "Erythromycin differentially inhibits lipopolysaccharide- or poly(I:C)-induced but not peptidoglycan-induced activation of human monocyte-derived dendritic cells," *Journal of Immunology*, vol. 175, no. 12, pp. 8069–8076, 2005.

[23] C. Pragnell and R. Wilson, "Fabricated or induced illness in children. Open mind is needed regarding origins of childhood symptoms and illnesses," *BMJ*, vol. 324, no. 7329, p. 114, 2002.

[24] A. Mencarelli, E. Distrutti, B. Renga et al., "Development of non-antibiotic macrolide that corrects inflammation-driven immune dysfunction in models of inflammatory bowel diseases and arthritis," *European Journal of Pharmacology*, vol. 665, no. 1–3, pp. 29–39, 2011.

[25] C. Blandizzi, T. Malizia, A. Lupetti et al., "Periodontal tissue disposition of azithromycin in patients affected by chronic inflammatory periodontal diseases," *Journal of Periodontology*, vol. 70, no. 9, pp. 960–966, 1999.

[26] S. L. Buset, N. U. Zitzmann, R. Weiger, and C. Walter, "Non-surgical periodontal therapy supplemented with systemically administered azithromycin: a systematic review of RCTs," *Clinical Oral Investigations*, vol. 19, no. 8, pp. 1763–1775, 2015.

[27] X. Feng and J. Liu, "A combination of irsogladine maleate and azithromycin exhibits addictive protective effects in LPS-induced human gingival epithelial cells," *Pharmazie*, vol. 72, no. 2, pp. 91–94, 2017.

[28] L. Gershenfeld, A. Kalos, T. Whittle, and S. Yeung, "Randomized clinical trial of the effects of azithromycin use in the treatment of Peri-implantitis," *Australian Dental Journal*, vol. 63, no. 3, pp. 374–381, 2018.

[29] T. Miyagawa, T. Fujita, H. Yumoto et al., "Azithromycin recovers reductions in barrier function in human gingival epithelial cells stimulated with tumor necrosis factor-α," *Archives of Oral Biology*, vol. 62, pp. 64–69, 2016.

[30] M. Nafar, R. Ataie, B. Einollahi, F. Nematizadeh, A. Firoozan, and F. Poorrezagholi, "A comparison between the efficacy of systemic and local azithromycin therapy in treatment of cyclosporine induced gingival overgrowth in kidney transplant patients," *Transplantation Proceedings*, vol. 35, no. 7, pp. 2727-2728, 2003.

[31] S. C. Gannon, M. D. Cantley, D. R. Haynes, R. Hirsch, and P. M. Bartold, "Azithromycin suppresses human osteoclast formation and activity in vitro," *Journal of Cellular Physiology*, vol. 228, no. 5, pp. 1098–1107, 2013.

[32] B.-M. Seo, M. Miura, S. Gronthos et al., "Investigation of multipotent postnatal stem cells from human periodontal ligament," *The Lancet*, vol. 364, no. 9429, pp. 149–155, 2004.

[33] J. Chang, F. Liu, M. Lee et al., "NF-κB inhibits osteogenic differentiation of mesenchymal stem cells by promoting β-catenin degradation," *Proceedings of the National Academy of Sciences of the United States of America*, vol. 110, no. 23, pp. 9469–9474, 2013.

[34] V. Baud and M. Karin, "Signal transduction by tumor necrosis factor and its relatives," *Trends in Cell Biology*, vol. 11, no. 9, pp. 372–377, 2001.

[35] W. C. Earnshaw, L. M. Martins, and S. H. Kaufmann, "Mammalian caspases: structure, activation, substrates, and functions during apoptosis," *Annual Review of Biochemistry*, vol. 68, no. 1, pp. 383–424, 1999.

[36] K. A. Bertrand, J. Shingala, A. Evens, B. M. Birmann, E. Giovannucci, and D. S. Michaud, "Periodontal disease and risk of non-Hodgkin lymphoma in the health professionals follow-up study," *International Journal of Cancer*, vol. 140, no. 5, pp. 1020–1026, 2017.

[37] P. Mark Bartold and T. E. Van Dyke, "Host modulation: controlling the inflammation to control the infection," *Periodontology 2000*, vol. 75, no. 1, pp. 317–329, 2017.

[38] F. Tang, R. Li, J. Xue et al., "Azithromycin attenuates acute radiation-induced lung injury in mice," *Oncology Letters*, vol. 14, no. 5, pp. 5211–5220, 2017.

[39] Y. F. Wan, Z. H. Huang, K. Jing et al., "Azithromycin attenuates pulmonary inflammation and emphysema in smoking-induced COPD model in rats," *Respiratory Care*, vol. 60, no. 1, pp. 128–134, 2015.

[40] A. Annibaldi and P. Meier, "Checkpoints in TNF-induced cell death: implications in inflammation and cancer," *Trends in Molecular Medicine*, vol. 24, no. 1, pp. 49–65, 2018.

[41] H. Kaneki, R. Guo, D. Chen et al., "Tumor necrosis factor promotes Runx2 degradation through up-regulation of Smurf1 and Smurf2 in osteoblasts," *Journal of Biological Chemistry*, vol. 281, no. 7, pp. 4326–4333, 2006.

[42] S. Mizunoe, J. Kadota, I. Tokimatsu, K. Kishi, H. Nagai, and M. Nasu, "Clarithromycin and azithromycin induce apoptosis of activated lymphocytes via down-regulation of Bcl-xL," *International Immunopharmacology*, vol. 4, no. 9, pp. 1201–1207, 2004.

[43] R. Stamatiou, K. Boukas, E. Paraskeva, P. A. Molyvdas, and A. Hatziefthimiou, "Azithromycin reduces the viability of human bronchial smooth muscle cells," *The Journal of Antibiotics*, vol. 63, no. 2, pp. 71–75, 2010.

[44] R. Nusse, "Wnt signaling," *Cold Spring Harbor Perspectives in Biology*, vol. 4, no. 5, 2012.

[45] M. D. Gordon and R. Nusse, "Wnt signaling: multiple pathways, multiple receptors, and multiple transcription factors," *Journal of Biological Chemistry*, vol. 281, no. 32, pp. 22429–22433, 2006.

[46] H. Huang and X. He, "Wnt/β-catenin signaling: new (and old) players and new insights," *Current Opinion in Cell Biology*, vol. 20, no. 2, pp. 119–125, 2008.

[47] N. Liu, S. Shi, M. Deng et al., "High levels of β-catenin signaling reduce osteogenic differentiation of stem cells in inflammatory microenvironments through inhibition of the noncanonical Wnt pathway," *Journal of Bone and Mineral Research*, vol. 26, no. 9, pp. 2082–2095, 2011.

[48] W. Liu, A. Konermann, T. Guo, A. Jager, L. Zhang, and Y. Jin, "Canonical Wnt signaling differently modulates osteogenic differentiation of mesenchymal stem cells derived from bone marrow and from periodontal ligament under inflammatory conditions," *Biochimica et Biophysica Acta (BBA) - General Subjects*, vol. 1840, no. 3, pp. 1125–1134, 2014.

[49] A. J. Bannister and T. Kouzarides, "Regulation of chromatin by histone modifications," *Cell Research*, vol. 21, no. 3, pp. 381–395, 2011.

[50] P. Deng, Q. M. Chen, C. Hong, and C. Y. Wang, "Histone methyltransferases and demethylases: regulators in balancing osteogenic and adipogenic differentiation of mesenchymal stem cells," *International Journal of Oral Science*, vol. 7, no. 4, pp. 197–204, 2015.

[51] Z. Fan, T. Yamaza, J. S. Lee et al., "BCOR regulates mesenchymal stem cell function by epigenetic mechanisms," *Nature Cell Biology*, vol. 11, no. 8, pp. 1002–1009, 2009.

[52] J. Du, Y. Ma, P. Ma, S. Wang, and Z. Fan, "Demethylation of epiregulin gene by histone demethylase FBXL11 and BCL6 corepressor inhibits osteo/dentinogenic differentiation," *Stem Cells*, vol. 31, no. 1, pp. 126–136, 2013.

[53] X. Wu, J. V. Johansen, and K. Helin, "Fbxl10/Kdm2b recruits polycomb repressive complex 1 to CpG islands and regulates H2A ubiquitylation," *Molecular Cell*, vol. 49, no. 6, pp. 1134–1146, 2013.

[54] E. Brookes, I. de Santiago, D. Hebenstreit et al., "Polycomb associates genome-wide with a specific RNA polymerase II variant, and regulates metabolic genes in ESCs," *Cell Stem Cell*, vol. 10, no. 2, pp. 157–170, 2012.

[55] A. Sparmann and M. van Lohuizen, "Polycomb silencers control cell fate, development and cancer," *Nature Reviews Cancer*, vol. 6, no. 11, pp. 846–856, 2006.

Research Article

Transcriptome and DNA Methylome Dynamics during Triclosan-Induced Cardiomyocyte Differentiation Toxicity

Guizhen Du [ID],[1,2,3] **Mingming Yu,**[1,2] **Lingling Wang,**[1,2] **Weiyue Hu,**[1,2] **Ling Song,**[1,2] **Chuncheng Lu,**[1,2,3] **and Xinru Wang** [ID][1,2,3]

[1]*State Key Laboratory of Reproductive Medicine, Institute of Toxicology, School of Public Health, Nanjing Medical University, Nanjing 211166, China*
[2]*Key Laboratory of Modern Toxicology of Ministry of Education, School of Public Health, Nanjing Medical University, Nanjing 211166, China*
[3]*Center for Global Health, School of Public Health, Nanjing Medical University, Nanjing 211166, China*

Correspondence should be addressed to Guizhen Du; guizhendu@njmu.edu.cn and Xinru Wang; xrwang@njmu.edu.cn

Cardiac development is a dynamic process and sensitive to environmental chemicals. Triclosan is widely used as an antibacterial agent and reported to transport across the placenta and affect embryonic development. Here, we used human embryonic stem cell- (hESC-) derived cardiomyocytes (CMs) to determine the effects of TCS exposure on cardiac development. After TCS treatment, the differentiation process was significantly blocked and spontaneous beating rates of CMs were also decreased. Transcriptome analysis showed the dysregulation of genes involved in cardiogenesis, including GATA4 and TNNT2. Additionally, DNA methylation was also altered by TCS exposure, especially in those regions with GATA motif enrichment. These alterations of transcriptome and DNA methylation were all associated with signaling pathways integral to heart development. Our findings indicate that TCS exposure might cause cardiomyocyte differentiation toxicity and provide the new insights into how environmental factors regulate DNA methylation and gene expressions during heart development.

1. Introduction

Cardiac development is a dynamic process, which occurs with complex transcriptional programs and signaling pathways [1]. Cardiomyogenesis is precisely controlled by sequential gene regulatory steps, in which cardiac transcription factors play essential roles in the early specification process [2]. Epigenetic modification especially DNA methylation plays a critical role in regulating the transcription of heart development-related genes [3]. Recent studies demonstrated that aberrant DNA methylation patterns were associated with heart diseases [4].

Human embryonic stem cells (hESCs), with their ability to differentiate into cardiomyocytes (CMs) in culture, serve as an *in vitro* model to investigate the molecular processes of embryonic cardiac development. Recent data indicate that this differentiation process recapitulates the similar developmental pattern of embryonic cardiogenesis *in vivo* [5]. hESC-derived CMs have cardiac-specific genes, proteins, and morphology structure and thus can properly predict the cardiotoxicity of environment factors including chemicals.

Triclosan (TCS), as broad spectrum antibacterial agents, is widely used in household and personal care products (PCPs) such as hand soaps, toothpastes, and deodorants. It is one of the most frequently detected and highly concentrated chemicals in the environment and humans [6]. TCS has been found in human samples including urine, serum, plasma, and human breast milk [7, 8]. The concentrations of TCS in humans are in the several μg/L levels (range: <2.3–3620 μg/L) [9]. Studies showed that TCS could transport across the placenta and further affect fetal development [7, 10]. High levels of TCS were detected in pregnant women. In a recent study, the median TCS in maternal urine samples was 21.6 μg/L (~0.1 μM) [11]. The maximal level of TCS was expected to reach 299 μg/L

(~1 μM) in maternal urine during pregnancy [12]. The study also showed the positive correlation between maternal sera and paired umbilical cord sera. Increased TCS levels detected in maternal serum were significantly correlated with abnormal births including heart disease and heart failure, but the underlying molecular mechanism of its effect on heart development is still unclear.

In the present study, to investigate whether TCS exposure could induce cardiac toxicity during embryo development, a hESC-based cardiac differentiation model was used to explore the potential effect of TCS. Interestingly, we found that TCS exposure inhibited the differentiation of hESCs into CMs and spontaneous beating rates of CMs. Through gene expression and DNA methylation analysis, we observed that TCS exposure affected the CM marker gene expression and DNA methylation. Our findings will provide epigenetic mechanism information on the cardiotoxicity of TCS.

2. Methods

2.1. H9 hESCs Differentiated into CMs.
H9 hESCs, purchased from the Institute of Biochemistry and Cell Biology at Shanghai, Chinese Academy of Sciences, were seeded onto 1% matrigel-coated 6-well plates in mTeSR1 medium (STEMCELL Technologies, cat. no. 05850) to 80–90% confluence. H9 hESCs were cultured and differentiated into CMs by using a monolayer-based directed differentiation protocol as previously reported [13]. Briefly, sequential treatment of Gsk3 inhibitor and Wnt signaling inhibitor was performed to stimulate cardiogenesis. H9 were cultured in mTeSR1 for 4 days before exposure to CHIR99021 (Selleck, cat. no. S1263) on day 0 and IWR-1 (Sigma, cat. no. I0161) on day 3 in RPMI/B27 without insulin medium (Life Technologies, cat. no. A1895601). The culture media were replaced with RPMI/B27 medium from day 7 to day 20. Differentiation was determined by microscopical inspection of cells starting at day 8 of differentiation. Cardiac mesoderm cells could spontaneously develop into functional contracting CMs.

2.2. TCS Treatment.
TCS (≥97.0%) was obtained from Sigma-Aldrich Co. (St. Louis, MO, USA). To evaluate the impact of TCS on CM genesis, TCS at a concentration of 1 μM was added on day 0 of differentiation. H9 were subjected to a 21-day differentiation procedure with TCS or vehicle control (DMSO only, 0.1% v/v) treatment. The final concentration of TCS used in the differentiation assay was set based on our preliminary cytotoxicity assay result.

Changes in morphology were examined and photographed under a microscope every day. Spontaneous beating rates of CMs were recorded using a video-based camera system under the inverted microscope. To characterize the structure of H9-derived CMs, immunostaining for cardiac troponin T (cTnT) and sarcomeric α-actinin was performed. For cardiac differentiation rate assessment, the NKX2.5 expression levels were detected. Briefly, CMs were fixed with paraformaldehyde and permeabilized with 0.1% Triton X-100. Then CMs were incubated with primary antibody cTnT (Life Technologies, cat. no. MA5-12960) together with antibody α-actinin (Sigma-Aldrich, cat. no. A7811) or antibody NKX2.5 (Cell Signaling Technology, cat. no. 8792) at 4°C overnight, followed by secondary antibody incubation. Signals of individual and merged image detection were performed using the fluorescence microscope (Olympus, Tokyo, Japan). The fluorescence density of cells in each group was quantified and calculated by using ImageJ software. The relative intensity values were compared between the control and exposure groups. In total, cardiac differentiation capability, the morphology, and the beating rates of CMs were examined and compared between the TCS-treated and control groups. All experiments were repeated at least three times, and the images provided represent typical results.

2.3. Genome-Wide Methylation Profiling.
At day 20 of differentiation, cells in culture were subsequently enriched by a commercial CM purification kit (Cellapy, Beijing, China, cat. no. CA2005100). Then the purified CM DNA was collected. Infinium MethylationEPIC BeadChips were used for the determination of methylation levels of more than 850000 CpG sites. Bisulfite-treated DNA sample was processed according to the protocol supplied by Illumina. The BeadChips were scanned with the Illumina HiScan SQ scanner, and raw data were imported to the GenomeStudio to extract the intensities. Probes located on the sex chromosomes and those that had a detection p value greater than 0.01 in one or more samples were removed. We also excluded probes that mapped to more than one location in a bisulfite-converted genome or overlapped with the location of known SNPs. Methylation data were processed using the ChAMP package [14]. The signal intensities for the methylated and unmethylated states were normalized using the beta-mixture quantile normalization (BMIQ) algorithm [15]. At each CpG site, the methylation level was reported as a β value and ranges from 0 (unmethylated) to 1 (methylated).

2.4. DNA Methylation Data Analysis.
Raw data were processed by ChAMP [14]. Differentially methylated regions (DMRs) were computed by Bumphunter, which could firstly cluster all probes into small regions and apply random per mutation method to find DMRs [16]. In this study, we chose to identify DMRs as 1 kb gap containing more than 5 probes. Functional annotation analysis of DMRs was performed using HOMER [17], linking DMRs to the nearest genes. Gene ontology analysis was done by DAVID [18, 19].

2.5. RNA Sequencing and Analysis.
At day 20 of differentiation, cells in culture were subsequently enriched by a commercial CM purification kit. CM RNA was extracted by RNeasy Kits (QIAGEN, Germany) and treated with DNase I (Life Technologies, USA) according to standard protocols. RNA sequencing was done in Novagene using TruSeq stranded mRNA library preparation (Novagene, China). Briefly, intact RNA was fragmented, end repaired, adapter ligated, and PCR amplified following the Illumina protocol. Libraries were sequenced by Illumina HiSeq 2000. After quality control, sequence data were processed with STAR [20] to generate read alignments with hg19. Raw read counts for

DMSO

(a)

TCS

(b)
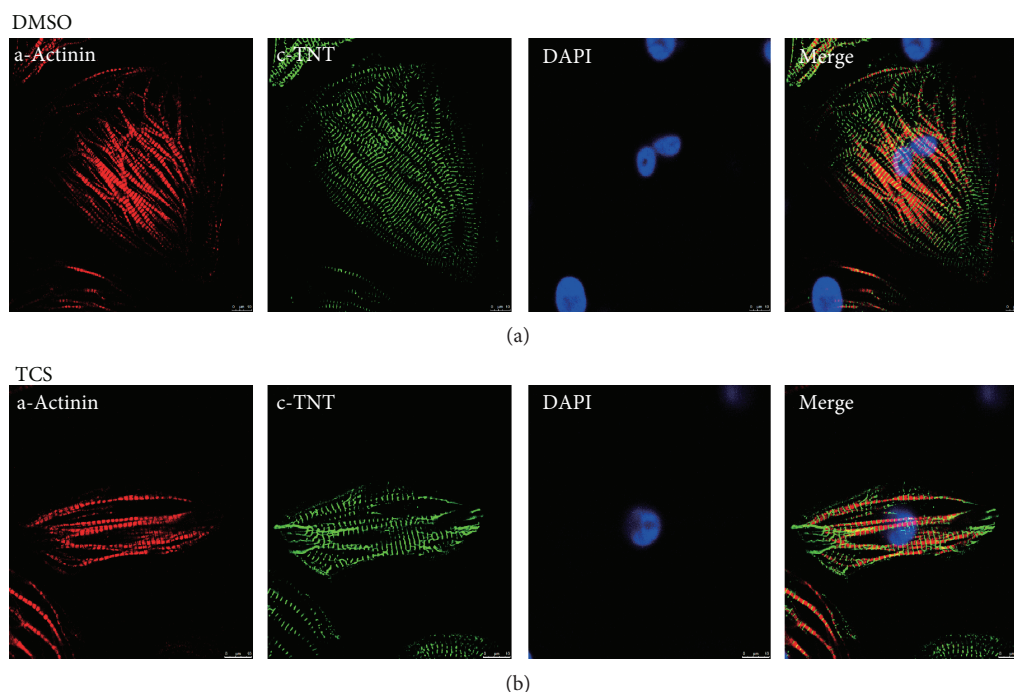
Figure 1: Structural characterization of H9-derived CMs. CMs were generated from H9 hESCs using the monolayer-based directed differentiation protocol. At day 20, CMs were immunostained for α-actinin (red) and cTnT (green). The cell nuclei were stained with DAPI (blue). Scale bar = 50 μm.

annotated genes were obtained with featureCounts with default settings [21] and normalized and analyzed using DEseq2 [22]. Real-time PCR was used to validate the RNA-seq data.

2.6. Statistical Analysis. Dates for the effect of TCS on cardiac differentiation were expressed as the mean ± standard error of mean (SEM). Statistical comparison between the TCS-treated and the control groups was determined by Student's *t*-test. All statistical analyses were performed using SPSS software, version 16.0 (SPSS Inc., Chicago, USA). Differences at $p < 0.05$ were considered as statistically significant. For DNA methylation and RNA-seq, all statistical tests were conducted in R (version 3.1.1). For DNA methylation and gene expression validation, all data are expressed as the mean ± standard deviation (SD) and Student's *t*-test was adopted to estimate the significance of the differences between the TCS-treated and the control groups.

3. Results

3.1. TCS Exposure Inhibited hESC Differentiation to CMs. Under the current experimental procedure, H9 hESCs were successfully differentiated into contracting CMs *in vitro*. The first beating cluster of cells was observed between day 8 and day 10. We observed that greater than 80% CMs were obtained at the end of differentiation in the control group, while around 60% CMs were obtained in the TCS-treated group. The changes in the morphology of hESCs during differentiation were examined and photographed under a microscope. The cardiac structure can be evaluated by cTnT and α-actinin. During differentiation, the sarcomere

structure was visualized by α-actinin and cTnT immuno-staining in H9-derived CMs. Results showed that most cells in culture were positive for cTnT and α-actinin. No significant differences in morphology were observed between TCS-treated cells and the control cells. Immunolabeling of these myofilament proteins indicates that well-organized sarcomeric structures were similarly developed in both the TCS and control groups (Figure 1, Supplementary Material, Figure S1).

To evaluate the effect of TCS on cardiac differentiation, we fixed the whole well of cells and performed immunostaining to quantify the average area of NKX2.5-positive regions for each well at day 20. Compared with the control group, TCS exposure significantly inhibited the expression level of NKX2.5 (Figure 2(a), Supplementary Material, Figure S2). We also used Western blotting to identify the expression of NKX2.5 protein. Results confirmed that the NKX2.5 protein level was reduced in the TCS-treated group (Supplementary Material, Figure S2). This indicated that persistent exposure to TCS at 1 μM could inhibit CM differentiation from hESCs. Spontaneously contracting CMs were initially observed on day 8 and progressively expanded throughout the time course. Robust beating occurred at day 12. TCS significantly inhibited the differentiation of CMs characterized by the decreased beating rates of CMs. Compared to 48 times per minute in control cells, heart rates were reduced to 27 times per minute after TCS exposure (Figure 2(b)).

3.2. TCS Exposure Altered CM Transcriptome. In order to understand how TCS exposure affects the transcriptome in CMs, we carried out RNA-seq in the TCS and control groups and 2163 differentially expressed genes (DEGs), including

(a)

(b)
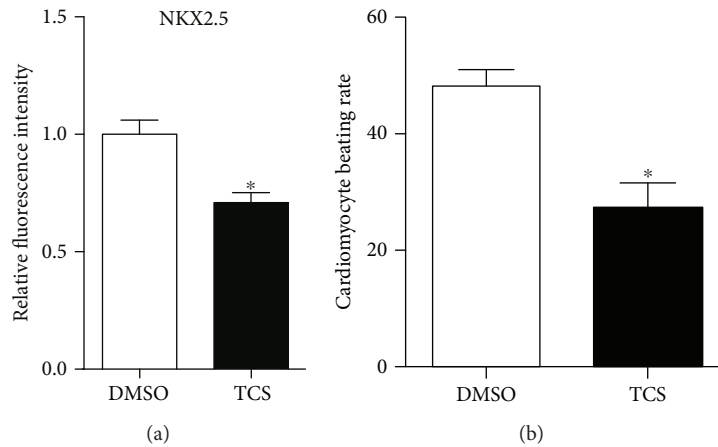
FIGURE 2: Quantitative analysis of CMs differentiated from hESCs. (a) Effect of TCS on cardiac differentiation. NKX2.5 expression in H9-derived CMs in the TCS-treated and the control groups was assessed and quantified. Data are expressed as average percentage of the positive area in each group. Error bars represent SEM. ∗ represents statistical significance ($p < 0.05$). (b) The spontaneous beating rates of CMs were counted. Data were analyzed from three independent experiments. Error bars represent SEM. $^*p < 0.05$.

917 upregulated and 1246 downregulated DEGs with fold change > 2 and FDR < 0.05, were identified using DESeq2 comparing the TCS group with the control group (Figures 3(a) and 3(b); Supplementary Material, Table S1). Represented UCSC Genome Browser shoot showed that the marker of CM differentiation was significantly repressed in the TCS-treated group (Figures 3(b) and 3(c)). To investigate the possible biological functions of significant DEGs, we performed gene ontology analysis. Our results demonstrated that the DEGs were significantly enriched with genes involved in aberrant cardiac development pathways, including arrhythmogenic right ventricular cardiomyopathy, dilated cardiomyopathy, and hypertrophic cardiomyopathy (Figure 3(d)). Besides, other signaling pathways involved in CM differentiation were also enriched in DEGs including the TGF-beta signaling pathway. These results suggested that during the differentiation of hESCs to CMs, the gene expression pattern was affected by TCS exposure.

3.3. TCS Shaped DNA Methylation Pattern in CMs. DNA methylation is the process of adding a methyl group to C5 position of the cytosine by DNA methyltransferases (DNMTs), which is a crucial epigenetic modification during CM differentiation [23]. To investigate the differential DNA methylation between the TCS and control groups, we performed Illumina EPIC BeadChip, which contains 850000 CpG sites. The genome-wide methylation levels in the TCS and control groups were showed in Figure 4(a). The CpG methylation levels were averaged in 1 Mbp windows and represented as histogram tracks. There was no global shift toward hypo- or hypermethylation after TCS treatment (Figure 4(a)). Biological functions have been reported to be associated with genomic regions rather than single CpG in general [24]. To this end, we used Bumphunter to identify the differentially methylated regions (DMRs) between the TCS and control groups. We detected only minor differences after TCS treatment. Totally, we generated a robust list of 1203 DMRs with 424 hypomethylated regions and 779

hypermethylated regions with FDR < 0.05 (Figure 4(b), Supplementary Material, Table S2).

Next, we analyzed conservation of TCS-related DMRs and the underlying DNA sequences of these DMRs were conserved across placental mammals (Figure 4(c)), which indicated that these DMRs had important functions. The overall distribution patterns of hypo- and hyper-DMRs were similar between the TCS and control groups (Figure 4(d)). The majority of DMRs was enriched in promoters, which suggested their roles in regulating gene expressions (Figure 4(d)). Altered DNA methylation near promoter regions will change the exposure of DNA sequence to transcription factors, which may affect the gene expression [25]. In order to identify the potential transcription factors binding in TCS-related DMRs, we used HORMER to predict the putative transcription factor binding sites. We found that several transcription factor binding sites were enriched in DMRs including GATA family members, which were reported to regulate differentiation of CMs (Figure 4(e)). Consistent with DMR analysis, GATA3 and GATA4 were also downregulated after TCS treatment. Functional annotation of genes near DMRs demonstrates enrichment for development of signaling pathways, including developmental process, anatomical structure development, and multicellular organismal development (Figure 4(f)). These findings suggested that TCS treatment compromised the tuning of DNA methylation during CM development.

4. Discussion

Human heart development requires fine tuning of CM-related genes, as well as other critical genes, and is sensitive to environmental factors [3]. As a widely used antibacterial agent, TCS has resulted in a global distribution and detection in various environments and human fluids (urine, serum, plasma, breast milk, and umbilical cord blood). Epidemiological and animal studies showed that TCS exposure increased the risks of developmental diseases [8, 26, 27].

(a)

(b)

(c)

(d)
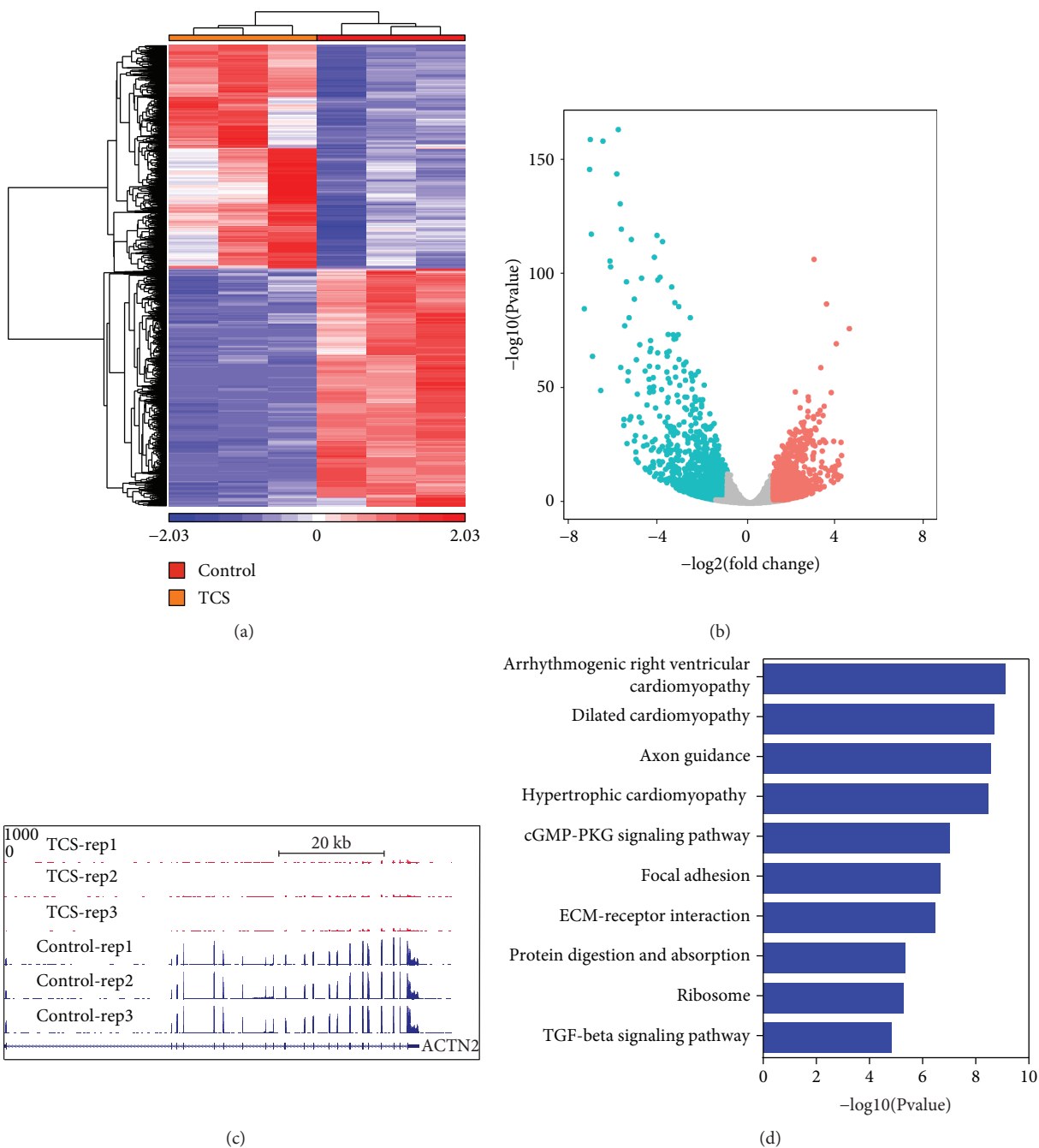
FIGURE 3: TCS exposure altered CM transcriptome. (a) Heatmap of differential expressed genes in the TCS and control groups. (b) Volcano plot of differential expressed genes in the TCS and control groups. (c) UCSC genome browser of DEGs. (d) GO analysis of differential methylated regions in TCS and control groups.

TCS can transport across the placenta and has a high potential for embryo-fetal developmental toxicity via maternal exposure. Our previous study also indicated that TCS exposure caused spontaneous abortion through affecting placental functions [8]. Some reports have confirmed that TCS exposure has been linked to heart disease and heart failure. Exposure to $400\,\mu$g/L ($\sim1.4\,\mu$M) TCS caused reduction in heart rate and resulted in a more substantial impact on end-diastolic volume, stroke volume, and ejection fraction in zebrafish [28]. Results of our previous study also suggested

that $300\,\mu$g/L ($\sim1\,\mu$M) TCS caused cardiovascular toxicity in zebrafish and $1\,\mu$M TCS could inhibit cardiogenesis in mouse embryonic stem cells. However, the relationship between TCS exposure and heart development defects is not well understood. By integration analysis of transcriptome and DNA methylome, we found that TCS could block the formation of CMs from hESCs through affecting the CM-related gene expressions and DNA methylations. Our findings highlight the TCS effects on key genes involved in heart development.

(a)

(b)

(c)

(d)

(e)

(f)
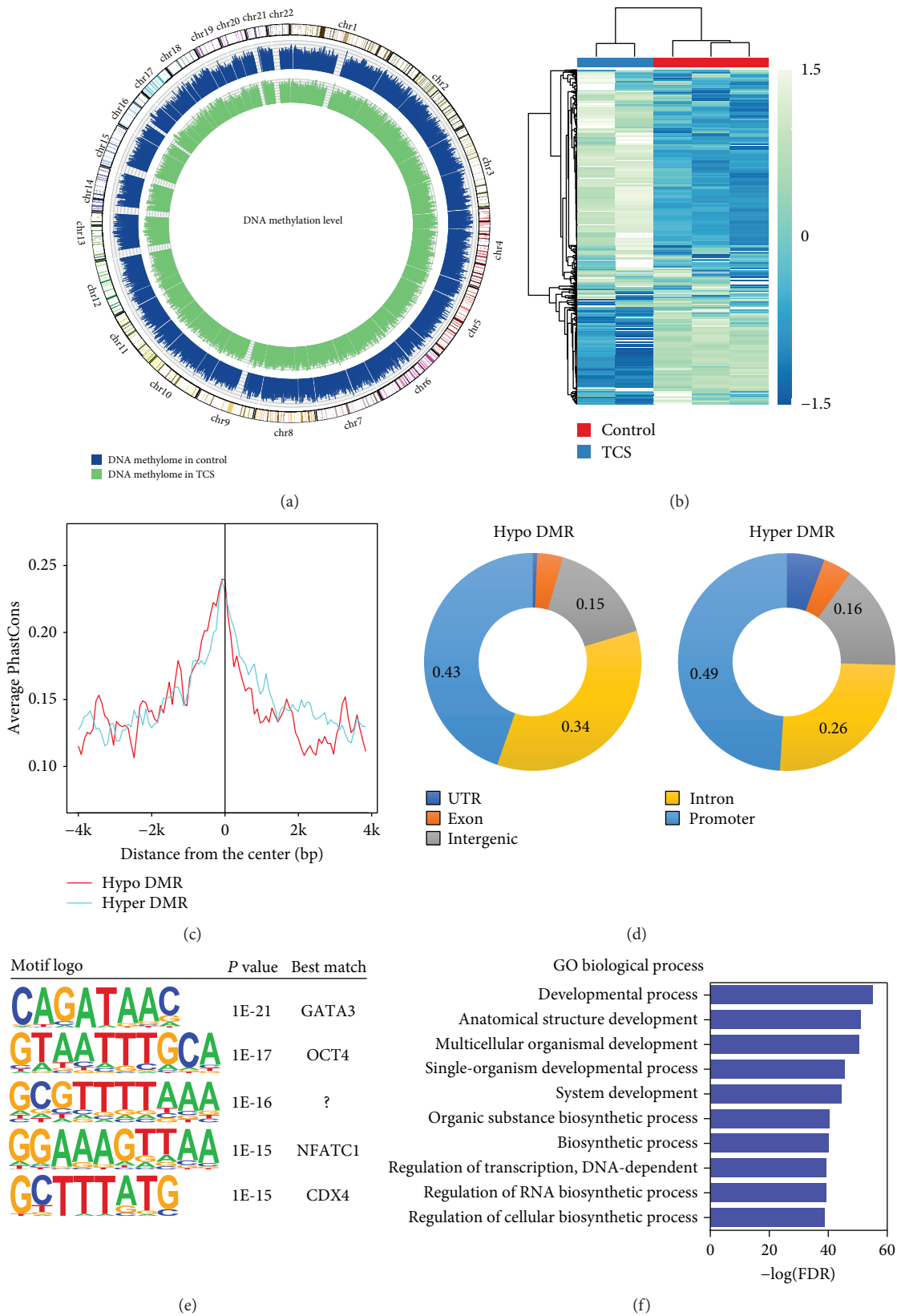
FIGURE 4: TCS shaped DNA methylation pattern in CMs. (a) Circos plot of DNA methylation levels in the TCS and control groups. (b) Heatmap of differential methylated regions in the TCS and control groups. (c) The underlying DNA sequences of DMRs are conserved across placental mammals. (d) Genome distribution of DMRs. (e) Motif analysis of DMRs. (f) GO analysis of DMRs.

In our previous study, we already found that TCS exposure affected the proliferation of mESC [29]. In the current study, to explore the mechanism behind TCS-induced CM differentiation toxicity at an environment-relevant level, $1\,\mu$M TCS was used as the test concentration. This is also the concentration used in most experiments that examine the effect of TCS on cells. Exposed to TCS, cardiac differentiation rates were significantly affected. Additionally, the spontaneously beating rates of CMs were also reduced at the TCS group. In agreement with these phenotypes, the mRNA level of ACTC1 was significantly decreased after TCS exposure. ACTC1, the cardiac α-actin gene, has been reported to play roles in sporadic congenital heart disease (CHD) [30]. Moreover, transcription factor GATA4, which is an important regulator of cardiomyogenesis, was also decreased after TCS exposure. The target genes of GATA4 were able to regulate CM beating [31]. Knocking down Gata4 in mESC during cardiomyogenesis led to decreased expression of Sox7 and heart muscle cell differentiation [31].

DNA methylation is one of several epigenetic mechanisms that regulate gene expressions [23]. We sought to determine the DNA methylation associated with differentiation of CMs and identify potential biomarkers for TCS exposure. By genome-wide analysis of DNA methylation in CMs, we had an overall glance at the gene regulation by DNA methylation. Majority of TCS-related DMRs was conserved and located near promoters, which indicates DMRs' roles in gene regulations. Additionally, our study uncovered that hypermethylation of DMRs near GATA4 and TNNT2 could downregulate their expressions after TCS exposure.

Overall, we have shown that the hESC-derived CM model enables quantitative screening of the potential cardiotoxicity of environmental chemicals by analyzing the changes of CM viability, contractility, gene expression, and epigenetic modification. Researchers can efficiently detect both the morphological and genetic toxicities of the cardiac toxicants in a short-term experiment. One limitation in our study is that we utilized a single hESC line. Differences in cell induction conditions and the epigenetic factors might affect the differentiation competence of hESCs into CMs, which might limit their ability to accurately predict cardiotoxicity. In a future study, using different hESC lines and multiple time point assays is needed to provide more insights into chemicals' cardiotoxicity.

5. Conclusion

In summary, by combining the DNA methylome and transcriptome analysis after TCS exposure, we observed the dynamic changes in transcriptome and DNA methylome in CMs. Our findings open new avenues in how TCS exposure affects the heart development and provide new insights into how environmental factors regulate DNA methylation and gene expressions.

Data Availability

The data used to support the findings of this study are available from the corresponding author upon request.

Conflicts of Interest

The authors declare that there is no conflict of interest regarding the publication of this paper.

Authors' Contributions

Guizhen Du and Mingming Yu contributed equally to the study, and they should be regarded as joint first authors.

Acknowledgments

Supplementary Materials

Supplementary 1. Figure S1: structural characterization of H9-derived CMs in the TCS-treated and the control groups.

Supplementary 2. Figure S2: assessment of NKX2.5 expression in H9-derived CMs in the TCS-treated and the control groups.

Supplementary 3. Table S1: gene expressions in H9-derived CMs in the TCS-treated and the control groups.

Supplementary 4. Table S2: differentially methylated regions in H9-derived CMs in the TCS-treated and the control groups.

References

[1] J. H. van Weerd, K. Koshiba-Takeuchi, C. Kwon, and J. K. Takeuchi, "Epigenetic factors and cardiac development," *Cardiovascular Research*, vol. 91, no. 2, pp. 203–211, 2011.

[2] M. S. Parmacek and J. A. Epstein, "An epigenetic roadmap for cardiomyocyte differentiation," *Circulation Research*, vol. 112, no. 6, pp. 881–883, 2013.

[3] Y. Gu, G. H. Liu, N. Plongthongkum et al., "Global DNA methylation and transcriptional analyses of human ESC-derived cardiomyocytes," *Protein & Cell*, vol. 5, no. 1, pp. 59–68, 2014.

[4] S. R. Martinez, M. S. Gay, and L. Zhang, "Epigenetic mechanisms in heart development and disease," *Drug Discovery Today*, vol. 20, no. 7, pp. 799–811, 2015.

[5] K. R. Boheler, J. Czyz, D. Tweedie, H. T. Yang, S. V. Anisimov, and A. M. Wobus, "Differentiation of pluripotent embryonic stem cells into cardiomyocytes," *Circulation Research*, vol. 91, no. 3, pp. 189–201, 2002.

[6] C. F. Wang and Y. Tian, "Reproductive endocrine-disrupting effects of triclosan: population exposure, present evidence and potential mechanisms," *Environmental Pollution*, vol. 206, pp. 195–201, 2015.

[7] M. Allmyr, M. Adolfsson-Erici, M. S. McLachlan, and G. Sandborgh-Englund, "Triclosan in plasma and milk from

Swedish nursing mothers and their exposure via personal care products," *Science of The Total Environment*, vol. 372, no. 1, pp. 87–93, 2006.

[8] X. Wang, X. Chen, X. Feng et al., "Triclosan causes spontaneous abortion accompanied by decline of estrogen sulfotransferase activity in humans and mice," *Scientific Reports*, vol. 5, no. 1, 2015.

[9] M. A. Adgent and W. J. Rogan, "Triclosan and prescription antibiotic exposures and enterolactone production in adults," *Environmental Research*, vol. 142, pp. 66–71, 2015.

[10] K. B. Paul, J. M. Hedge, R. Bansal et al., "Developmental triclosan exposure decreases maternal, fetal, and early neonatal thyroxine: a dynamic and kinetic evaluation of a putative mode-of-action," *Toxicology*, vol. 300, no. 1-2, pp. 31–45, 2012.

[11] L. Weiss, T. E. Arbuckle, M. Fisher et al., "Temporal variability and sources of triclosan exposure in pregnancy," *International Journal of Hygiene and Environmental Health*, vol. 218, no. 6, pp. 507–513, 2015.

[12] B. F. G. Pycke, L. A. Geer, M. Dalloul, O. Abulafia, A. M. Jenck, and R. U. Halden, "Human fetal exposure to triclosan and triclocarban in an urban population from Brooklyn, New York," *Environmental Science & Technology*, vol. 48, no. 15, pp. 8831–8838, 2014.

[13] X. Lian, J. Zhang, S. M. Azarin et al., "Directed cardiomyocyte differentiation from human pluripotent stem cells by modulating Wnt/β-catenin signaling under fully defined conditions," *Nature Protocols*, vol. 8, no. 1, pp. 162–175, 2013.

[14] Y. Tian, T. J. Morris, A. P. Webster et al., "ChAMP: updated methylation analysis pipeline for Illumina BeadChips," *Bioinformatics*, vol. 33, no. 24, pp. 3982–3984, 2017.

[15] A. E. Teschendorff, F. Marabita, M. Lechner et al., "A beta-mixture quantile normalization method for correcting probe design bias in Illumina Infinium 450 k DNA methylation data," *Bioinformatics*, vol. 29, no. 2, pp. 189–196, 2013.

[16] A. E. Jaffe, P. Murakami, H. Lee et al., "Bump hunting to identify differentially methylated regions in epigenetic epidemiology studies," *International Journal of Epidemiology*, vol. 41, no. 1, pp. 200–209, 2012.

[17] S. Heinz, C. Benner, N. Spann et al., "Simple combinations of lineage-determining transcription factors prime cis-regulatory elements required for macrophage and B cell identities," *Molecular Cell*, vol. 38, no. 4, pp. 576–589, 2010.

[18] D. W. Huang, B. T. Sherman, and R. A. Lempicki, "Systematic and integrative analysis of large gene lists using DAVID bioinformatics resources," *Nature Protocols*, vol. 4, no. 1, pp. 44–57, 2009.

[19] D. W. Huang, B. T. Sherman, and R. A. Lempicki, "Bioinformatics enrichment tools: paths toward the comprehensive functional analysis of large gene lists," *Nucleic Acids Research*, vol. 37, no. 1, pp. 1–13, 2009.

[20] A. Dobin, C. A. Davis, F. Schlesinger et al., "STAR: ultrafast universal RNA-seq aligner," *Bioinformatics*, vol. 29, no. 1, pp. 15–21, 2013.

[21] Y. Liao, G. K. Smyth, and W. Shi, "featureCounts: an efficient general purpose program for assigning sequence reads to genomic features," *Bioinformatics*, vol. 30, no. 7, pp. 923–930, 2014.

[22] M. I. Love, W. Huber, and S. Anders, "Moderated estimation of fold change and dispersion for RNA-seq data with DESeq2," *Genome Biology*, vol. 15, no. 12, p. 550, 2014.

[23] D. M. Messerschmidt, B. B. Knowles, and D. Solter, "DNA methylation dynamics during epigenetic reprogramming in the germline and preimplantation embryos," *Genes & Development*, vol. 28, no. 8, pp. 812–828, 2014.

[24] A. J. Svendsen, K. Gervin, R. Lyle et al., "Differentially methylated DNA regions in monozygotic twin pairs discordant for rheumatoid arthritis: an epigenome-wide study," *Frontiers in Immunology*, vol. 7, 2016.

[25] R. E. Thurman, E. Rynes, R. Humbert et al., "The accessible chromatin landscape of the human genome," *Nature*, vol. 489, no. 7414, pp. 75–82, 2012.

[26] M. S. Jackson-Browne, G. D. Papandonatos, A. Chen et al., "Identifying vulnerable periods of neurotoxicity to triclosan exposure in children," *Environmental Health Perspectives*, vol. 126, no. 5, article 057001, 2018.

[27] F. Ouyang, N. Tang, H. J. Zhang et al., "Maternal urinary triclosan level, gestational diabetes mellitus and birth weight in Chinese women," *Science of The Total Environment*, vol. 626, pp. 451–457, 2018.

[28] A. Saley, M. Hess, K. Miller, D. Howard, and T. C. King-Heiden, "Cardiac toxicity of triclosan in developing zebrafish," *Zebrafish*, vol. 13, no. 5, pp. 399–404, 2016.

[29] X. Chen, B. Xu, X. Han et al., "The effects of triclosan on pluripotency factors and development of mouse embryonic stem cells and zebrafish," *Archives of Toxicology*, vol. 89, no. 4, pp. 635–646, 2015.

[30] H. K. Jiang, G. R. Qiu, J. Li-Ling, N. Xin, and K. L. Sun, "Reduced ACTC1 expression might play a role in the onset of congenital heart disease by inducing cardiomyocyte apoptosis," *Circulation Journal*, vol. 74, no. 11, pp. 2410–2418, 2010.

[31] B. A. Afouda, A. T. Lynch, E. de Paiva Alves, and S. Hoppler, "Genome-wide transcriptomics analysis identifies sox7 and sox18 as specifically regulated by gata4 in cardiomyogenesis," *Developmental Biology*, vol. 434, no. 1, pp. 108–120, 2018.

Research Article

D-Mannose Enhanced Immunomodulation of Periodontal Ligament Stem Cells via Inhibiting IL-6 Secretion

Lijia Guo [iD],[1] Yanan Hou [iD],[2] Liang Song [iD],[3] Siying Zhu [iD],[4] Feiran Lin [iD],[4] and Yuxing Bai [iD][1]

[1]*Department of Orthodontics School of Stomatology, Capital Medical University, Beijing, China*
[2]*Department of Orthodontics, Peking University School of Stomatology, The Third Dental Center, Beijing, China*
[3]*Department of Stomatology, The Fifth People's Hospital of Shanghai, Fudan University, Shanghai, China*
[4]*Laboratory of Tissue Regeneration and Immunology and Department of Periodontics, Beijing Key Laboratory of Tooth Regeneration and Function Reconstruction, School of Stomatology, Capital Medical University, Beijing, China*

Correspondence should be addressed to Yuxing Bai; byuxing@ccmu.edu.cn

Periodontal ligament stem cell- (PDLSC-) mediated periodontal tissue regeneration has recently been proposed for the new therapeutic method to regenerate lost alveolar bone and periodontal ligament. It was reported that both autogenic and allogeneic PDLSCs could reconstruct damaged periodontal tissues but the regeneration effects were not consistent. The effective methods to improve the properties of PDLSCs should be further considered. In this study, we investigated if D-mannose could affect the immunomodulatory properties of hPDLSCs. After being pretreated with D-mannose, hPDLSCs could inhibit T cell proliferation and affect T cell differentiation into Treg cells. We found that less IL-6 could be detected in D-mannose-pretreated hPDLSCs. In the D-mannose pretreatment group, induced Treg cell number would decrease if increased IL-6 levels could be detected. Our data uncovered a previously unrecognized function of D-mannose to regulate the immunomodulatory function of PDLSCs and that IL-6 might play a key role in this process. The results provided a property method to improve PDLSC-based periodontal regeneration.

1. Introduction

Periodontitis, as one of the major oral infectious diseases, has high incidence in human. Periodontitis could cause damage to periodontal tissues, such as gingiva recession, attachment loss, alveolar bone loss, and teeth loss [1]. There is still no efficient therapy to recover the lost tissue. Stem cell-mediated periodontal tissue reconstruction is a promising strategy. Recently, periodontal ligament stem cells (PDLSCs) have received more and more attention in periodontal tissue reconstruction because of its multiple differentiation capacity and immunomodulation [2].

Recently, mesenchymal stem cells (MSCs) have been confirmed to have immunosuppressive and immunomodulatory properties and are extensively used to treat autoimmune diseases. Under the stimulation of inflammatory cytokines in microenvironment, MSCs inhibit the activation and proliferation of a variety of immune cells. Nevertheless, the role of MSCs on immune cells in different microenvironments remains partly unknown. More importantly, the diverse results suggested that the immunomodulatory functions of MSCs are involved in multiple factors. PDLSCs belong to one of various tooth-derived MSCs, which owned immunosuppressive abilities and mediate suppression by secreting inhibitory factors such as IFNγ, IDO, TGFβ1, and HGF [3–6]. PDLSCs could inhibit T cell proliferation though PGE2 and promote T cell differentiation into Treg cells [7, 8]. When minipigs are transplanted with periodontal defects, PDLSCs could remodel the local immune microenvironment and obtain new tissue regeneration [9]. However, the detailed mechanisms were unknown, which caused unstable therapeutic outcomes in periodontal tissue regeneration.

Glucose plays critical roles in cell metabolism during energy generation and storage. At same time, glucose participates in some pathogenic processes, such as diabetes and obesity. D-Mannose is one of the important proteins in the

glycosylation. The blood concentration of D-mannose is less than one-fiftieth of that of glucose. However, D-mannose has not received much attention. D-Mannose is a kind of C-2 epimer of glucose, which has been reported to as an effective therapy for urinary tract infections [10–15]. Currently, the function of T cell regulation of D-mannose has been found. D-Mannose could stimulate Treg differentiation by promoting TGFβ signaling [16]. But whether D-mannose could affect immunomodulation of stem cell is still unknown. In this study, we cocultured T cells with D-mannose-pretreated human PDLSCs (hPDLSCs) to investigate the effect of D-mannose on hPDLSC immunomodulation function.

2. Materials and Method

2.1. Antibodies and Reagents. Purified anti-human CD3 (OKT3) and purified anti-human CD28 (CD28.2) were purchased from eBioscience. All fluorochrome-conjugated antibodies (anti-human CD4 (RPA-T4), anti-human CD45RA (HI100), anti-human CD25 (BC96), anti-human FoxP3 (PCH101), anti-human IFNγ, anti-human IL-4, anti-human IL-17, and anti-mouse IL-6) were from eBioscience. Recombinant human IL-2 (202-IL), human TGFβ1 (240-B), and human latent TGFβ1 (299-LT) were purchased from R&D Systems. Anti-TGFβ (1D11.16.8), anti-CD25 (PC-61.5.3), and their isotype control antibodies (MOPC-21, HRPN) were from Bio X Cell. PGE2, TGFβ, and IL-6 ELISA Ready-SET-Go! kits were purchased from eBioscience.

2.2. PDLSC Culture. PDLSCs were isolated and cultured from periodontal ligament tissues of periodontal healthy donors. The protocols for handling human tissues had been approved by the Research Ethical Committee of Capital Medical University. Healthy periodontal tissues from nine patients (age 18–36 years) were obtained. The periodontal ligament from the extracted teeth was separated from the surface of the roots and cut to small pieces. Then the small tissues were digested in 3 mg/ml collagenase type I (Worthington Biochemical, Freehold, NJ) and 4 mg/ml dispase (Roche Diagnostics, Basel, Switzerland) for 1 hour at 37°C. To get the single cells, all the cells were passed through a 70 μm strainer (BD Labware, Franklin Lakes, NJ). Then about 1×10^5 single cells were seeded into 10 cm culture dishes (Corning Costar, Cambridge, MA) with culture medium. The culture medium included α-modification of Eagle's medium (Gibco, Carlsbad, CA) and 10% fetal bovine serum (Equitech-Bio Inc., Kerrville, TX) supplemented with 100 mol/l ascorbic acid 2-phosphate (Wako Chemical, Tokyo), 2 mmol/l glutamine, 100 U/ml penicillin, and 100 μg/ml streptomycin (Invitrogen, Carlsbad, CA). Then the cells were incubated at 37°C in 5% carbon dioxide. The colony cells were passed on day 14. PDLSCs in the study were three to four passages. All cells used in this study were at 3-4 passages. For each experiment, the same passages of hPDLSCs were used.

2.3. Surface Marker of PDLSCs after Glucose or D-Mannose Treatment. PDLSCs were cultured in "complete" glucose-free α-MEM culture medium supplemented with 25 mM D-mannose (M-hPDLSCs) or in the normal culture medium supplemented with 25 mM glucose (G-hPDLSCs). Three days later, surface marker expressions were analyzed by FACS staining. The treated PDLSCs were harvested with 0.25% trypsin, and cell suspensions (1.0×10^6 cells) were incubated for 1 h at room temperature with monoclonal antibodies specific for CD90, CD45, CD44, CD73, and CD105 (BD Biosciences, Franklin Lakes, NJ, USA). Expression profiles of PDLSCs were analyzed by flow cytometry (BD Biosciences).

2.4. Osteogenic Differentiation Assay. PDLSCs were cultured in osteogenic medium. The inducing medium contained 2 mM β-glycerophosphate (Sigma-Aldrich, St. Louis, MO), 10 nM dexamethasone (Sigma-Aldrich, St Louis, MO), and 100 μM L-ascorbic acid 2-phosphate (Wako Chemicals USA, Richmond, VA). The total protein was collected from induced PDLSCs after ten days. The gene expression levels of BGLAP and ALPL were assayed by RT-PCR analysis. The primer set for PCR included BGLAP (sense, 5-CGCT ACCTGTATCAATGGCTGG-3, antisense, 5-CTCCTGAA AGCCGATGTGGTCA-3); ALPL (sense, 5-ATGGGATGG GTGTCTCCACA-3, antisense, 5-CCACGAAGGGGAACT TGTC-3); and GAPDH (sense, 5-AGCCGCATCTTCTTTT GCGTC-3, antisense, 5-TCATATTTGGCAGGTTTTT CT-3). To detect mineralized nodule formation, the cultured PDLSCs were stained with alizarin red after 4 weeks of induction.

2.5. Adipogenic Differentiation Assay. PDLSCs were cultured in adipogenic culture medium. The medium contained 500 μM isobutylmethylxanthine (Sigma-Aldrich, St. Louis, MO), 500 nM hydrocortisone (Sigma-Aldrich, St. Louis, MO), 60 μM indomethacin (Sigma-Aldrich, St. Louis, MO), 100 μM L-ascorbic acid 2-phosphate, and 10 μg/ml insulin (Sigma-Aldrich, St. Louis, MO). The gene expressions of peroxisome proliferator-activated receptor g ($PPA\gamma G$) and FABP4 were analyzed via RT-PCR after adipogenic induction. The primer set for PCR included PPAγG (sense, 5-CTCCTATTGACCCAGAAAGC-3, antisense, 5-GTAGAG CTGAGTCTTCTCAG-3); FABP4 (sense, 5-GTCCAGGCT GGAATGCAGTG-3, antisense, 5-CACACAGACGTACA GAGTGG-3); and GAPDH (sense, 5-AGCCGCATCTT CTTTTGCGTC-3, antisense, 5-TCATATTTGGCAGGTT TTTCT-3).

2.6. Alizarin Red Staining. After being induced for four weeks, the PDLSCs were fixed with 70% ethanol and stained with 2% alizarin red (Sigma-Aldrich). After being stained with alizarin red, the cells were destained for 30 min at room temperature with 10% cetylpyridinium chloride in 10 mM sodium phosphate and the calcium content was determined.

2.7. Oil Red O Staining. The cells were induced for 14 days in adipogenic medium and stained with Oil Red O (Sigma-Aldrich, St. Louis, MO). After being fixed with 4% paraformaldehyde, the cells were incubated with Oil Red O solution for 1 h. Then lipid droplets could be observed by microscopy.

2.8. Real-Time RT-PCR. Total RNA was derived from PDLSCs with an RNeasy mini kit (Qiagen). For real-time

RT-PCR, cDNA was synthesized with a high-capacity cDNA reverse transcription kit (Applied Biosystems). Quantitative real-time PCR was performed using TaqMan gene expression assay kits (Applied Biosystems). The gene expression levels were normalized to the expression of *Hprt*.

2.9. Peripheral Blood Mononuclear Cells and $CD4^+$ T Cells. Human peripheral blood mononuclear cells (PBMCs) from healthy volunteers were approved by the Research Ethical Committee of Capital Medical University. Blood samples were provided by the Capital Medical University School of Stomatology. All donors signed informed consent. Naive $CD4^+$ T cells were purified by using Naive T Cell Isolation Kit II (Miltenyi Biotec). Then all the isolated cells were resuspended in T cell culture medium (Roswell Park Memorial Institute (RPMI))—1640 medium (GIBCO, Carlsbad, CA) with 10% FBS, 2 mmol/l glutamine, 20 mol/l HEPES, 100 U/ml penicillin, and 100 μg/ml streptomycin (Invitrogen). To stimulate the naive $CD4^+$ T cells, the cells were cultured in the anti-human CD3 (5 μg/ml) precoated plate and soluble anti-human CD28 (2.5 μg/ml) plus IL-2 (10 ng/ml). Three days after stimulation, the cells were analyzed by FACS staining.

2.10. T Cells Cocultured with PDLSCs. 2×10^4 human PDLSCs were seeded in 24-well plates in triplicate, and cells adhered to the plates and stayed overnight. Then the glucose- or D-mannose-pretreated PDLSCs were cocultured with $CD4^+$ T cells (T + G-hPDLSCS/T + M-hPDLSCs) for 3 days in T cell culture medium stimulated with soluble anti-human CD3 (5 μg/ml), anti-human CD28 (2.5 μg/ml), and IL-2 (10 ng/ml).

2.11. T Cell Proliferation Assay. Activated T lymphocytes (1×10^6/well) were cocultured with or without 0.2×10^6 PDLSCs (pretreated with glucose or D-mannose) on 24-well multiplates with T cell-stimulated medium for 3 days. 1×10^4 cells were incubated with 5 mM carboxyfluorescein succinimidyl ester (CFSE, Invitrogen) for 10 min. Five volumes of ice-cold medium were added to stop the staining process. After being washed three times, T cells were cultured for 72 h and analyzed by CFSE flow cytometry. A percentage of divided cells were analyzed by FSC Express 3.0 software.

2.12. In Vitro Th1 and Th2 Induction by PDLSCs. $CD4^+$ T cells (1×10^6/well) were cocultured with 0.2×10^6 glucose- or D-mannose-pretreated PDLSCs on 24-well multiplates for 3 days in T cell culture medium stimulated with soluble anti-human CD3 (5 μg/ml), soluble anti-human CD28 (2.5 μg/ml), and IL-2 (10 ng/ml). After 3 days, cells in suspension were collected and detected Th1, Th2, Th17, and Treg via flow cytometry analysis. The concentrations of PGE2 and TGFβ1 in supernatant were analyzed by ELISA Ready-SET-Go! kits (eBioscience) following the manufacturer's instructions. Gene expression of Nos2 and IDO1 in cocultured PDLSCs were analyzed by RT-PCR.

2.13. Flow Cytometry Analysis. Cells were incubated with PMA (10 ng/ml), ionomycin (250 ng/ml), and Golgi plug (1 : 1000 dilution; BD PharMingen) at 37°C for 4 h. For intracellular cytokine staining, cells were fixed with the fixation/permeabilization buffer solution (BD Biosciences). The collected T cells (1×10^6) were stained with anti-CD4-FITC, anti-IFNγ-PE, anti-IL-6-PerCP, anti-IL-4-APC, and anti-CD25-PerCP. For intranuclear staining, the cells were continuously treated with fixation/permeabilization buffer solution (eBioscience) and stained with anti-FoxP3-PacBlue antibodies (each 1 mg/ml; eBioscience). Cells were carried out on a FACSCalibur, and data were analyzed with FlowJo software.

2.14. Statistical Analysis. All data were repeated in three to five independent experiments. Unless otherwise noted, statistical significance comparison was analyzed by two-tailed Student's *t*-test between two groups and by one-way ANOVA between more than two groups. Statistical analysis was performed with GraphPad Prism 6. *P* values less than 0.05 were determined statistically significant.

3. Results

3.1. D-Mannose-Pretreated PDLSCs Modulated T Cell Proliferation Better. In order to examine the effects of D-mannose on hPDLSCs, we used D-mannose or glucose medium to culture hPDLSCs. Surface makers of hPDLSCs, CD44, CD73, CD90, and CD105 were detected by flow cytometry Figure 1(a) and there was no difference between the two groups. There were no significant differences in apoptosis and proliferation of hPDLSCs between D-mannose and glucose treatment. We have added the data in (Figures 1(b) and 1(c)). We also found that D-mannose-pretreated hPDLSCs had no difference compared with the glucose-pretreated group on osteogenic differentiation and adipogenic differentiation potentials (Figures 1(d)–1(i)). Then we cocultured mannose- or glucose-pretreated hPDLSCs with T cells, and the results showed that mannose-pretreated PDLSCs (M-hPDLSCs) had more inhibitory ability to proliferate T cells than G-hPDLSCs (Figures 1(j) and 1(k)).

3.2. More Regulatory T Cells Were Generated When Cocultured with D-Mannose-Pretreated PDLSCs. To investigate how D-mannose affects hPDLSC immunomodulation function, T cells were cocultured with M-hPDLSCs or G-hPDLSCs. No difference was found in PGE2, TGFβ1, Nos2, and IDO1 between both groups (Figures 2(a)–2(d)). However, more FoxP3+ T cells could be found in the T + M-hPDLSCs coculture system, suggesting that M-hPDLSCs induced more T cells differentiated to Tregs (Figures 2(e) and 2(f)). Furthermore, less Th1 could be found in the M-hPDLSC coculture system (Figures 2(g) and 2(h)) compared with G-hPDLSCs and there was no significant difference in Th17 (Figures 2(g) and 2(i)) or Th2 (Figures 2(j) and 2(k)) between these two groups.

3.3. D-Mannose-Pretreated hPDLSCs Secret Less IL-6 and Induced More Tregs. In order to know why the T cell M-hPDLSCs coculture system had more Tregs, we screened different cytokines (data not shown) and found that IL-6 was significantly lower in the T + M-hPDLSC coculture system. (Figure 3(a)). Interestingly, the number of Tregs increased
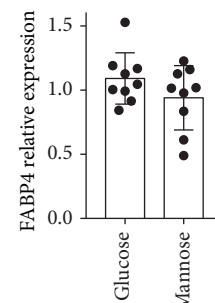
(a)

(b)

(c)

(d)

(e)

(f)

(g)

(h)

(i)
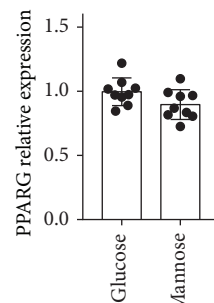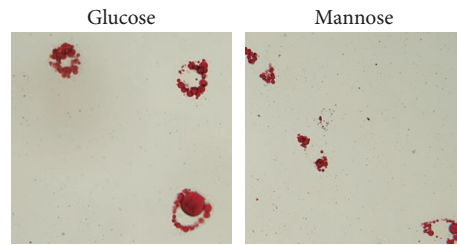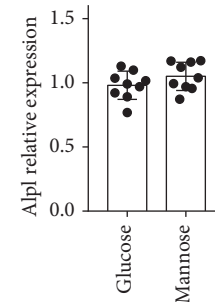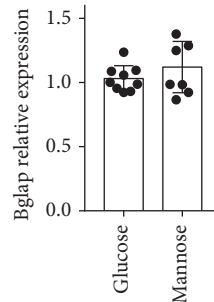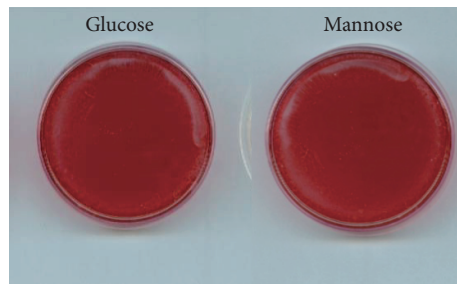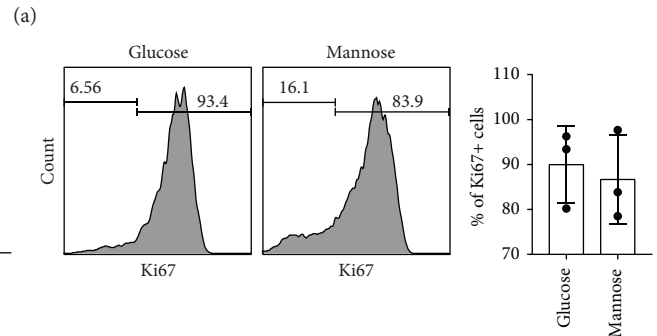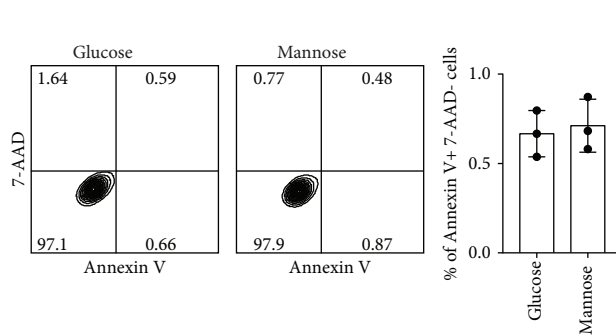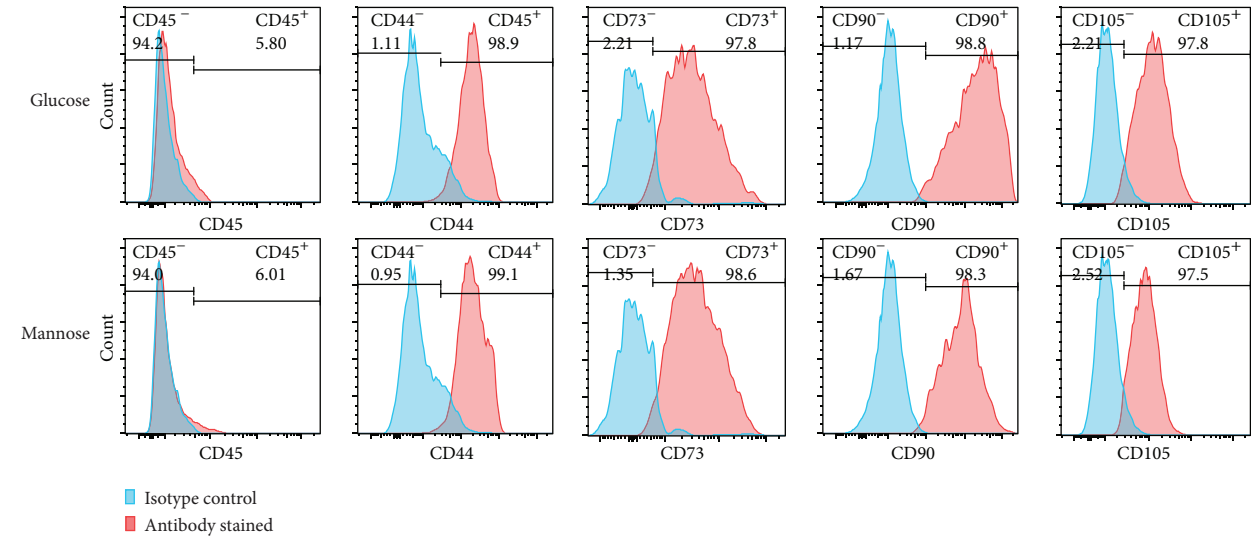
Figure 1: Continued.

(j)

(k)
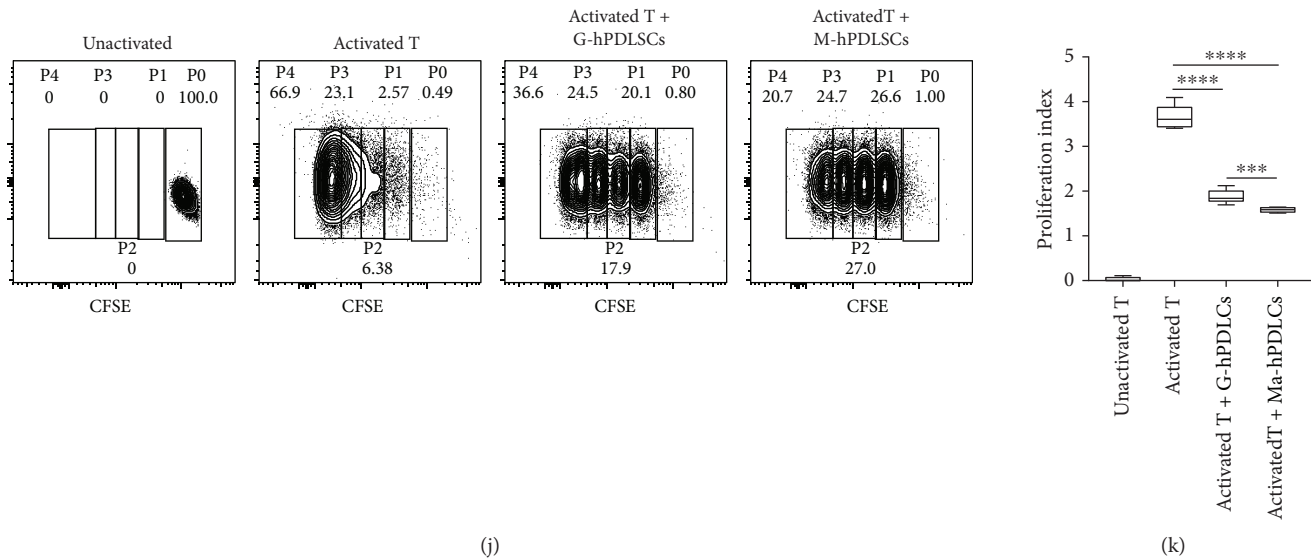
FIGURE 1: M-hPDLSCs have more inhibitory ability to proliferate T cells. (a) CD45, CD44, CD73, CD90, and CD105 have been detected by flow cytometry. There is no difference between M-hPDLSCs and G-hPDLSCs. (b, c) The apoptosis and proliferation of hPDLSCs between D-mannose and glucose treatment had no significant differences. (d–f) Osteogenic differentiation ability of M-hPDLSCs and G-PDLSCs has been detected. M-hPDLSCs and G-hPDLSCs were induced osteogenic differentiation. Alizarin red staining, BGLAP, and ALPL levels showed that M-PDLSCs have the same osteogenic differentiation ability as G-PDLSCs. (g–i) M-hPDLSCs and G-hPDLSCs were induced to adipogenic differentiation. Oil Red O staining, PPARG, and FABP4 levels showed that M-PDLSCs have the same adipogenic differentiation ability as G-hPDLSCs. (j, k) M-hPDLSCs and G-PDLSCs were cocultured with T cell to detect the effect of both on T cell proliferation. Both M-PDLSCs and G-PDLSCs could impair T cell proliferation. Compared with G-PDLSCs, M-hPDLSCs has more T cell proliferation inhibitory ability. Student's t test was used to analyze statistical significance. All error bars represent s.d. ($n = 9$). $^{***}P \leq 0.001$ and $^{****}P \leq 0.0001$.

after we neutralized IL-6 in T + G-hPDLSCs Figures 3(b) and 3(c) and decreased after we supply more IL-6 in the T + M-hPDLSC culture system (Figures 3(d) and 3(e)).

3.4. D-Mannose-Pretreated hPDLSCs Induced More Tregs In Vivo by Decreasing IL-6 Secretion. To verify previous results, we transplanted human T + G-hPDLSCs or human T + M-hPDLSC mixed cells with or without anti hIL-6 into nude mice. 2 days later, we extracted the spleen to examine T cells by flow cytometry. Without anti IL-6, the number of Tregs in the T + G-hPDLSCs group was much less than it in the T + M-hPDLSCs group. With anti hIL-6, the frequency of Tregs increased significantly in the T + G-hPDLSCs group (Figures 4(a) and 4(b)). These findings suggested that D-mannose could inhibit IL-6 in hPDLSCs to induce more Treg in vivo. On the other hand, more Th1 could be detected in the T + G-hPDLSCs group (Figures 4(c) and 4(d)) and IL-6 neutralizing could also reduce the number of Th17 (Figures 4(c) and 4(e)).

4. Discussion

Periodontitis is one of chronic infectious diseases destructing the alveolar bone and the supportive tissue of the teeth; it is also associated with a variety of systemic diseases such as diabetes, cardiovascular disease, and premature low birth weight [17–19]. The periodontal ligament comes from dental follicle, derived from neural crest cells, and PDLSCs play critical roles in periodontal ligament. PDLSCs could express the

stem cell markers such as CD105, CD166, STRO-1, and CD146/MUC18 and own the properties of self-renewal and multipotency differentiation to osteo-like cells, adipocytes [20, 21]. PDLSCs participated into the whole process of periodontal tissue regeneration.

PDLSC-mediated periodontal tissue regeneration has been proposed for the development of new periodontal tissue. It is reported that both autogeneic and allogeneic PDLSCs could reconstruct damaged periodontal tissues but the regeneration effects were not consistent [22, 23]. Although lots of studies confirm that MSCs, such as PDLSCs, are generally thought to be poorly immunogenic, PDLSC transplantation in periodontal tissue engineering would not eliminate host immune rejection against the donor cells. Recently, many studies reported that MSC-mediated bone regeneration could be regulated by the host immune system, especially T lymphocytes. Proliferation of allogeneic lymphocytes could be elicited in both differentiated and undifferentiated MSCs [24–27]. On the other hand, it is well known that MSCs own immunomodulatory properties both *in vitro* and *in vivo*. MSCs could suppress the proliferation and differentiation of Th1 and Th17 cells [28, 29], as well as their productions (IFNγ and interleukin 17), while MSCs could enhance Th2 cells and the production (IL-4) [30, 31]. So, the crosstalk between immune cells and PDLSCs decided the tissue regeneration effects.

Previous studies found that the immunomodulatory properties of PDLSCs partially depended on soluble factors, which could be produced by PDLSCs after being stimulated

(a)

(b)

(c)

(d)

(e)

(f)

(g)
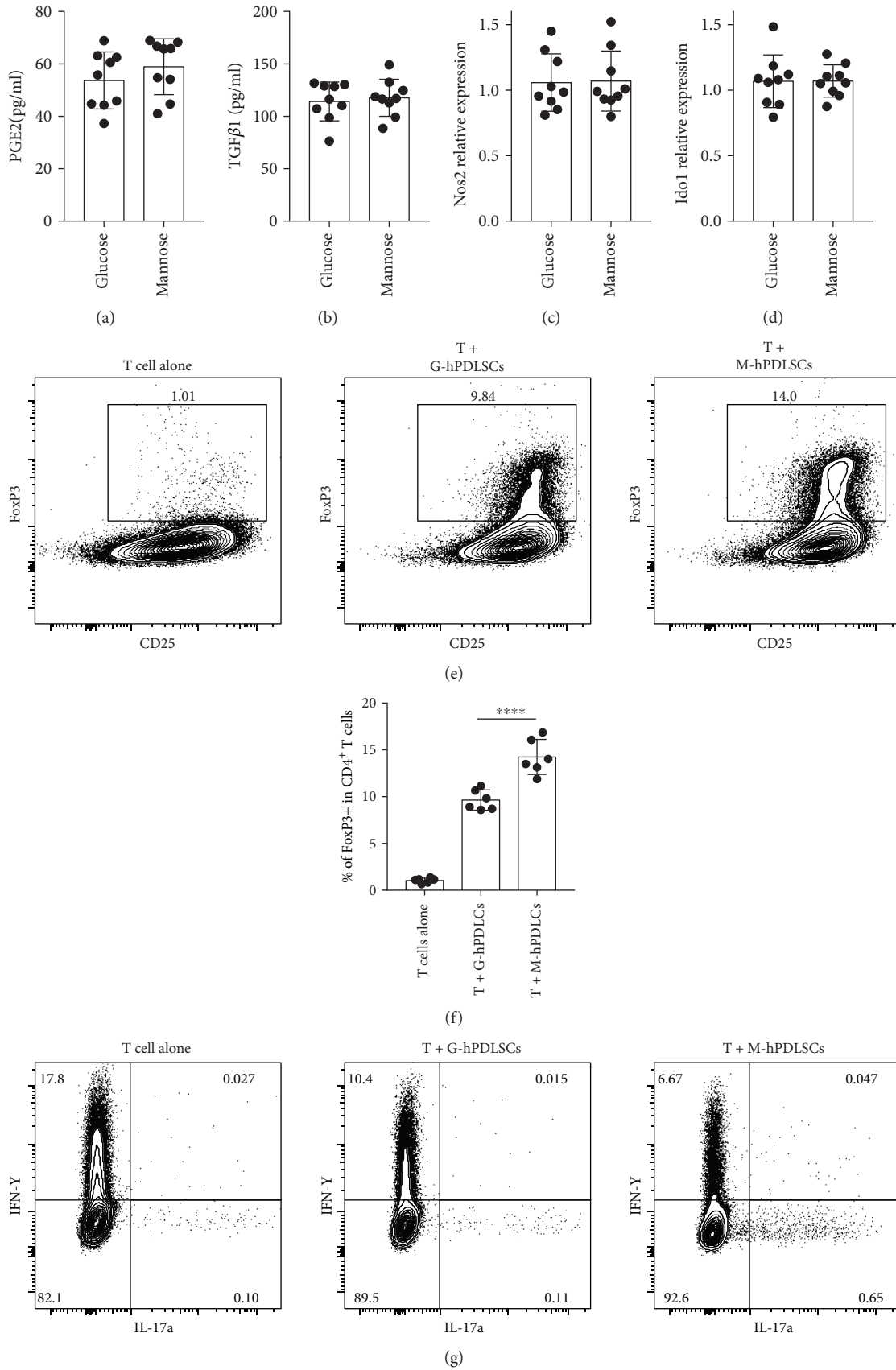
FIGURE 2: Continued.

(h)

(i)

(j)

(k)
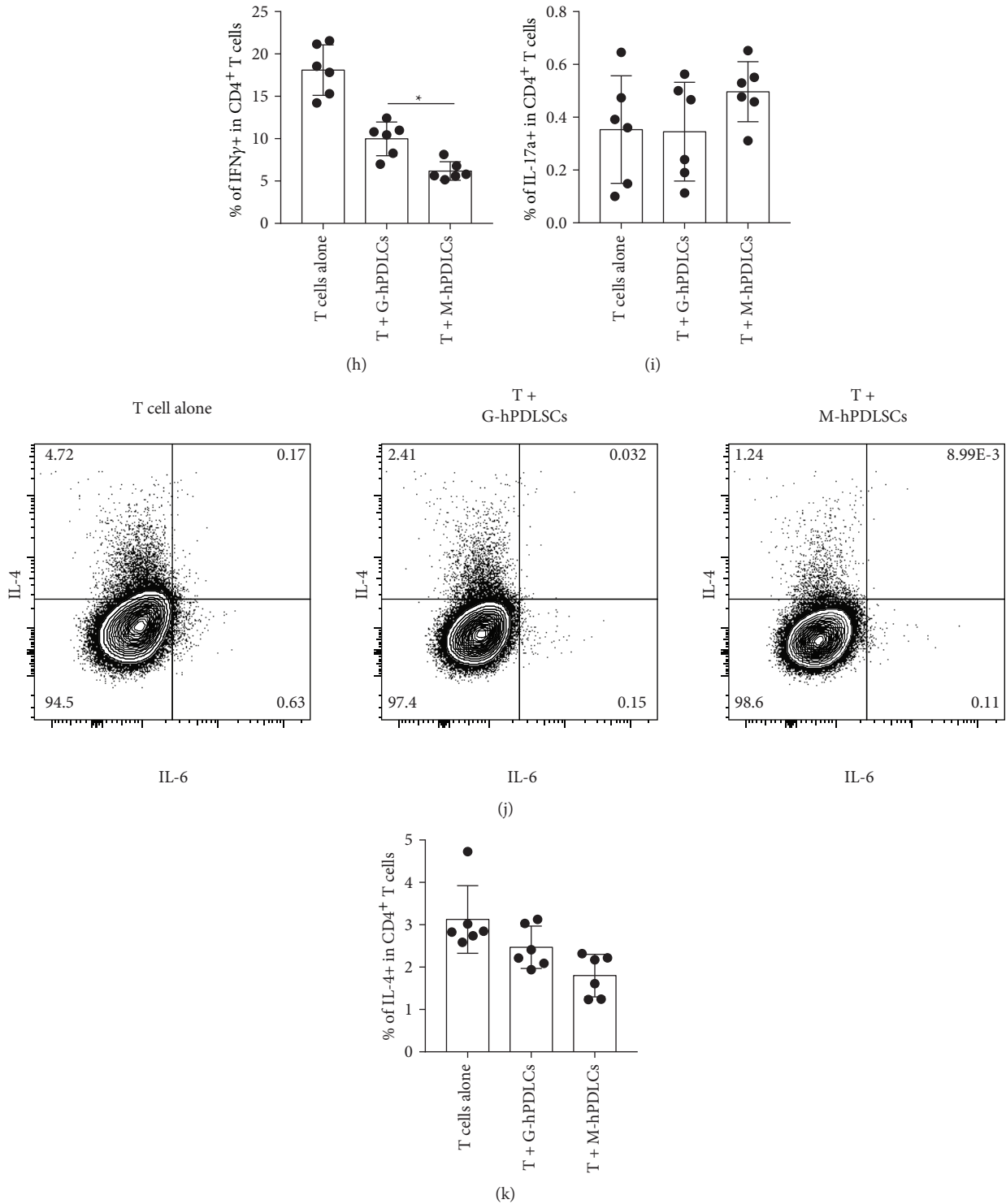
FIGURE 2: M-hPDLSCs induced more T cell differentiation into Tregs. (a, b) The results of ELISA showed that there was no difference in PGE2 and TGFβ1 between T + M-hPDLSCs and T + G-hPDLSCs. (c, d) RT-PCR results showed that there is no difference in Nos2 and Ido1 between T + M-hPDLSCs and T + G-hPDLSCs. (e, f) FoxP3 have been detected by flow cytometry. Compared with T + G-hPDLSCs, more FoxP3 was detected in T + M-hPDLSCs. (g, h) IFNγ and IL-17 have been detected by flow cytometry. More IFNγ could be detected in T + M-hPDLSCs. There was no difference in IL-17 between T + G-hPDLSCs and T + M-hPDLSCs. (j, k) There was no difference in IL-4 between T + G-hPDLSCs and T + M-hPDLSCs. Student's t-test was used to analyze statistical significance. All error bars represent s.d. ($n = 9$). $^{*}P \leq 0.05$ and $^{****}P \leq 0.0001$.

(a)

(b)

(c)

(d)

(e)
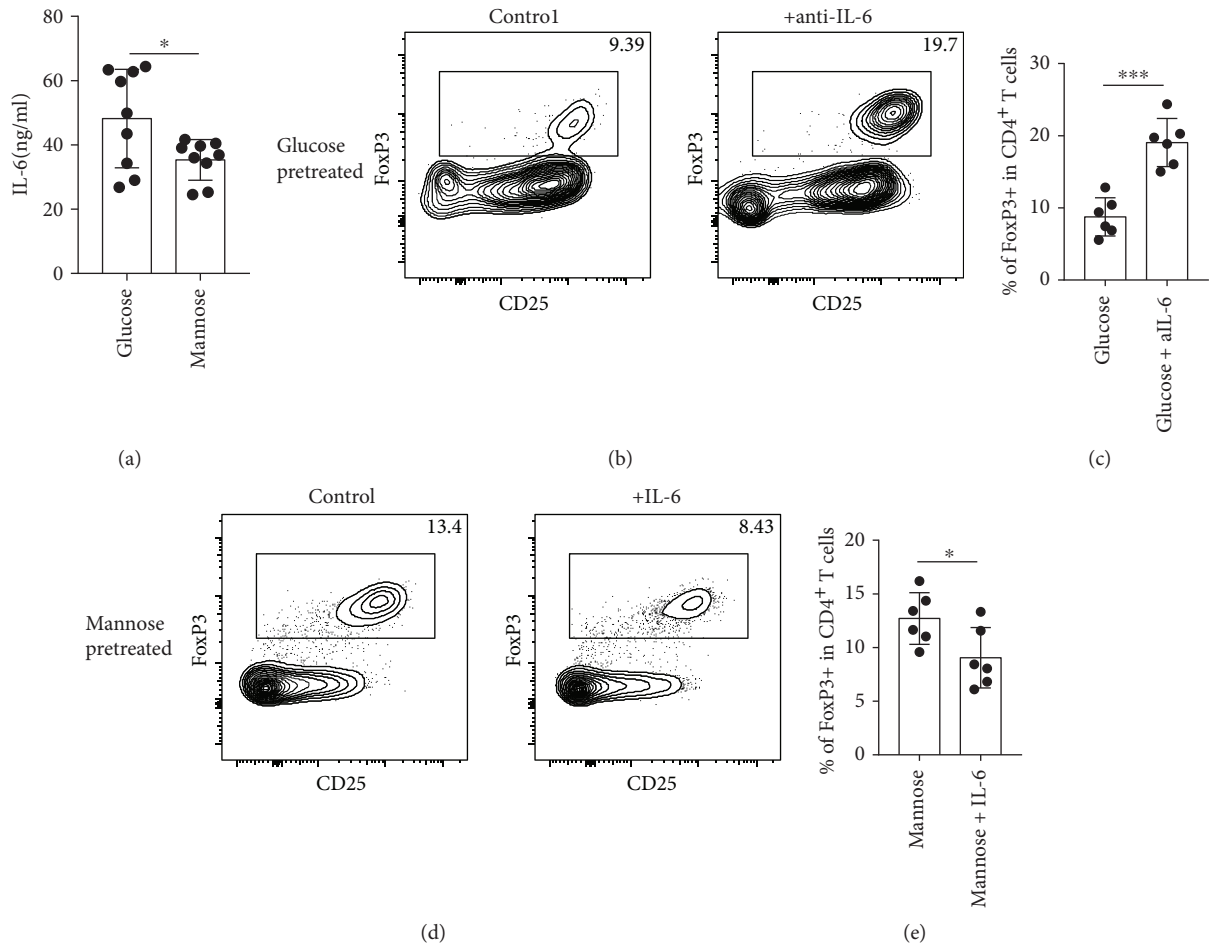
Figure 3: D-mannose inhibited IL-6 secretion of hPDLSCs to induce more T cell differentiation into Tregs. (a) Compared with T + G-hPDLSCs, less IL-6 could be detected in T + M-hPDLSCs. (b, c) Anti-IL-6 could increase the FoxP3 level in T + G-hPDLSCs. (d, e) Increased IL-6 could reduce the FoxP3 level in T + M-hPDLSCs. Student's t-test was used to analyze statistical significance. All error bars represent s.d. ($n = 9$). $^{*}P \le 0.05$ and $^{***}P \le 0.001$.

by activated PBMNCs. When PDLSCs were cocultured with activated PBMNCs, PDLSCs could produce more TGFβ1, indoleamine 2, 3-dioxygenase (IDO), and hepatocyte growth factor (HGF) [4]. hPDLSCs also could regulate the function of B cells. On the one hand, hPDLSCs could inhibit human B cell proliferation, differentiation, and chemotactic behavior. On the other hand, hPDLSCs could increase B cell viability by secreting interleukin-6. It was reported that the immunoregulatory capability of hPDLSCs to human B cells was through cell-to-cell contact manner, and programmed death-1 (PD-1) as well as its ligand (PD-L1) interaction was one of the critical ways in the process [32]. However, the interplay between host and transplanted PDLSCs during periodontal regeneration is unclear.

Recently, mannose was found as an important function in immune cell activity. D-Mannose could promote activation of the latent form of TGFβ and enhance naive CD4$^+$ T cell differentiation to Treg cells. However, the affection of D-mannose on the PDLSC characteristics was unclear. In this study, we found that D-mannose could affect hPDLSCs immunomodulation. hPDLSCs pretreated by D-mannose could inhibit T cell proliferation. As more results have shown,

hPDLSCs pretreated by D-mannose could induce more T cell differentiation into Tregs and IL-6 played a key role in this process. Less IL-6 has been detected in T + M-hPDLSCs. When we increased the IL-6 level, less Treg cells could be detected in T + M-hPDLSCs; and when IL-6 was reduced, the number of Treg cells was increased in T + G-hPDLSCs. As we know, TGFβ is an essential cytokine for inducing Foxp3+ Treg cells and enhanced TGFβ signaling is an underlying mechanism. In our current study, TGFβ levels between glucose- and D-mannose-pretreated groups had no significant difference.

IL-6 is a common cytokine and participates in almost every organ system's physiology. IL-6 could stimulate acute-phase responses, hematopoiesis, and immune reactions of the host to contribute to host defense. IL-6 plays an important role in the process of innate-acquired immune response. IL-6 could stimulate naïve CD4$^+$ T cell differentiation [33]. It has been reported that IL-6 combined with TGFβ is necessary for the process of naïve CD4$^+$ T cell differentiation into Th17 [34]. IL-6 also could inhibit Treg differentiation induced by TGFβ [35]. IL-6 plays a very important role in regulating Treg/Th17 balance. Breaking of the Treg/

(a)

(b)

(c)

(d)

(e)

(f)
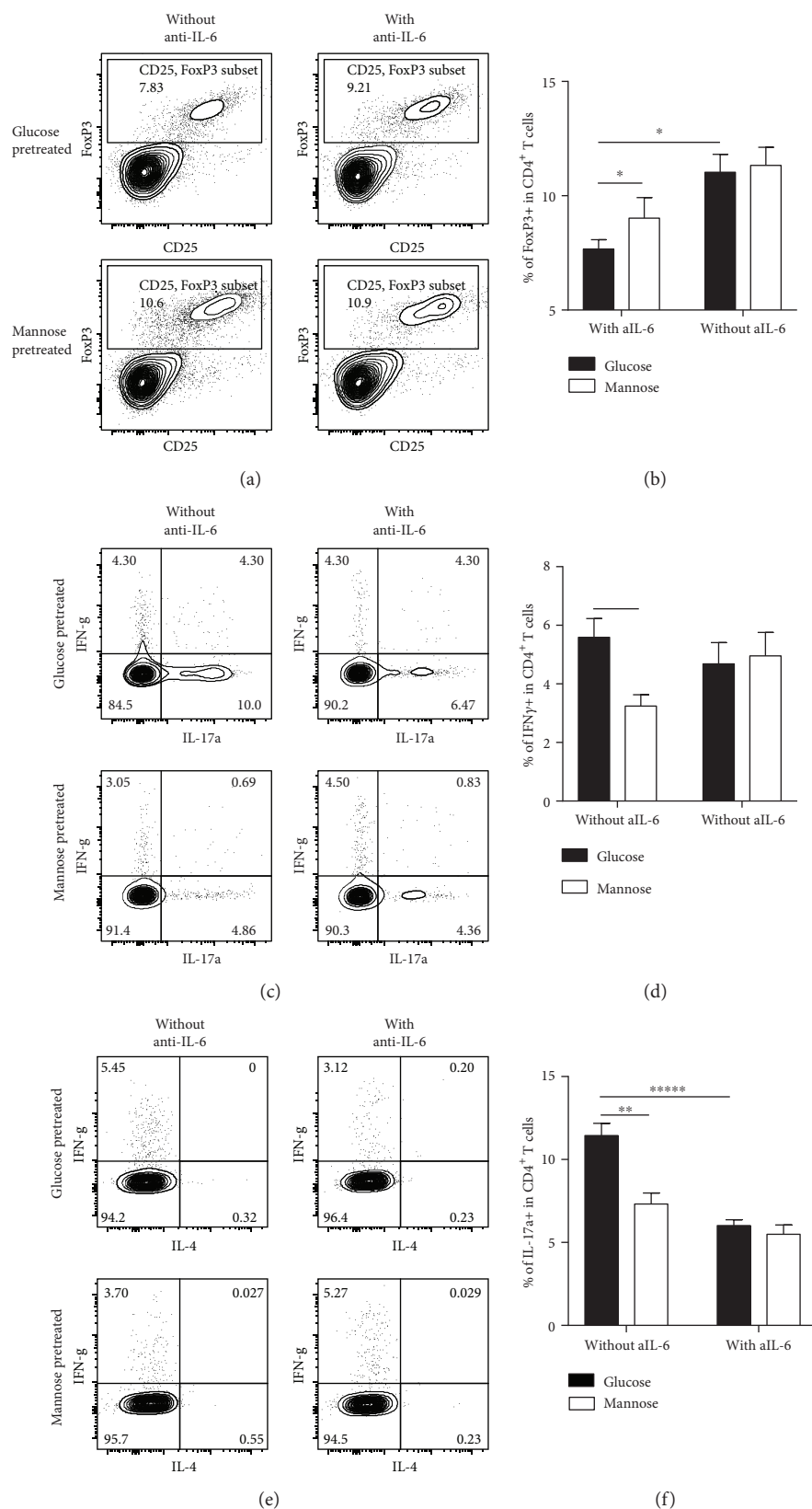
FIGURE 4: D-mannose inhibited IL-6 secretion of hPDLSCs to induce more T cell differentiation into Tregs in vivo. (a, b) IL-6 reduction could increase the number of FoxP3 and CD25 double positive cells in T + G-hPDLSC mixed cell-injected mice. (c, d) In vivo, compared with the T + G-hPDLSCs group, there was less Th1 cell in T + M-hPDLSC mixed cell-injected mice. (c, e) In vivo, IL-6 reduction could decrease the number of Th17 cell in T + G-hPDLSC mixed cell-injected mice. Student's t-test and one way ANOVA were used to analyze statistical significance. All error bars represent s.d. ($n = 9$). $*P \leq 0.05$, $**P \leq 0.01$, and $*****P \leq 0.00001$.

Th17 balance could be responsible for the collapse of immunological tolerance [36]. Further in vivo results also verified the important function of IL-6 in the process of D-mannose-regulating hPDLSC-stimulating Treg differentiation from T cells. It was reported that integrin $\alpha v \beta 8$ and reactive oxygen species (ROS) were essential for D-mannose-treated activation of TGFβ T cells. However, how the detailed mechanism of D-mannose mediated IL-6 inhibition remains unknown.

In conclusion, our present results showed a new function of D-mannose on hPDLSC immunomodulation, exploring the important role of IL-6 in the process of D-mannose-regulating hPDLSC immunomodulation. Our findings provide more information for the basic immunological mechanisms of hexose sugars and provided the possible clinical applications of D-mannose.

Data Availability

The data used to support the findings of this study are available from the corresponding author upon request.

Conflicts of Interest

The authors declare no conflicts of interest.

Authors' Contributions

Lijia Guo and Yanan Hou contributed equally to this work.

Acknowledgments

References

[1] B. L. Pihlstrom, B. S. Michalowicz, and N. W. Johnson, "Periodontal diseases," *Lancet*, vol. 366, no. 9499, pp. 1809–1820, 2005.

[2] H. Ikeda, Y. Sumita, M. Ikeda et al., "Engineering bone formation from human dental pulp- and periodontal ligament-derived cells," *Annals of Biomedical Engineering*, vol. 39, no. 1, pp. 26–34, 2011.

[3] N. Wada, D. Menicanin, S. Shi, P. M. Bartold, and S. Gronthos, "Immunomodulatory properties of human periodontal ligament stem cells," *Journal of Cellular Physiology*, vol. 219, no. 3, pp. 667–676, 2009.

[4] K. A. Cho, J. K. Lee, Y. H. Kim, M. Park, S. Y. Woo, and K. H. Ryu, "Mesenchymal stem cells ameliorate B-cell-mediated immune responses and increase IL-10-expressing regulatory B cells in an EBI3-dependent manner," *Cellular & Molecular Immunology*, 2017.

[5] D. Wang, S. P. Li, J. S. Fu, L. Bai, and L. Guo, "Resveratrol augments therapeutic efficiency of mouse bone marrow mesenchymal stem cell-based therapy in experimental autoimmune encephalomyelitis," *International Journal of Developmental Neuroscience*, vol. 49, pp. 60–66, 2016.

[6] R. A. Contreras, F. E. Figueroa, F. Djouad, and P. Luz-Crawford, "Mesenchymal stem cells regulate the innate and adaptive immune responses dampening arthritis progression," *Stem Cells International*, vol. 2016, 10 pages, 2016.

[7] R. Tang, F. Wei, L. Wei, S. Wang, and G. Ding, "Osteogenic differentiated periodontal ligament stem cells maintain their immunomodulatory capacity," *Journal of Tissue Engineering and Regenerative Medicine*, vol. 8, no. 3, pp. 226–232, 2014.

[8] D. Liu, J. Xu, O. Liu et al., "Mesenchymal stem cells derived from inflamed periodontal ligaments exhibit impaired immunomodulation," *Journal of Clinical Periodontology*, vol. 39, no. 12, pp. 1174–1182, 2012.

[9] A. D. Sawant, A. T. Abdelal, and D. G. Ahearn, "Purification and characterization of the anti-Candida toxin of Pichia anomala WC 65," *Antimicrobial Agents and Chemotherapy*, vol. 33, no. 1, pp. 48–52, 1989.

[10] B. Kranjčec, D. Papeš, and S. Altarac, "D-mannose powder for prophylaxis of recurrent urinary tract infections in women: a randomized clinical trial," *World Journal of Urology*, vol. 32, no. 1, pp. 79–84, 2014.

[11] S. Altarac and D. Papeš, "Use of D-mannose in prophylaxis of recurrent urinary tract infections (UTIs) in women," *BJU International*, vol. 113, no. 1, pp. 9-10, 2014.

[12] L. Domenici, M. Monti, C. Bracchi et al., "D-mannose: a promising support for acute urinary tract infections in women: a pilot study," *European Review for Medical and Pharmacological Sciences*, vol. 20, no. 13, pp. 2920–2925, 2016.

[13] J. R. Etchison and H. H. Freeze, "Enzymatic assay of D-mannose in serum," *Clinical Chemistry*, vol. 43, no. 3, pp. 533–538, 1997.

[14] A. Schneider, C. Thiel, J. Rindermann et al., "Successful prenatal mannose treatment for congenital disorder of glycosylation-Ia in mice," *Nature Medicine*, vol. 18, no. 1, pp. 71–73, 2011.

[15] G. Alton, M. Hasilik, R. Niehues et al., "Direct utilization of mannose for mammalian glycoprotein biosynthesis," *Glycobiology*, vol. 8, no. 3, pp. 285–295, 1998.

[16] D. Zhang, C. Chia, X. Jiao et al., "D-mannose induces regulatory T cells and suppresses immunopathology," *Nature Medicine*, vol. 23, no. 9, pp. 1036–1045, 2017.

[17] Z. Rutter-Locher, T. O. Smith, I. Giles, and N. Sofat, "Association between systemic lupus erythematosus and periodontitis: a systematic review and meta-analysis," *Frontiers in Immunology*, vol. 8, p. 1295, 2017.

[18] D. F. Kinane and G. J. Marshall, "Periodontal manifestations of systemic disease," *Australian Dental Journal*, vol. 46, no. 1, pp. 2–12, 2001.

[19] D. F. Kinane, P. G. Stathopoulou, and P. N. Papapanou, "Periodontal diseases," *Nature Reviews Disease Primers*, vol. 3, p. 17038, 2017.

[20] L. Huang, J. Liang, Y. Geng et al., "Directing adult human periodontal ligament-derived stem cells to retinal fate," *Investigative Ophthalmology & Visual Science*, vol. 54, no. 6, pp. 3965–3974, 2013.

[21] B. M. Seo, M. Miura, S. Gronthos et al., "Investigation of multipotent postnatal stem cells from human periodontal ligament," *Lancet*, vol. 364, no. 9429, pp. 149–155, 2004.

[22] Y. Liu, Y. Zheng, G. Ding et al., "Periodontal ligament stem cell-mediated treatment for periodontitis in miniature swine," *Stem Cells*, vol. 26, no. 4, pp. 1065–1073, 2008.

[23] G. Ding, Y. Liu, W. Wang et al., "Allogeneic periodontal ligament stem cell therapy for periodontitis in swine," *Stem Cells*, vol. 28, no. 10, pp. 1829–1838, 2010.

[24] C. D. Li, W. Y. Zhang, H. L. Li et al., "Mesenchymal stem cells derived from human placenta suppress allogeneic umbilical cord blood lymphocyte proliferation," *Cell Research*, vol. 15, no. 7, pp. 539–547, 2005.

[25] K. Le Blanc, C. Tammik, K. Rosendahl, E. Zetterberg, and O. Ringdén, "HLA expression and immunologic properties of differentiated and undifferentiated mesenchymal stem cells," *Experimental Hematology*, vol. 31, no. 10, pp. 890–896, 2003.

[26] F. Djouad, P. Plence, C. Bony et al., "Immunosuppressive effect of mesenchymal stem cells favors tumor growth in allogeneic animals," *Blood*, vol. 102, no. 10, pp. 3837–3844, 2003.

[27] Y. Liu, L. Wang, T. Kikuiri et al., "Mesenchymal stem cell-based tissue regeneration is governed by recipient T lymphocytes via IFN-γ and TNF-α," *Nature Medicine*, vol. 17, no. 12, pp. 1594–1601, 2011.

[28] M. Di Nicola, C. Carlo-Stella, M. Magni et al., "Human bone marrow stromal cells suppress T-lymphocyte proliferation induced by cellular or nonspecific mitogenic stimuli," *Blood*, vol. 99, no. 10, pp. 3838–3843, 2002.

[29] D. V. Krysko, G. Denecker, N. Festjens et al., "Macrophages use different internalization mechanisms to clear apoptotic and necrotic cells," *Cell Death and Differentiation*, vol. 13, no. 12, pp. 2011–2022, 2006.

[30] S. Aggarwal and M. F. Pittenger, "Human mesenchymal stem cells modulate allogeneic immune cell responses," *Blood*, vol. 105, no. 4, pp. 1815–1822, 2005.

[31] S. Zhao, R. Wehner, M. Bornhauser, R. Wassmuth, M. Bachmann, and M. Schmitz, "Immunomodulatory properties of mesenchymal stromal cells and their therapeutic consequences for immune-mediated disorders," *Stem Cells and Development*, vol. 19, no. 5, pp. 607–614, 2010.

[32] O. Liu, J. Xu, G. Ding et al., "Periodontal ligament stem cells regulate B lymphocyte function via programmed cell death protein 1," *Stem Cells*, vol. 31, no. 7, pp. 1371–1382, 2013.

[33] T. Tanaka, M. Narazaki, and T. Kishimoto, "IL-6 in inflammation, immunity, and disease," *Cold Spring Harbor Perspectives in Biology*, vol. 6, no. 10, article a016295, 2014.

[34] T. Korn, E. Bettelli, M. Oukka, and V. K. Kuchroo, "IL-17 and Th17 cells," *Annual Review of Immunology*, vol. 27, no. 1, pp. 485–517, 2009.

[35] E. Bettelli, Y. Carrier, W. Gao et al., "Reciprocal developmental pathways for the generation of pathogenic effector TH17 and regulatory T cells," *Nature*, vol. 441, no. 7090, pp. 235–238, 2006.

[36] A. Kimura and T. Kishimoto, "IL-6: regulator of Treg/Th17 balance," *European Journal of Immunology*, vol. 40, no. 7, pp. 1830–1835, 2010.

Research Article

Bone Morphogenetic Protein 6 Inhibits the Immunomodulatory Property of BMMSCs via Id1 in Sjögren's Syndrome

Yingying Su [iD],[1] **Yi Gu,**[2] **Ruiqing Wu** [iD],[1] **and Hao Wang** [iD][1]

[1]*Department of Stomatology, Beijing Tiantan Hospital, Capital Medical University, Beijing, China*
[2]*Department of Pediatrics, Beijing Chaoyang Hospital, Capital Medical University, Beijing, China*

Correspondence should be addressed to Hao Wang; 13701131933@139.com

Mesenchymal stem cells (MSCs) treatment has emerged as a promising approach for treating Sjögren's syndrome (SS). Impaired immunoregulatory activities of bone marrow mesenchymal stem cells (BMMSCs) are found in both SS patients and animal models, and the underlying mechanism is poorly understood. Increased expression of BMP6 is reported to be related to SS. The aim herein was to determine the effects of BMP6 on BMMSCs function. BMMSCs were isolated from SS patients and NOD mice and showed a high level of BMP6 expression. The effects of BMP6 on BMMSCs function were investigated using *in vitro* BMMSCs differentiation and *in vitro* and *in vivo* T cell proliferation and polarization assays. BMP6 increased osteogenic differentiation of BMMSCs and inhibited the immunomodulatory properties of BMMSCs. BMP6 enhanced T cell proliferation and Th1/Th17 differentiation in a T cell-BMMSC coculture system. Mechanistically, BMP6 downregulated PGE2 and upregulated IFN-gamma via Id1 (inhibitor of DNA-binding protein 1). Neutralizing BMP6 and knockdown of Id1 could restore the BMMSCs immunosuppressive function both *in vitro* and *in vivo*. The present results suggest a novel role of Id1 in BMP-mediated MSCs function, which may contribute to a better understanding of the mechanism of action of MSCs in treating autoimmune diseases.

1. Introduction

Sjögren's syndrome (SS) is a chronic and systemic autoimmune disease that mainly affects middle-aged women. SS is characterized by lymphocytic infiltration of salivary and lacrimal glands, leading to dry eyes and mouth [1, 2]. The etiology of SS is not fully delineated, and some genetic and environmental factors are suggested to be involved [1]. Current treatment strategies include punctual occlusion, artificial tears, use of saliva substitutes, and pharmacological therapy such as anti-inflammatory agents and immunosuppressive drugs [3]. However, these strategies are considered unable to modify the course of the disease and remain symptom-based [4].

In recent years, an accumulating body of evidence has supported the promising effects of mesenchymal stem cells (MSCs) in the treatment of autoimmune diseases. MSCs are multipotent stem cells characterized by colony-forming ability, multilineage differentiation, and self-renewal capacity [5]. Importantly, MSCs have an immunosuppressive capacity that enables their role in the treatment of a variety of immune diseases. Impaired immunoregulatory activities of MSCs are found in both SS patients and animal models [6]. MSCs treatment can suppress autoimmunity and restore salivary and lacrimal gland secretory function in both animal models and SS patients [6, 7]. However, the underlying mechanisms responsible for the impaired immunoregulatory function of MSCs in SS remain unclear. Elevated expression of bone morphogenetic protein 6 (BMP6) was recently reported in the epithelia of SS patients, and hypofunction and increased lymphocytic infiltration of the salivary gland were induced by the overexpression of BMP6 in normal mice [8]. Whether BMP6 is involved in the dysfunction of MSCs immunoregulatory capacity is unclear. In the present study, we found that

BMP6 impaired immunomodulatory properties of normal BMMSCs via Id1 and anti-BMP6 treatment, and blockage of Id1 rescued BMMSC function.

2. Materials and Methods

2.1. Animals. Female NOD/Ltj (referred to as NOD) mice were purchased from Beijing HFK Bioscience Co. and served as the SS animal model. OT-II transgenic mice, CD45.1 transgenic mice, and BALB/c mice were obtained from the Institute of Laboratory Animal Science, Chinese Academy of Medical Sciences. Animals were housed in a specific pathogen-free animal facility. All the animal procedures were approved by the Animal Care and Use Committee of Capital Medical University.

2.2. BMMSC Isolation and Culture. Total mRNA of BMMSCs from six SS patients and nine healthy volunteers was obtained from Drum Tower Hospital of Nanjing University Medical School. Mouse BMMSCs were isolated and cultured as described previously [9]. In brief, bone marrow cells were flashed out from bone cavity of femurs and tibias with 2% heat-inactivated fetal bovine serum (FBS; Gibco, USA) in phosphate-buffered saline (PBS; Hyclone, China). Single-cell suspension was obtained by passing bone marrow cells through a 70 mm cell strainer (BD Bioscience, USA), and cells were then seeded onto 100 mm culture dishes (Corning, USA). After culture for 14 days, colony-forming attached cells were passaged for further experiments. To confirm the BMMSC phenotypes, flow cytometric analysis was used to ensure that the cells were positive for CD90, CD105, and CD146 and negative for CD34 and CD45.

2.3. BMMSC In Vitro Differentiation Assays. To assess the osteogenic ability of BMMSCs, BMMSCs were cultured in osteoinductive medium containing 10 mM β-glycerophosphate (Sigma, USA), 100 μM L-ascorbic acid 2-phosphate (Sigma), and 10 nM dexamethasone (Sigma, USA). After 7 days of induction, the cells were stained with an alkaline phosphatase (ALP) staining kit (Sigma, USA) or collected for ALP activity testing using alkaline phosphatase yellow (pNPP) liquid ELISA substrate (Sigma, USA). For the adipo-induction, an adipogenic differentiation kit (Invitrogen, USA) was used. After 4 weeks of induction, the cells were stained with Oil Red O (Sigma, USA). After photographing, lipid droplets were then dissolved with 100% isopropanol, and OD value was measured at 492 nm. For real-time RT-PCR assays, total mRNA was isolated from BMMSCs after one week of induction. All assays were done in duplicate from at least three independent experiments.

2.4. Coculture of BMMSCs and T Cells and T Cell Proliferation Assay. Mouse lymph nodes were derived from BALB/c mice. T cells were isolated from lymphocytes using a naïve CD4$^+$ T Cell isolation kit (Miltenyi Biotec, German) following the manufacturer's instructions. The proliferation of CD4$^+$ T cells was detected using carboxyfluorescein succinimidyl ester (CFSE; Invitrogen, USA) labeling according to the manufacturer's instructions. To activate naïve CD4$^+$ T cells, naïve CD4$^+$ T cells were stimulated with immobilized 5 μg/ml anti-mouse CD3 antibody and 1 μg/ml anti-mouse CD28 (BD Pharmingen, USA) for 2-3 days. Activated CD4$^+$ T cells were then cocultured with BMMSCs from NOD or BALB/c mice at the ratio of 1:1 for 3 days. The proliferation of T cells was determined by loss of CFSE fluorescence.

2.5. Real-Time RT-PCR. Total RNA was isolated from BMMSCs using Trizol reagents (Invitrogen, USA), and cDNA was synthesized using the PrimeScript™ RT reagent kit (Takara, Dalian, China). Real-time RT-PCR was analyzed using SYBR *Premix Ex Taq*™ (Takara, Dalian, China). The following primers were used: *BMP6* (Hs01099594_m1, Invitrogen), *GAPDH* (Hs02786624_g1, Invitrogen), *Bmp6* (Mm01332882_m1, Invitrogen), *Gapdh* (Mm99999915_g1, Invitrogen), *Bglap* (Mm03413826_mH, Invitrogen), *Alp* (Mm01187117_m1, Invitrogen), *Pparg* (Mm00440940_m1, Invitrogen), *Fabp4* (Mm00445878_m1, Invitrogen), *Ido1* (Mm00492590_m1, Invitrogen), *Nos2* (Mm00440502_m1, Invitrogen), *TGFb1* (Mm00441727_g1, Invitrogen), *Id1* (Mm00775963_g1, Invitrogen), *Id2* (Mm00711781_m1, Invitrogen), *Id3* (Mm00492575_m1, Invitrogen), *Id4* (Mm 00499701_m1, Invitrogen), and *Cox2* (Mm03294838_g1, Invitrogen).

2.6. Enzyme-Linked Immunosorbent Assay (ELISA). Mice peripheral blood serum was collected from the retro-orbital plexus. The salivary gland was grounded with protein extraction reagent; the ground tissue was then centrifuged, and the supernatant was collected for cytokine measurement. The cytokine levels of IFN-gamma, IL-17, and PGE2 were measured by using a mouse ELISA kit (R&D Systems, USA) according to the manufacturer's instructions.

2.7. BMP6 Neutralization Antibody Treatment. BMP6 present in the T cell and BMMSCs coculture system was neutralized using an anti-mouse BMP6 antibody (R&D Systems, USA) at a concentration of 10 μg/ml/5×10^5 cells. Monoclonal rat IgG2B (R&D Systems, USA) served as a control.

2.8. siRNA Transfection. Id1 siRNA (sc-35632, Santa Cruz, USA) and the control scrambled sequence siRNA (sc-36869, Santa Cruz, USA) were transfected using Lipofectamine™ 2000 (Invitrogen, USA). Twenty-four or 48 hours after transfection, the cells or the supernatants were collected for further experiments.

2.9. In Vivo Immunosuppression. Naïve CD4$^+$ T cells were isolated and purified from the spleen and lymph nodes of OT-II transgenic mice. Approximately 1×10^6 CFSE-labeled naïve CD4$^+$ T cells and 5×10^5 BMMSCs were cotransferred, by tail vein injection, to recipient CD45.1 transgenic C57BL/6 mice. Four hours later, 25 μg OVA (Sigma-Aldrich, USA) emulsified in the complete Freund's adjuvant (CFA) was injected into the footpad of recipient mice. The popliteal lymph nodes of recipient mice were removed, and flow cytometry was carried out to measure CD45.2$^+$ T cell proliferation and differentiation.

2.10. Flow Cytometry. Cell suspensions from the spleen and lymph nodes were stained with fluorescence-conjugated anti-CD4, anti-IFN-gamma, and anti-IL-17 (BD Biosciences, USA) for analysis of $CD4^+$ T, Th1, and Th17 cells.

2.11. Statistical Analyses. The salivary flow rates were analyzed with repeated measurement, and other data were analyzed by Student's t-test or one-way analysis of variance analysis. All data are presented as the mean ± SEM (infiltrating area statistics) or SD (other data). Analysis was performed using SPSS 13.0 Software. A P value less than 0.05 was considered statistically significant.

3. Results

3.1. BMP6 Was Overexpressed in BMMSCs of SS Patients and NOD Mice and Regulated BMMSCs Differentiation. BMP6 was reported to be overexpressed in the epithelia of salivary glands of SS patients and NOD mice [8]. Here, we first investigated BMP6 expression in BMMSCs of SS patients and NOD mice. Real-time RT-PCR results indicated that the mRNA level of *Bmp6* is about five times higher in SS patient BMMSCs and eight times higher in NOD BMMSCs than in normal BMMSCs (Figures 1(a) and 1(b)). The elevated BMP6 protein in the supernatant of NOD BMMSCs culture medium when compared with BALB/c was also detected by ELISA (Figure 1(c)). We next treated BALB/c BMMSCs with BMP6 to examine its role in the differentiation of BMMSCs. BMMSCs cultured with BMP6 showed a significant increase in ALP activity relative to untreated controls (Figures 1(d) and 1(e)). This effect was confirmed by real-time RT-PCR analysis. Expression of osteogenic markers ALP and BGLAP (bone gamma-carboxyglutamate protein) showed a significant increase in BMP6-treated cells (Figures 1(h) and 1(i)). After adipogenic induction, BMMSCs treated with BMP6 showed no detectable difference in cellular lipid accumulation from control cells, as evidenced by Oil Red O staining (Figures 1(f) and 1(g)). Consistently, expression of adipogenesis-induced genes, including PPARγ (peroxisome proliferator-activated receptor-γ) and FABP4 (fatty acid-binding protein 4) demonstrated no significant changes in the presence of BMP6 (Figures 1(j) and 1(k)).

3.2. BMP6 Impaired Immunomodulatory Properties of BMMSCs by Downregulating PGE2 and Upregulating Th1 and Th17 Cells. To investigate whether BMP6 treatment impaired the immunomodulatory properties of BMMSCs, activated T cells were cocultured with BMMSCs for 48 hours. Proliferation of T cells was inhibited by normal BMMSCs from 87% to 51.2%, while BMP6-treated BMMSCs could only inhibit T cell proliferation by 62.4% (Figures 2(a) and 2(b)). Normal BMMSCs can regulate T cell differentiation into Th1 and Th17 cells, but BMP6 treatment significantly inhibited BMMSC-mediated downregulation of Th1 and Th17 cells (Figures 2(c)–2(e)). ELISA revealed that BMP6-treated BMMSCs showed a decreased concentration of PGE2 (Figure 2(f)) and increased concentration of IFN-gamma (Figure 2(g)) in the supernatants of the BMMSCs/T cell coculture system. Although no significant difference

was detected, there was an increasing trend in IL-17 concentration in the supernatants of the BMMSCs/T cell coculture system (Figure 2(h)). In contrast, BMP6-neutralizing antibodies (anti-BMP6) could significantly enhance the immunomodulatory properties of BMMSCs from NOD mice. T cells proliferated less when cocultured with anti-BMP6-pretreated NOD BMMSCs compared with the isotype antibody group (Figures 2(i) and 2(j)). Furthermore, anti-BMP6-pretreated NOD BMMSCs showed an increased effect on downregulating Th1 and Th17 cells (Figures 2(k)–2(m)). Consistently, anti-BMP6-pretreated NOD BMMSCs significantly increased the levels of T cell-produced PGE2 (Figure 2(n)) and decreased the levels of IFN-gamma (Figure 2(o)), but had no effect on IL-17 (Figure 2(p)) in the supernatants of the BMMSCs/T cell coculture system.

3.3. BMP6 Impaired Immunomodulatory Properties of BMMSCs and Downregulated PGE2 via Id1. Given that Ids are suggested to be the main targets of BMPs [10], we predicted that Ids were involved in BMP6-mediated impairment of BMMSCs immunoregulatory function. Real-time RT-PCR results demonstrated a higher level of *Id1* and *Id4* mRNA expression in BMMSCs derived from NOD mice compared with BALB/c mice (Figures 3(a), 3(c), and 3(d)), while *Id2* and *Id3* transcripts showed no significant difference between the two groups (Figure 3(a)). When treated with BMP6, BALB/c BMMSCs showed an increase in *Id1*, rather than in *Id2*, *Id3*, or *Id4* mRNA expression (Figures 3(b), 3(e), and 3(f)). To evaluate the effects of Id1 on BMMSC immunoregulatory function at the molecular level, we examined the expression levels of PGE2 and its synthase Cox2 in BMMSCs treated with or without BMP6 or Id1 siRNA. Knockdown of Id1 increased BMP6-induced Cox2 (Figure 3(g)) and PGE2 (Figure 3(h)) downregulation. In addition, Id1 knockdown dramatically increased the inhibitory capacity of BMMSCs on T cells proliferation reduced by BMP6 (Figure 3(i)). Our results suggested that Id1 mediated BMP6-induced impairment of BMMSC immunomodulatory properties by downregulating PGE2.

3.4. Knockdown of Id1 Rescued Impaired Immunosuppressive Capacity of BMMSCs Induced by BMP6 In Vivo. To further confirm the role of Id1 in BMP6-induced BMMSC immunosuppressive function impairment, we adoptively transferred OT-II T cells plus BMMSCs treated with or without BMP6 or Id1 siRNA to CD45.1 transgenic C57BL/6 mice. BMMSC treatment significantly reduced the number of proliferated $CD4^+$ T cells, while BMP6-treated BMMSCs showed no significant reduction. When Id1 was blocked by siRNA in BMP6-treated BMMSCs, a greater reduction in $CD4^+$ T cell number was observed (Figures 4(a) and 4(b)). The effects of Id1 on BMMSC-induced differentiation of T cells *in vivo* were also checked. A greater ratio of Th1 cells was detected in the presence of BMP6 compared with BMMSCs alone. Knockdown of Id1 significantly decreased the proportion of Th1 cells (Figures 4(c) and 4(d)). Together, these data showed that knockdown of Id1 could rescue impaired immunosuppressive capacity of BMMSCs induced by BMP6 *in vivo*.
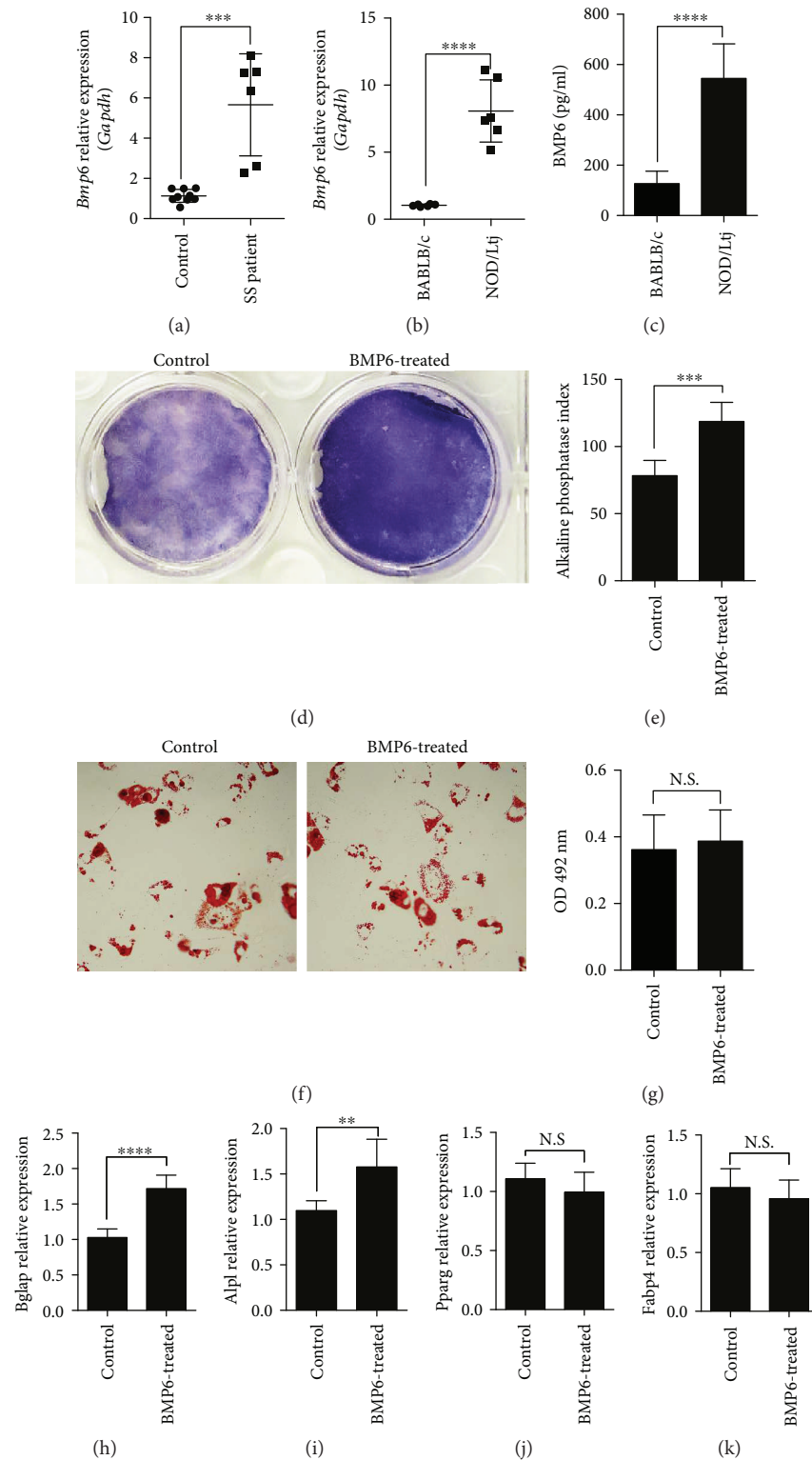
FIGURE 1: BMP6 was overexpressed in BMMSCs of SS patients and NOD mice and regulated BMMSCs differentiation. Real-time RT-PCR results indicated that the mRNA level of BMP6 is about five times higher in SS patient BMMSCs (a) and eight times higher in NOD BMMSCs (b) than in normal BMMSCs (***$P < 0.001$, ****$P < 0.0001$). (c) ELISA showed that the BMP6 protein level is higher in the supernatant of NOD BMMSCs culture medium compared with BALB/c (****$P < 0.0001$). (d, e) BMP6-treated BMMSCs showed a significant increase in ALP activity compared to untreated controls (***$P < 0.001$). Real-time RT-PCR analysis demonstrated elevated expression of BGLAP mRNA (h) and ALP mRNA (i) in BMP6-treated cells (**$P < 0.01$, ****$P < 0.0001$). (f, g) Oil Red O staining showed that BMP6 has no effect on cellular lipid accumulation in BMMSCs. Real-time RT-PCR results revealed that BMP6 do not increase the expression of PPARγ mRNA (j) and FABP4 mRNA (k). N.S.: no significant difference.

(a)

(b)

(c)

(d)

(e)

(f)

(g)

(h)

(i)

(j)

(k)

(l)

(m)

(n)

(o)

(p)
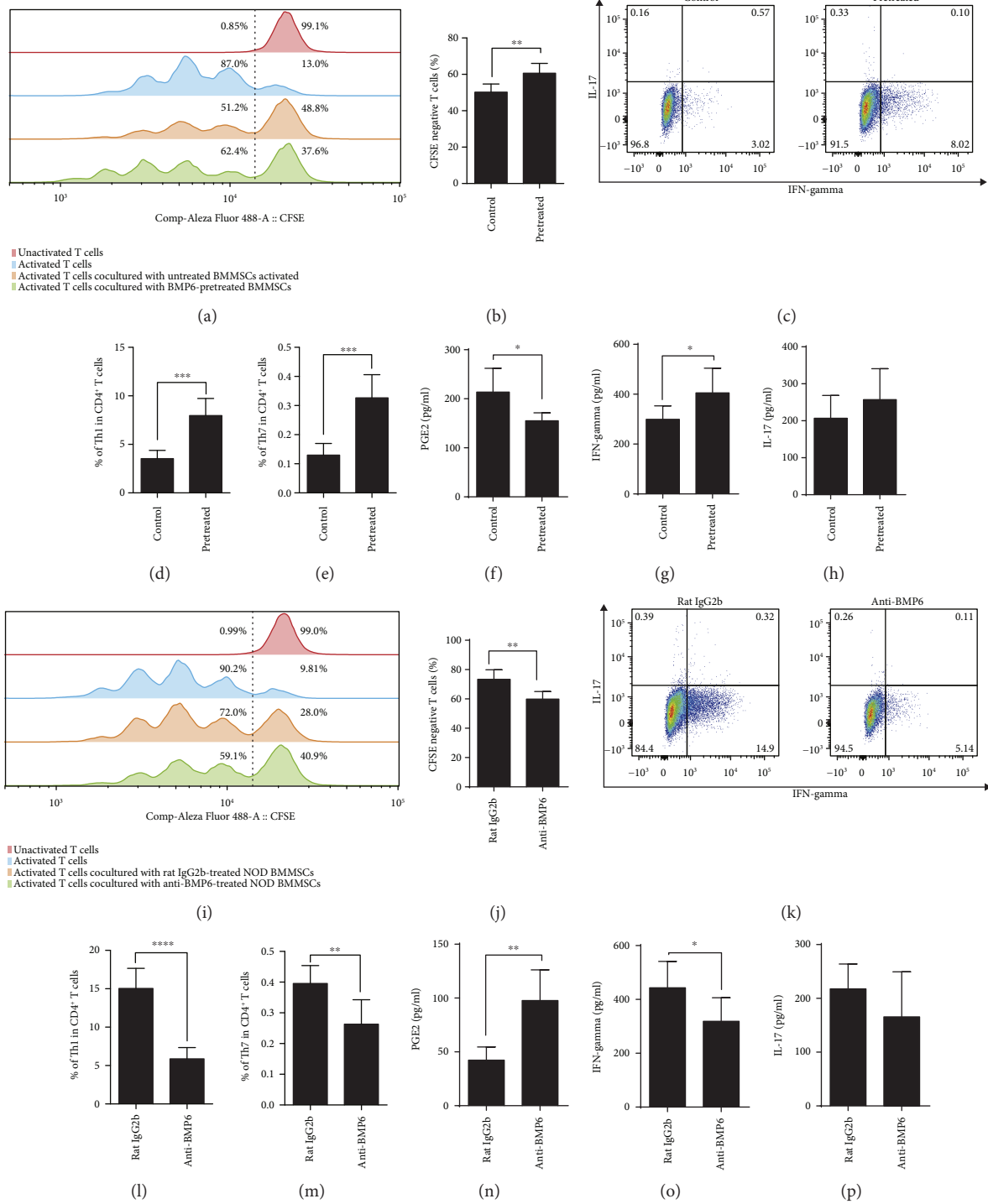
FIGURE 2: BMP6 impaired the immunomodulatory properties of BMMSCs by downregulating PGE2 and upregulating Th1 and Th17 cells. (a, b) CFSE assays showed T cells proliferation was inhibited by BMMSCs, and this effect could be attenuated by BMP6 ($^{**}P < 0.01$). (c, d, e) Flow cytometric analysis indicated that BMP6 significantly inhibited BMMSC-mediated downregulation of Th1 and Th17 cells ($^{***}P < 0.001$). ELISA assays revealed that BMP6-treated BMMSCs showed a decreased concentration of PGE2 (f) and increased concentration of IFN-gamma (g) in the supernatants of the BMMSCs/T cell coculture system ($^{*}P < 0.05$). (h) Although no significant difference was detected, there was an increasing trend in IL-17 concentration in the supernatants of the BMMSCs/T cell coculture system (i, j). CFSE assays showed that T cells proliferated less when cocultured with anti-BMP6-pretreated NOD BMMSCs compared with the isotype antibody group ($^{**}P < 0.01$). (k, l, m) Flow cytometric analysis showed that anti-BMP6-treated NOD BMMSCs exert an effect on downregulating Th1 and Th17 cells ($^{**}P < 0.01$, $^{****}P < 0.0001$). ELISA assays revealed that anti-BMP6-pretreated NOD BMMSCs significantly increased the levels of PGE2 (n) and decreased the levels of IFN-gamma (o) but had no effect on IL-17 (p) in the supernatants of the BMMSCs/T cell coculture system ($^{*}P < 0.05$, $^{**}P < 0.01$).

(a)

(b)

(c)

(d)

(e)

(f)

(g)

(h)

(i)
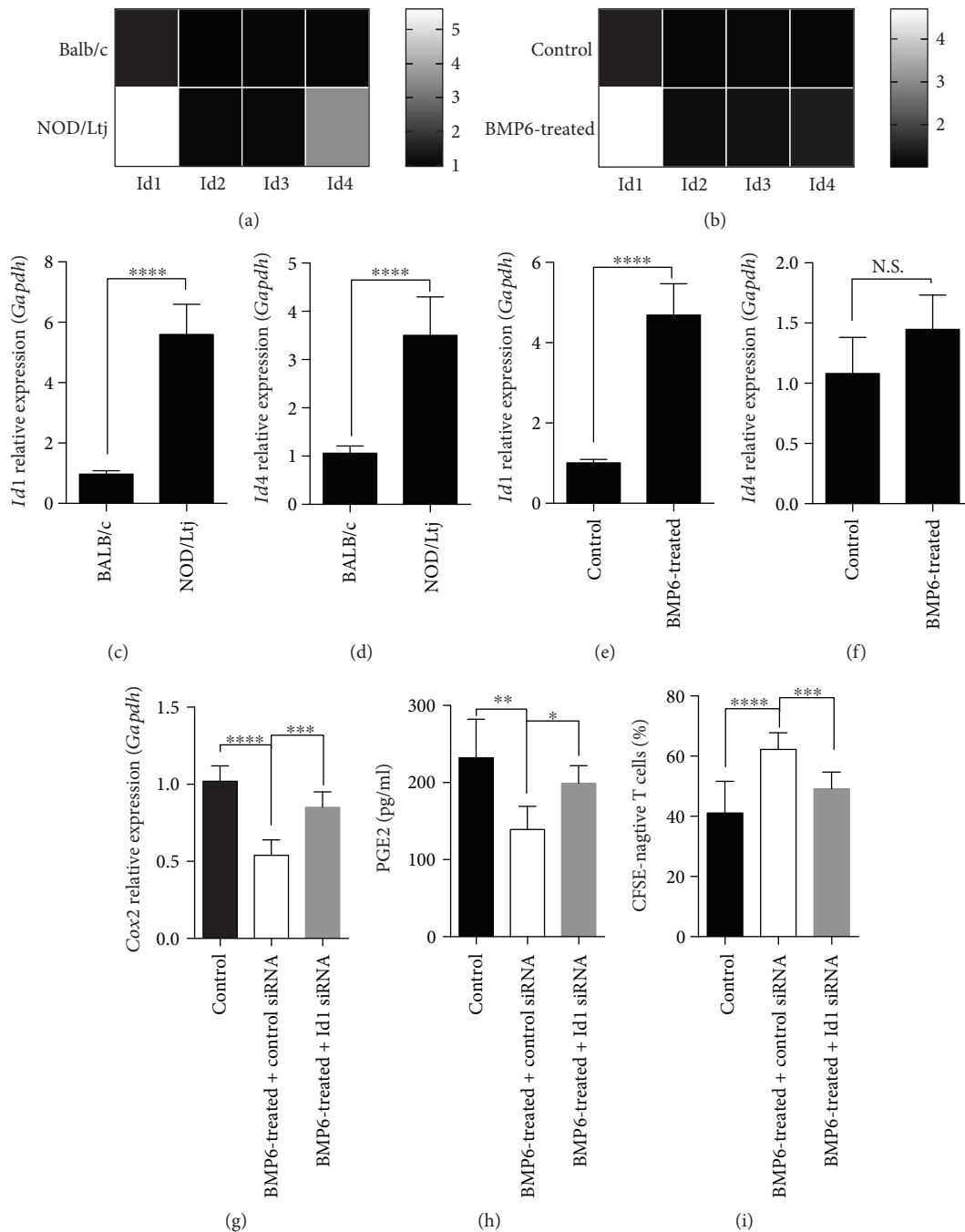
FIGURE 3: BMP6 impaired immunomodulatory properties of BMMSCs and downregulated PGE2 via Id1. (a, c, d) Real-time RT-PCR results demonstrated a higher level of Id1 and Id4 mRNA expression in BMMSCs derived from NOD mice compared with BALB/c, while Id2 and Id3 transcripts showed no significant difference between two groups (a) (****$P < 0.0001$). (b, e, f) BMP6-treated BALB/c BMMSCs showed an increase in Id1, rather than in Id2, Id3, or Id4 mRNA expression (****$P < 0.0001$) Knockdown of Id1 increased BMP6-induced Cox2 (g) and PGE2 (h) downregulation, as evidenced by real-time RT-PCR and ELISA, respectively. (*$P < 0.05$, **$P < 0.01$, ***$P < 0.001$, ****$P < 0.0001$). (i) CFSE assays indicated that BMP6 inhibited downregulation of T cells proliferation mediated by BMMSCs, while Id1 knockdown attenuated this effect (***$P < 0.001$, ****$P < 0.0001$). N.S.: no significant difference.

4. Discussion

MSCs have been known to have immunoregulatory functions for decades [11–16], and it was reported that MSCs from many autoimmune disease patients, including those with SS, have deficient immunoregulatory functions and

biological properties [6, 17, 18], which was one of the critical mechanisms for "MSCs therapy". In the present study, we found that the differentiation potentials and immunoregulatory activities of BMMSCs are impaired in SS patients and disease mice. BMP6 was expressed at a higher level in BMMSCs derived from SS patients as well as NOD mice

(a)

(b)

(c)

(d)
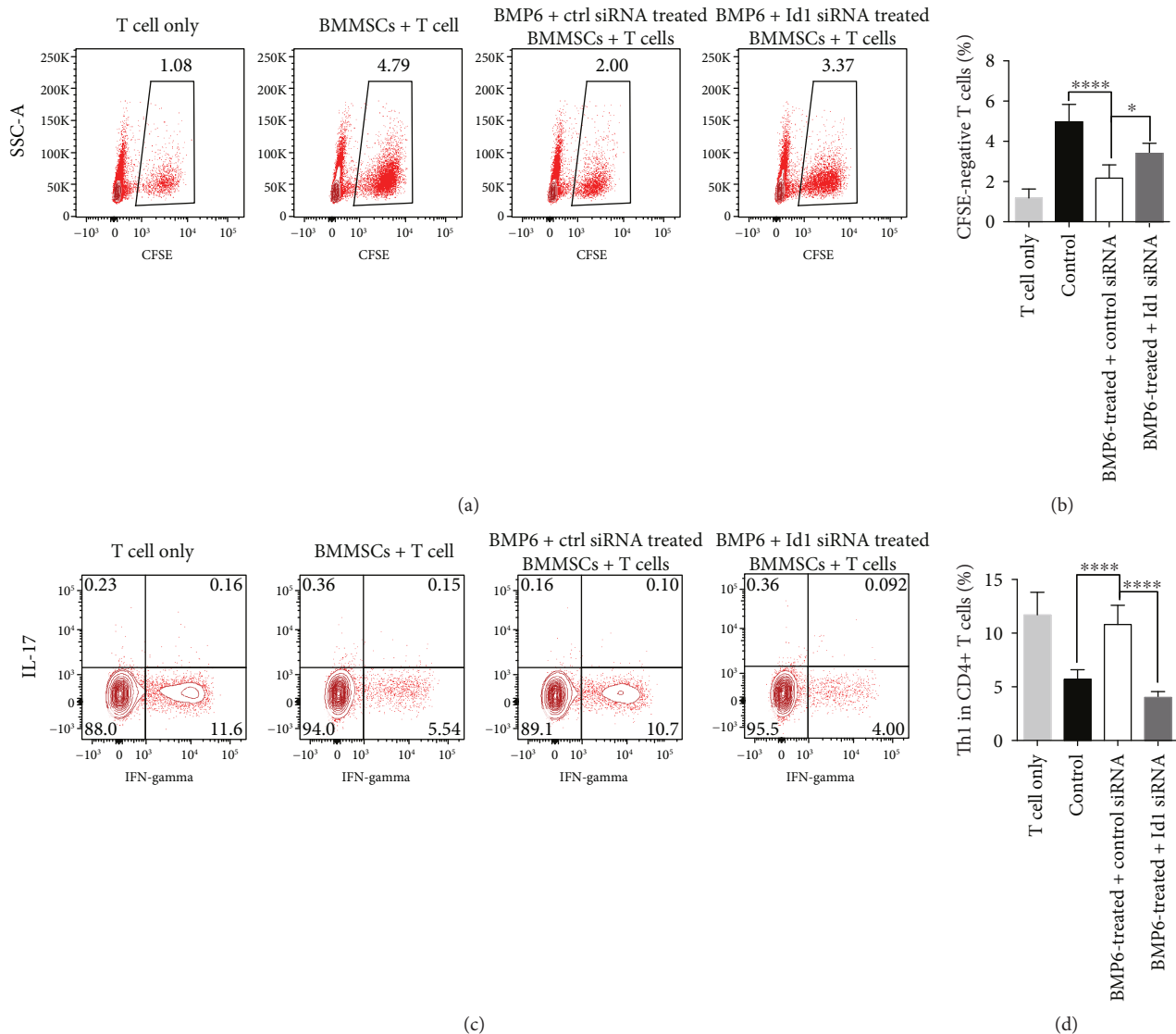
FIGURE 4: Knockdown of Id1 rescued impaired immunosuppressive capacity of BMMSCs induced by BMP6 *in vivo*. (a, b) BMMSCs treatment significantly reduced the number of CD4^{+} T cells, while BMP6-treated BMMSCs showed no significant reduction. When Id1 was blocked by siRNA in BMP6-treated BMMSCs, a greater reduction in CD4^{+} T cells number was observed (*$P < 0.05$, ****$P < 0.0001$). (c, d) A greater ratio of Th1 cells were detected in the presence of BMP6 compared with BMMSCs alone. Knockdown of Id1 significantly decreased the proportion of Th1 cells. (****$P < 0.0001$).

and regulated BMMSCs function, especially the immunomodulatory properties via Id1. Neutralizing the BMP6 and knockdown Id1 significantly restored the BMMSCs function both *in vitro* and *in vivo*.

BMP6 was reported to be highly expressed in the epithelia of the salivary gland in patients with SS, and overexpression of BMP6 locally could induce loss of cellular water permeability and salivary gland hypofunction [2, 8]. However, proinflammatory cytokines or autoantibodies associated with SS after BMP6 overexpression locally were not found, which suggests that the loss of salivary gland activity in SS patients may result from changes in epithelial function by BMP6 expression rather than the direct immune response [8]. In the present study, for the first time, we found that BMP6 was also highly expressed in BMMSCs from SS patients and animal models. BMP6 treatment can improve

the osteogenic differentiation but impair the immunoregulatory function of BMMSCs. These results indicate that BMP6 could not lead to the dysfunction of the salivary gland but may influence the tissue repair and immune functions of systemic MSCs, which may collectively contribute to the inflammation of the salivary gland in SS.

BMMSCs from NOD mice were reported to have lower osteogenic and adipogenic differentiation capacity [6]. BMP6 is one of the most potent regulators of osteoblast differentiation [19]. We showed here, BMP6 was highly expressed in BMMSCs from SS patients and disease mice, and enhanced osteogenic fate determination was observed in BMP6-treated BMMSCs. These findings suggested that high level of BMP6 in BMMSCs from SS patients and NOD mice may not contribute to the decreased osteogenic potential of BMMSCs.

A predominance of Th1 and Th17 cell responses and their products, notably INF-gamma and IL-17, in primary SS patients has been reported [20, 21]. MSCs can regulate the adaptive and innate immune systems by suppression of T cells and maturation of dendritic cells, reducing B-cell activation and proliferation, inhibiting proliferation and cytotoxicity of natural killer (NK) cells, and promoting the generation of regulatory T cells [22]. We found that BMMSCs significantly reduced the frequency of Th1 and Th17 cells in T cells-BMMSCs coculture system. BMP6 abolished this suppressive effect, demonstrating that BMMSCs suppressed Th1 and Th17 responses in SS.

Several soluble factors, including prostaglandin E2 (PGE2) [12], indoleamine-pyrrole 2,3-dioxygenase (IDO) [11], nitric oxide (NO) [23], and transforming growth factor-β1 (TGF-β1) [22], have been proposed to mediate this immunosuppressive effect. In the present study, we found that BMP6 can only downregulate the expression of PGE2 in BMMSCs. It has been known for over 30 years that PGE2 has a largely immunosuppressive role in T-cell activation and proliferation [24]. Here, we reported that BMP6 decreased PGE2 secretion in a T cells-BMMSCs coculture system and promoted T cell proliferation and Th1 and Th17 polarization, indicating that PGE2 is involved in the BMP6-induced impaired immunomodulatory ability of BMMSCs.

Id1 is a negative regulator of basic helix-loop-helix (bHLH) protein [25]. It was reported that Id1 promoter is a BMP-responsive element [26]. It is one of the most critical targets of BMPs and is responsible for various biological activities of BMPs [27–29]. Ids are also suggested to be involved in the determination of function of MSCs induced by BMPs [10]. We found that BMMSCs derived from the SS mice model expressed a higher level of BMP6 and Id1, and treatment with BMP6 upregulated Id1 gene expression in BMMSCs derived from control mice. Further experiments demonstrated that Id1 was involved in BMP6-induced impairment of BMMSC immunomodulatory function. Id1 was found to inhibit PGE2 secretion and stimulate T cell proliferation and Th1/Th17 differentiation in a T cells-BMMSCs coculture system. These data reveal a novel role of Id1 in BMP-mediated MSC function.

5. Conclusion

In conclusion, BMP6 was found to be expressed at a higher level in BMMSCs derived from SS patients as well as in animal models. BMP6 inhibited the immunomodulatory properties of BMMSCs by promoting T cell proliferation and Th1/Th17 differentiation. Mechanistically, BMP6 downregulated PGE2 and upregulated IFN-gamma via Id1. Neutralizing the BMP6 and knockdown Id1 could restore the BMMSC immunosuppressive function both *in vitro* and *in vivo*.

Data Availability

The data used to support the findings of this study are available from the corresponding author upon request.

Conflicts of Interest

The authors declare that there is no conflict of interest regarding the publication of this paper.

Authors' Contributions

Yingying Su and Yi Gu contributed equally to this work as first authors.

Acknowledgments

Supplementary Materials

Supplementary Figure 1: Surface makers of BMMSCs. (*Supplementary Materials*)

References

[1] R. I. Fox, "Sjögren's syndrome," *The Lancet*, vol. 366, no. 9482, pp. 321–331, 2005.

[2] Z. Lai, H. Yin, J. Cabrera-Pérez et al., "Aquaporin gene therapy corrects Sjögren's syndrome phenotype in mice," *Proceedings of the National Academy of Sciences of the United States of America*, vol. 113, no. 20, pp. 5694–5699, 2016.

[3] G. E. Katsifis, N. M. Moutsopoulos, and S. M. Wahl, "T lymphocytes in Sjögren's syndrome: contributors to and regulators of pathophysiology," *Clinical Reviews in Allergy & Immunology*, vol. 32, no. 3, pp. 252–264, 2007.

[4] C. P. Mavragani, N. M. Moutsopoulos, and H. M. Moutsopoulos, "The management of Sjögren's syndrome," *Nature Clinical Practice Rheumatology*, vol. 2, no. 5, pp. 252–261, 2006.

[5] P. S. Frenette, S. Pinho, D. Lucas, and C. Scheiermann, "Mesenchymal stem cell: keystone of the hematopoietic stem cell niche and a stepping-stone for regenerative medicine," *Annual Review of Immunology*, vol. 31, no. 1, pp. 285–316, 2013.

[6] J. Xu, D. Wang, D. Liu et al., "Allogeneic mesenchymal stem cell treatment alleviates experimental and clinical Sjögren syndrome," *Blood*, vol. 120, no. 15, pp. 3142–3151, 2012.

[7] H. S. Aluri, M. Samizadeh, M. C. Edman et al., "Delivery of bone marrow-derived mesenchymal stem cells improves tear production in a mouse model of Sjögren's syndrome," *Stem Cells International*, vol. 2017, Article ID 3134543, 10 pages, 2017.

[8] H. Yin, J. Cabrera-Perez, Z. Lai et al., "Association of bone morphogenetic protein 6 with exocrine gland dysfunction in patients with Sjögren's syndrome and in mice," *Arthritis & Rheumatism*, vol. 65, no. 12, pp. 3228–3238, 2013.

[9] Y. Liu, R. Yang, and S. Shi, "Systemic infusion of mesenchymal stem cells improves cell-based bone regeneration via upregulation of regulatory T cells," *Tissue Engineering Part A*, vol. 21, no. 3-4, pp. 498–509, 2015.

[10] K. Miyazono and K. Miyazawa, "Id: a target of BMP signaling," *Science Signaling*, vol. 2002, no. 151, article pe40, 2002.

[11] R. Meisel, A. Zibert, M. Laryea, U. Gobel, W. Daubener, and D. Dilloo, "Human bone marrow stromal cells inhibit allogeneic T-cell responses by indoleamine 2,3-dioxygenase–mediated tryptophan degradation," *Blood*, vol. 103, no. 12, pp. 4619–4621, 2004.

[12] S. Aggarwal and M. F. Pittenger, "Human mesenchymal stem cells modulate allogeneic immune cell responses," *Blood*, vol. 105, no. 4, pp. 1815–1822, 2005.

[13] X. Chen, M. A. Armstrong, and G. Li, "Mesenchymal stem cells in immunoregulation," *Immunology & Cell Biology*, vol. 84, no. 5, pp. 413–421, 2006.

[14] M. E. Castro-Manrreza and J. J. Montesinos, "Immunoregulation by mesenchymal stem cells: biological aspects and clinical applications," *Journal of Immunology Research*, vol. 2015, Article ID 394917, 20 pages, 2015.

[15] L. Fan, Z. Yu, J. Li, X. Dang, and K. Wang, "Immunoregulation effects of bone marrow-derived mesenchymal stem cells in xenogeneic acellular nerve grafts transplant," *Cellular and Molecular Neurobiology*, vol. 34, no. 7, pp. 999–1010, 2014.

[16] F. Gao, S. M. Chiu, D. A. L. Motan et al., "Mesenchymal stem cells and immunomodulation: current status and future prospects," *Cell Death & Disease*, vol. 7, no. 1, article e2062, 2016.

[17] L. Sun, K. Akiyama, H. Zhang et al., "Mesenchymal stem cell transplantation reverses multi-organ dysfunction in systemic lupus erythematosus mice and humans," *Stem Cells*, vol. 27, no. 6, pp. 1421–1432, 2009.

[18] K. Akiyama, C. Chen, D. Wang et al., "Mesenchymal-stem-cell-induced immunoregulation involves FAS-ligand-/FAS-mediated T cell apoptosis," *Cell Stem Cell*, vol. 10, no. 5, pp. 544–555, 2012.

[19] M. S. Friedman, M. W. Long, and K. D. Hankenson, "Osteogenic differentiation of human mesenchymal stem cells is regulated by bone morphogenetic protein-6," *Journal of Cellular Biochemistry*, vol. 98, no. 3, pp. 538–554, 2006.

[20] Y. Ohyama, S. Nakamura, G. Matsuzaki et al., "Cytokine messenger RNA expression in the labial salivary glands of patients with Sjögren's syndrome," *Arthritis & Rheumatism*, vol. 39, no. 8, pp. 1376–1384, 1996.

[21] J. M. van Woerkom, A. A. Kruize, M. J. Wenting-van Wijk et al., "Salivary gland and peripheral blood T helper 1 and 2 cell activity in Sjögren's syndrome compared with non-Sjögren's sicca syndrome," *Annals of the Rheumatic Diseases*, vol. 64, no. 10, pp. 1474–1479, 2005.

[22] Y. Wang, X. Chen, W. Cao, and Y. Shi, "Plasticity of mesenchymal stem cells in immunomodulation: pathological and therapeutic implications," *Nature Immunology*, vol. 15, no. 11, pp. 1009–1016, 2014.

[23] G. Ren, L. Zhang, X. Zhao et al., "Mesenchymal stem cell-mediated immunosuppression occurs via concerted action of chemokines and nitric oxide," *Cell Stem Cell*, vol. 2, no. 2, pp. 141–150, 2008.

[24] V. Sreeramkumar, M. Fresno, and N. Cuesta, "Prostaglandin E_2 and T cells: friends or foes?," *Immunology & Cell Biology*, vol. 90, no. 6, pp. 579–586, 2012.

[25] R. Benezra, R. L. Davis, D. Lockshon, D. L. Turner, and H. Weintraub, "The protein Id: a negative regulator of helix-loop-helix DNA binding proteins," *Cell*, vol. 61, no. 1, pp. 49–59, 1990.

[26] O. Korchynskyi and P. ten Dijke, "Identification and functional characterization of distinct critically important bone morphogenetic protein-specific response elements in the Id1 promoter," *Journal of Biological Chemistry*, vol. 277, no. 7, pp. 4883–4891, 2002.

[27] Y. Ueki and T. A. Reh, "Activation of BMP-Smad1/5/8 signaling promotes survival of retinal ganglion cells after damage in vivo," *PLoS One*, vol. 7, no. 6, article e38690, 2012.

[28] F. Vinals and F. Ventura, "Myogenin protein stability is decreased by BMP-2 through a mechanism implicating Id1," *Journal of Biological Chemistry*, vol. 279, no. 44, pp. 45766–45772, 2004.

[29] J. Yang, X. Li, Y. Li et al., "Id proteins are critical downstream effectors of BMP signaling in human pulmonary arterial smooth muscle cells," *American Journal of Physiology-Lung Cellular and Molecular Physiology*, vol. 305, no. 4, pp. L312–L321, 2013.

Research Article

Effect of a Combination of Prednisone or Mycophenolate Mofetil and Mesenchymal Stem Cells on Lupus Symptoms in MRL.*Fas*^lpr Mice

Hong Kyung Lee,[1] Ki Hun Kim,[1] Hyung Sook Kim,[1] Ji Sung Kim,[1] Jae Hee Lee,[1] Ayoung Ji,[1] Kyung Suk Kim,[2] Tae Yong Lee,[2] In Young Chang,[2] Sang-Cheol Bae,[3] Jin Tae Hong,[1] Youngsoo Kim,[1] and Sang-Bae Han [ID][1]

[1]*College of Pharmacy, Chungbuk National University, Cheongju, 28160 Chungcheongbuk-do, Republic of Korea*
[2]*Corestem Inc., Seongnam, 13486 Gyeonggi-do, Republic of Korea*
[3]*Hanyang University Hospital for Rheumatic Diseases, Seoul 04763, Republic of Korea*

Correspondence should be addressed to Sang-Bae Han; shan@chungbuk.ac.kr

The combination of immunosuppressants and mesenchymal stem cells (MSCs) is a promising therapeutic strategy for systemic lupus erythematosus, since this approach reduces doses of immunosuppressants while maintaining the same therapeutic outcome. However, it is unavoidable for MSCs to be exposed to immunosuppressants. Here, we examined the combination effect of prednisone (PD) or mycophenolate mofetil (MMF) and MSCs. We showed that PD or MMF in combination with MSCs showed better therapeutic effect than single therapy in lupus-prone MRL.*Fas*^lpr mice, as assessed by using the following readouts: prolongation of survival, decrease in anti-dsDNA and total IgG levels in serum, decrease in cytokine gene expression in spleen cells, and decrease in inflammatory cell infiltration into the kidney. *In vitro*, immunosuppressants and MSCs inhibited T cell proliferation in a synergistic manner. However, immunosuppressants did not affect MSC viability and functions such as TGF-β1 and PGE$_2$ production, migration, and immunosuppressive capacity. In summary, our study demonstrates that a combination of immunosuppressants and MSCs is a good strategy to reduce the side effects of PD and MMF without the loss of therapeutic outcome.

1. Introduction

Systemic lupus erythematosus (SLE) is a multiorgan disease characterized by abnormalities of T and B cells and production of autoantibodies [1]. Nephritis occurs in 40–75% of patients and is associated with increased morbidity and mortality. SLE has been traditionally treated using immunosuppressants, such as cyclophosphamide, prednisone (PD), and mycophenolate mofetil (MMF) [1]. PD, which is metabolized to prednisolone *in vivo*, acts through a genomic and a nongenomic pathway. In the genomic pathway, PD binds cytosolic receptors to form a regulatory complex, which translocates to the nucleus, binds to DNA,

and represses the transcription of many inflammatory mediators [2]. PD also activates the expression of genes associated with osteoporosis, cataracts, hyperglycemia, coronary heart disease, and cognitive impairment, which are thought to be responsible for the most serious adverse effects of PD [3]. In the nongenomic pathway, PD interacts with diverse proteins in cytosol and membranes [4]. PD is a strong anti-inflammatory agent that inhibits proliferation of and inflammatory mediator production by immune cells [2]. MMF is a prodrug of mycophenolic acid (MPA), an inhibitor of inosine monophosphate dehydrogenase (IMPDH), which is the rate-limiting enzyme in the de novo synthesis of guanosine nucleotides [5]. MMF

is a potent cytostatic agent and strongly inhibits the proliferation of T and B cells [5].

Mesenchymal stem cells (MSCs) alone or in combination with the currently used immunosuppressive therapy have been investigated as a promising therapeutic strategy for SLE [6]. MSCs can be isolated from various tissues including the skeletal muscle, umbilical cord blood, adipose tissue, and bone marrow (BM); they are self-renewable and can differentiate into osteocytes, myocytes, adipocytes, and other cell types [7, 8]. They adhere under normal culture conditions and express CD73, CD90, and CD105, but not CD34 or CD45 [9]. Interestingly, MSCs can regulate immune responses through soluble mediators and cell-cell contacts: they inhibit T cell proliferation and cytokine production, decrease B cell proliferation and antibody secretion, inhibit the maturation and functions of dendritic cells, and reduce proliferation and functions of NK cells but enhance the activity of Treg cells [8].

A combination of MSCs and immunosuppressants significantly ameliorated symptoms in SLE patients [10]. Yet, an important question remains: do immunosuppressants interfere with MSC functions in combination therapy? MSC functions might be inhibited by immunosuppressants, since they express the molecular targets of immunosuppressants. To address this issue, we examined the effects of an immunosuppressant-MSC combination on lupus-prone MRL.Fas^lpr mice and investigated the effects of PD and MMF on survival, soluble mediator production, migration, and immunosuppressive capacity of human BM-derived MSCs.

2. Materials and Methods

2.1. Mesenchymal Stem Cells and Immunosuppressants.
Human BM-derived MSCs were obtained from Corestem Inc. (Seoul, Korea). In brief, BM was aspirated from the posterior iliac crest of healthy donors and mononuclear cells were purified by density gradient centrifugation [11]. These cells were cultured in CSMB-A06 medium (Corestem Inc.) containing 10% fetal bovine serum (BD Biosciences, Franklin Lakes, NJ, USA), 2.5 mM L-glutamine, and penicillin/streptomycin (WelGene, Gyeonggi, Korea) in a 5% CO_2 incubator at 37°C for 3–5 passages. After washing out nonadherent cells, the adherent cells retained the canonical phenotype of MSCs (CD29$^+$CD44$^+$-CD73$^+$CD105$^+$CD90$^+$CD34$^-$CD45$^-$HLA-DR$^-$) and were used in the experiments. All human MSC experiments were approved by the Institutional Review Board of Hanyang University Hospital and were carried out in accordance with their approved guidelines; all participants provided written informed consent. PD, prednisolone (PDL), and MPA were purchased from Sigma-Aldrich (St. Louis, MO, USA). MMF was purchased from Kyongbo Pharmaceutical Co. Ltd. (Asan, Korea).

2.2. MRL.Fas^{lpr} Mouse Model.
MRL.Fas^lpr mice were purchased from the Jackson Laboratory (Bar Harbor, ME, USA). Mice were housed in specific pathogen-free conditions at 21–24°C and 40%–60% relative humidity under a 12 h light/dark cycle. In each experiment, female mice were divided into four groups (6 mice per group): control (vehicle), PD (0.5 mg/kg) or MMF (50 mg/kg), MSC (4×10^4 cells/injection), and a combination of PD or MMF and MSCs. MSCs were injected intravenously once at the age of 12 weeks. PD was injected intraperitoneally once a week from 10 to 16 weeks of age. MMF was administered orally twice a week from 10 to 19 weeks of age. Survival rate and body weight were measured weekly. The serum levels of anti-dsDNA IgG and total IgG were measured by using an anti-dsDNA IgG ELISA kit (Alpha Diagnostic International, San Antonio, TX, USA) and a total IgG ELISA kit (eBioscience, San Diego, CA, USA) [11]. All animal experiments were approved by the Chungbuk National University Animal Experimentation Ethics Committee and were carried out in accordance with their approved guidelines.

2.3. Flow Cytometry.
Spleens were isolated from MRL.Fas^lpr mice at 25 weeks of age, and immune cell composition was analyzed by flow cytometry. Spleen cells were stained with the following monoclonal antibodies in 0.5% BSA/PBS at 4°C for 15 min: FITC-labeled anti-B220, APC-labeled anti-CD3, PE-labeled anti-CD4, FITC-labeled anti-CD8, FITC-labeled anti-CD11c, PE-labeled anti-CD11b, APC-labeled anti-CD138, FITC-labeled anti-IgG1 (BD Biosciences, San Jose, CA, USA), FITC-labeled anti-CD4, and PE-labeled anti-Foxp3 (eBioscience). Data were collected using FACSCalibur and analyzed with CellQuest Pro software (BD Biosciences).

2.4. RT-PCR.
Total RNA was isolated from spleen cells of MRL.Fas^lpr mice using TRIzol reagent (Thermo Fisher Scientific, Waltham, MA, USA). RNA was quantified using a spectrophotometer and stored at −80°C at a concentration of 1 mg/ml [12]. Reverse transcription polymerase chain reaction (RT-PCR) was performed to determine the relative quantities of mRNAs for IL-1β, TNF-α, IFN-γ, and IL-12 and housekeeping gene β-actin. cDNA was synthesized from 3 μg total RNA using an RT kit (Bioneer, Daejeon, Korea). All of the PCRs were performed with a GenePro thermal cycler (Bioer, Hangzhou, China) by using a final volume of 50 μl containing reaction buffer (1 mM Tris-HCl, 5 mM KCl, and 0.1% Triton X-100), 2 mM $MgCl_2$, 200 μM deoxynucleoside triphosphates, 0.2 μM each primer, 1.25 U of Taq thermostable polymerase (Promega), and template cDNA. After an initial incubation at 95°C for 2 min, temperature cycling was begun. The cycles consisted of 20 sec of denaturation at 94°C, 30 sec of primer annealing at 56°C, and 30 sec of primer extension at 72°C for 30 cycles. All PCR products were analyzed by electrophoresis on 1% agarose gels and visualized by staining with ethidium bromide staining (0.5 μg/ml). The primer sequences were as follows: IL-1β, sense, 5$'$-ATG GCA ATG TTC CTG AAC TCA ACT-3$'$, antisense, 5$'$-CAG GAC AGG TAT AGA TTC TTT CCT TT-3$'$; IFN-γ, sense, 5$'$-AGC GGC TGA CTG AAC TCA GAT TGT AG-3$'$, antisense, 5$'$-GTC ACA GTT TTC AGC TGT ATA GGG-3$'$; TNF-α, sense, 5$'$-AGG TTC TGT CCC TTT CAC TCA CTG-3$'$, antisense, 5$'$-AGA

FIGURE 1: Effect of a combination of PD and MSCs in lupus-prone MRL.*Fas*[lpr] mice. Mice were intravenously injected with MSCs once at 12 weeks of age and with PD intraperitoneally once a week from 10 to 16 weeks of age. Survival (a) and body weight (b) were measured weekly. The levels of anti-dsDNA IgG (c) and total IgG (d) in serum were measured every 3 weeks. (e) Total RNA was purified from spleen cells, which were isolated from surviving mice at 20 weeks of age, and the expression of IL-1β, TNF-α, IFN-γ, and IL-12 was examined by RT-PCR. (f) Subset ratios were analyzed by flow cytometry. $^*p < 0.01$ versus control.

GAA CCT GGG AGT CAA GGT A-3$'$; IL-12, sense, 5$'$-AGA GGT GGA CTG GAC TCC CGA-3$'$, antisense, 5$'$-TTT GGT GCT TCA CAC TTC AG-3$'$; and β-actin, sense, 5$'$-TGG AAT CCT GTG GCA TCC ATG AAA C-3$'$, antisense, 5$'$-TA A AAC GCA GCT CAG TAACAG TCC G-3$'$.

2.5. *Immunohistochemistry.* Kidneys were also isolated from MRL.*Fas*[lpr] mice at 25 weeks of age, fixed with 4% formalin, and immersed in PBS. After dehydration with ethanol and xylene, the tissues were embedded in paraffin and cut into 4 μm sections. After deparaffinization and dehydration, sections were heated in a microwave oven (650 W,

20 min) for antigen retrieval, after which endogenous peroxidase activity was blocked by 3% hydrogen peroxide [13]. Thereafter, sections were incubated with the primary antibodies: goat antibody against mouse CD19 (diluted 1 : 100; Biolegend, San Diego, CA, USA), CD3 (diluted 1 : 100, Santa Cruz Biotechnology, Dallas, TX, USA), F4/80 (diluted 1 : 100, Santa Cruz Biotechnology), CD209b (diluted 1 : 100, Santa Cruz Biotechnology), and Foxp3 (diluted 1 : 50, Abcam, Cambridge, England) at 4°C overnight. Sections were then incubated with secondary antibody, anti-goat IgG conjugated with horseradish peroxidase (Vector Laboratories, Burlingame, CA, USA), for 1 h at room temperature. Signals were developed with a two-component high-sensitivity
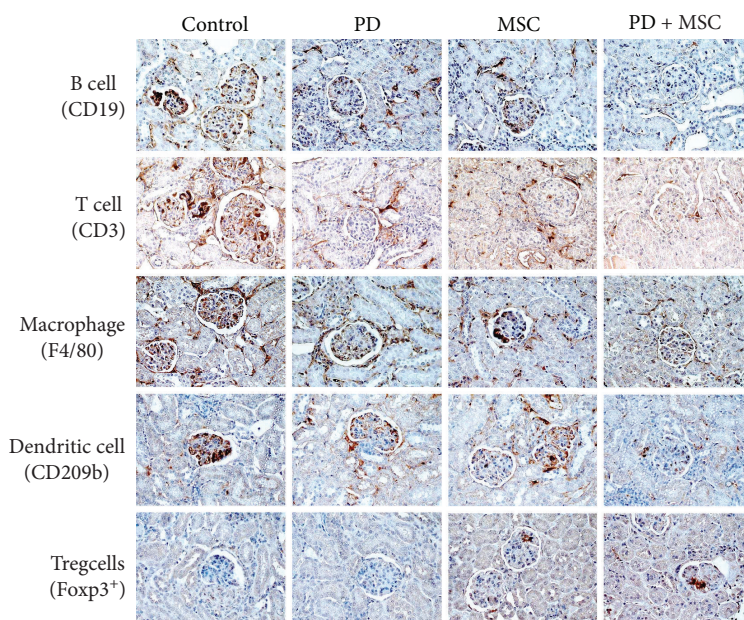
FIGURE 2: Representative images of immunohistochemical staining of kidneys after treatment with a PD-MSC combination. MRL.Fas^{lpr} mice were intravenously injected with MSCs once at 12 weeks of age and with PD intraperitoneally once in a week from 10 to 16 weeks of age. Kidneys were isolated from surviving mice at 20 weeks of age. Kidney sections were stained with antibodies against CD19 (B cells), CD3 (T cells), F4/40 (macrophages), CD209b (dendritic cells), and Foxp3$^+$ (Treg cells).

diaminobenzidine chromogenic substrate (Vector Laboratories) for 10 min and counter stained with hematoxylin.

2.6. Viability Test. Effect of immunosuppressants on MSC viability was determined with XTT assay. MSCs were seeded in a 96-well plate at 1×10^4 cells/well and incubated with immunosuppressants for 24 h. XTT reagent (50 μl; Roche, Mannheim, Germany) was then added, cells were incubated for an additional 6 h, and absorbance was read at 450 nm using a SpectraMax 190 Microplate Reader (Molecular Devices, Sunnyvale, CA, USA). The levels of TGF-β and PGE$_2$ in culture medium were determined by ELISA kits (R&D Systems, Minneapolis, MN, USA).

2.7. Migration Assay. Effect of immunosuppressants on MSC migration was examined in transwell plates with 8 μm pore filters (Corning, Cambridge, MA, USA) [14]. Upper wells were precoated with 0.1% gelatin (Sigma-Aldrich) for 2 h at 37°C. Upper wells were loaded with 2×10^4 MSCs in 200 μl of medium and the lower wells with 500 μl of medium containing 10% fetal bovine serum and 100 ng/ml CXCL10 (R&D Systems). After 24 h, nonmigrated cells on the upper side of the filters were removed and the membranes were fixed in 10% formalin. MSCs that migrated to the lower side of the filter were stained with 0.5% crystal violet for 10 min and were counted under an inverted light microscope.

2.8. T Cell Function Assay. MSCs were pretreated with immunosuppressants for 24 h, harvested, washed three times with medium, and seeded at 1×10^4 cells/well in a 96-well plate. T cells were purified from spleen cells of MRL.Fas^{lpr} mice by a negative depletion method using biotinylated antibodies specific for B220, GR-1, and CD11c (BD Biosciences) and

Dynabeads M-280 Streptavidin (Thermo Fisher Scientific) [11]. Purity was typically >90%. Splenic T cells were added at 1×10^5 cells/well, and concanavalin A (ConA; 1 μg/ml) was added to activate the cells. After 52 h incubation, T cells were pulsed with 1 μCi ^{3}H-thymidine/well (113 Ci/nmol; NEN, Boston, MA, USA) and harvested 18 h later. Incorporated radioactivity was measured using a Microbeta scintillation counter (Wallac, Turku, Finland) [15]. In some experiments, culture medium was collected after 72 h incubation and the level of IFN-γ was quantified by an ELISA kits (R&D Systems). We also examined the effect of a combination of MSCs and immunosuppressants on T cell proliferation. MSCs and/or immunosuppressants were added to splenic cells and ConA (1 μg/ml) was added to induce T cell proliferation. After 52 h incubation, cells were pulsed with 1 μCi ^{3}H-thymidine/well and harvested 18 h later. Incorporated radioactivity was measured using a Microbeta scintillation counter.

2.9. Statistical Analysis. Data are the mean ± SEM of at least three independent experiments each performed in triplicate (in vitro) or six mice (in vivo); p values were calculated using one-way ANOVA in GraphPad Prism software (GraphPad, San Diego, CA, USA).

3. Results

3.1. Effect of a Combination of PD and MSCs in Lupus-Prone MRL.Fas^{lpr} Mice. In our preliminary study, we observed that only 10% of untreated mice survived until 24 weeks of age, but >80% of mice treated with PD (1 mg/kg) and >70% of mice treated with MSCs (4×10^5 cells/injection) lived until this age. Thus, we injected lower doses of PD (0.5 mg/kg)
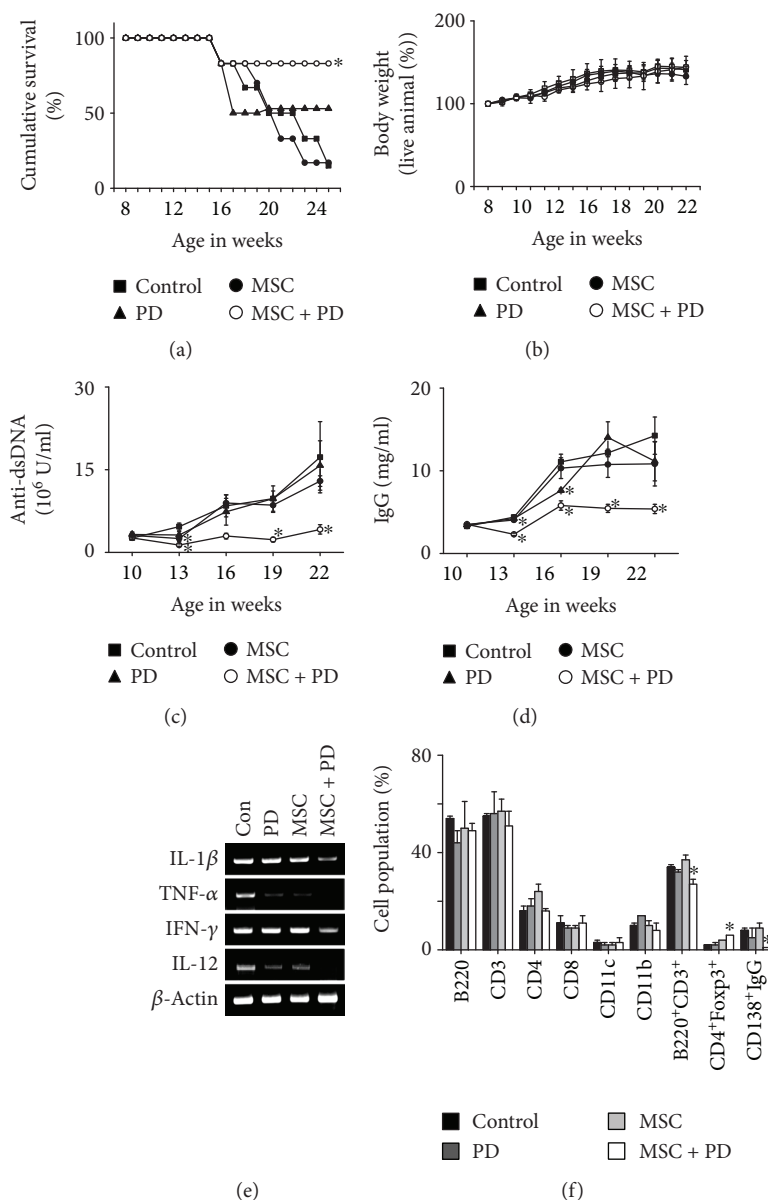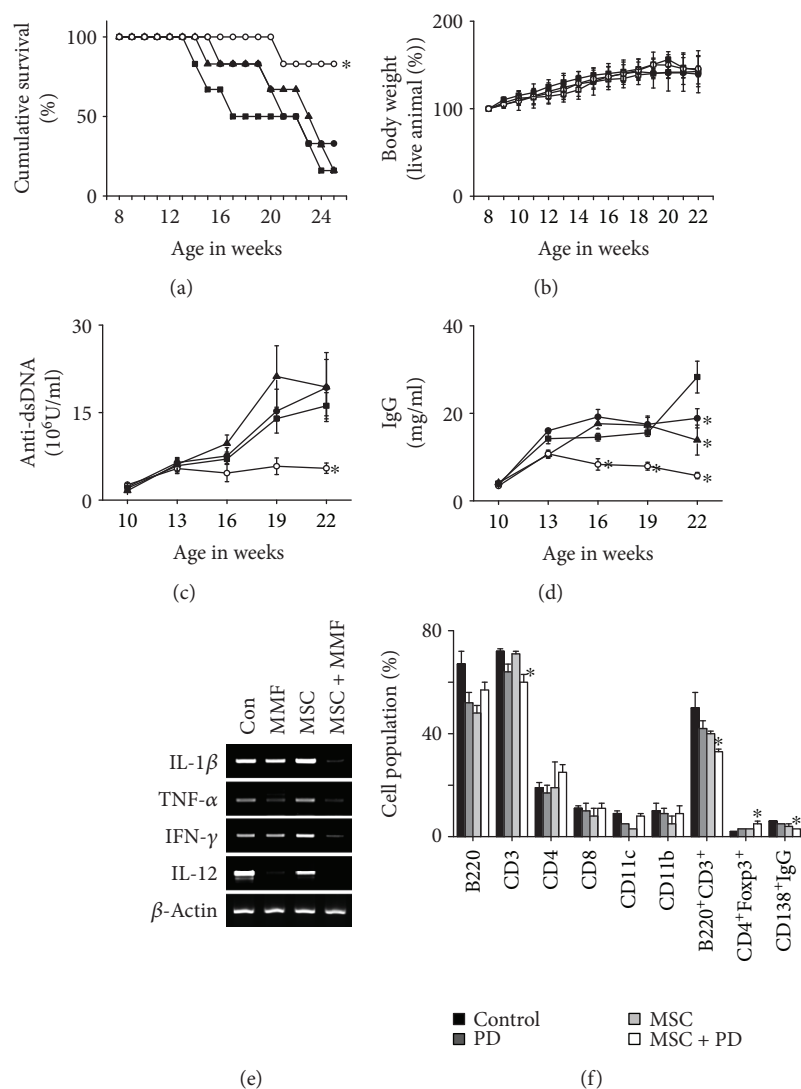
FIGURE 3: Effect of a combination effect of MMF and MSCs in lupus-prone MRL.Fas[lpr] mice. Mice were intravenously injected with MSCs once at 12 weeks of age and with MMF orally twice a week from 10 to 19 weeks of age. Survival (a) and body weight (b) were measured weekly. The levels of anti-dsDNA IgG (c) and total IgG (d) in serum were measured every 3 weeks. (e) Total RNA was purified from spleen cells, which were isolated from surviving mice at 20 weeks of age, and the expression of IL-1β, TNF-α, IFN-γ, and IL-12 was examined by RT-PCR. (f) Subset ratios were analyzed by flow cytometry. $^*p < 0.01$ versus control.

and MSCs (4×10^4 cells/injection) to determine the effect of their combination. The combination of PD and MSCs significantly prolonged survival compared to each therapy alone: 90% of the mice receiving PD and MSCs survived up to 25 weeks of age, whereas only 10% of control and MSC-treated mice and 50% of PD-treated mice survived (Figure 1(a)). None of the therapies affected body weight (Figure 1(b)), and no untoward effects were noted. The serum level of anti-dsDNA IgG (Figure 1(c)) and total IgG antibodies (Figure 1(d)) decreased in mice treated with the PD-MSC combination compared to each therapy alone.

We isolated spleen cells from surviving 25-week-old mice. The expression of all inflammatory cytokines tested (IL-1β, TNF-α, IFN-γ, and IL-12) decreased in the spleens of mice treated with the PD-MSC combination compared to each therapy alone (Figure 1(e)), whereas the frequency

of CD4^{+}Foxp3^{+} Treg cells increased and that of CD138[+-] IgG^{+} plasma cells decreased (Figure 1(f)). No infiltration of B cells, T cells, macrophages, dendritic cells, or Treg cells into the kidney was detected before disease onset (5 weeks of age; data not shown); their infiltration strongly increased with disease progression (25 weeks of age) and decreased in mice treated with a combination of PD and MSCs (Figure 2). The infiltration of Treg cells decreased with the progression of disease in control mice, and this trend was reversed by the combination of PD and MSCs (Figure 2). Single therapies did not affect immune cell infiltration into the kidney due to suboptimal dosage of PD or MSCs. These data show that treatment with a combination of PD and MSCs strongly ameliorates the development of lupus symptoms in MRL.Fas[lpr] mice compared to single therapies.

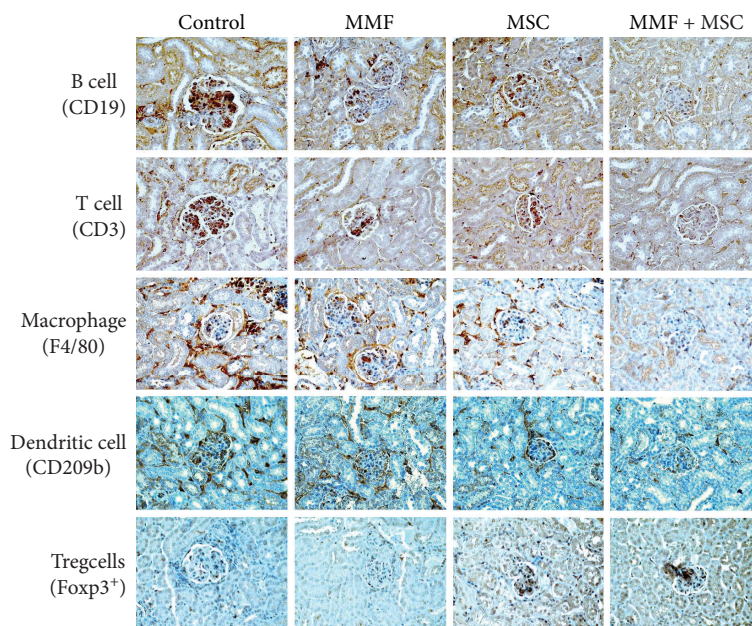FIGURE 4: Representative images of immunohistochemical staining of kidneys after treatment with a MMF-MSC combination. MRL.Fas^{lpr} mice were intravenously injected with MSCs once at 12 weeks of age and with MMF orally twice a week from 10 to 19 weeks of age. Kidneys were isolated from surviving mice at 20 weeks of age. Kidney sections were stained with antibodies against CD19 (B cells), CD3 (T cells), F4/40 (macrophages), CD209b (dendritic cells), and Foxp3^{+} (Treg cells).

3.2. Combination Effect of MMF and MSCs in MRL.Fas^{lpr} Mice. Next, we examined the therapeutic activity of a combination of MMF and MSCs. Since 90% of the mice receiving MMF at 100 mg/kg survived up to 24 weeks of age, we injected lower doses of MMF (50 mg/kg). A combination of MMF and MSCs significantly prolonged survival (by 90%) at 25 weeks of age, which was higher than single therapy of MMF or MSCs (Figure 3(a)). None of the therapies affected body weight (Figure 3(b)). The serum level of anti-dsDNA (Figure 3(c)) and total IgG antibodies (Figure 3(d)) decreased by the combination therapy compared to each therapy alone. At 25 weeks of age, we isolated spleen cells from several surviving mice. Combination therapy decreased the expression of all inflammatory cytokines tested (IL-1β, TNF-α, IFN-γ, and IL-12) in comparison with each therapy alone (Figure 3(e)). The frequency of CD4^{+}Foxp3^{+} Treg cells increased and that of CD138^{+}IgG^{+} plasma cells in the spleen was lower after combination therapy than after each therapy alone (Figure 3(f)). Immunohistological data showed that the infiltration of B cells, T cells, macrophages, dendritic cells, and Treg cells into the kidney was decreased by combination therapy in comparison with each therapy alone (Figure 4). The infiltration of Treg cells decreased with the progression of disease in control mice, and this trend was reversed by the combination therapy (Figure 4). These data show that treatment with a combination of MMF and MSCs strongly ameliorates the development of lupus symptoms in MRL.Fas^{lpr} mice compared to single therapies.

3.3. Effect of Combinations of Immunosuppressants and MSCs In Vitro. Next, we examined the effects of combinations of immunosuppressants and MSCs on T cell proliferation *in vitro*. PD alone inhibited ConA-induced T cell proliferation with an IC$_{50}$ of 37.5 nM and MSCs with 6819 cells/injection; their combination synergistically inhibited T cell proliferation (Figure 5(a)). PDL, a metabolite of PD, inhibited T cell proliferation with an IC$_{50}$ of 8.2 nM, and its combination with MSCs synergistically inhibited T cell proliferation (Figure 5(b)). MMF alone inhibited T cell proliferation with an IC$_{50}$ of 0.4 nM (Figure 5(c)); MPA, a metabolite of MMF, had an IC$_{50}$ of 149.6 nM (Figure 5(d)). MMF or MPA in combination with MSCs synergistically inhibited T cell proliferation (Figures 5(c) and 5(d)). These data confirm that immunosuppressants in combination with MSCs synergistically inhibit T cell proliferation [16].

3.4. Direct Effect of Immunosuppressants on MSC Functions. We reasoned that immunosuppressants might affect MSC functions and examined this possibility. In our preliminary experiments, none of the immunosuppressants (PD, PDL, MMF, and MPA) affected MSC functions at concentration below 1 μM. At higher concentrations (3–100 μM), all immunosuppressants inhibited the proliferation of and IFN-γ production by ConA-activated T cells (data not shown), but did not affect MSC viability (Figure 6(a)), TGF-β1 production (Figure 6(b)), or PGE$_2$ production (Figure 6(c)). These data suggest that immunosuppressants up to 100 μM do not affect the soluble factor production by MSCs. Next, we examined whether immunosuppressant-treated MSCs had normal functions. MSCs treated with 100 μM immunosuppressants for 24 h showed the same potency of migration toward CXCL10 as control MSCs
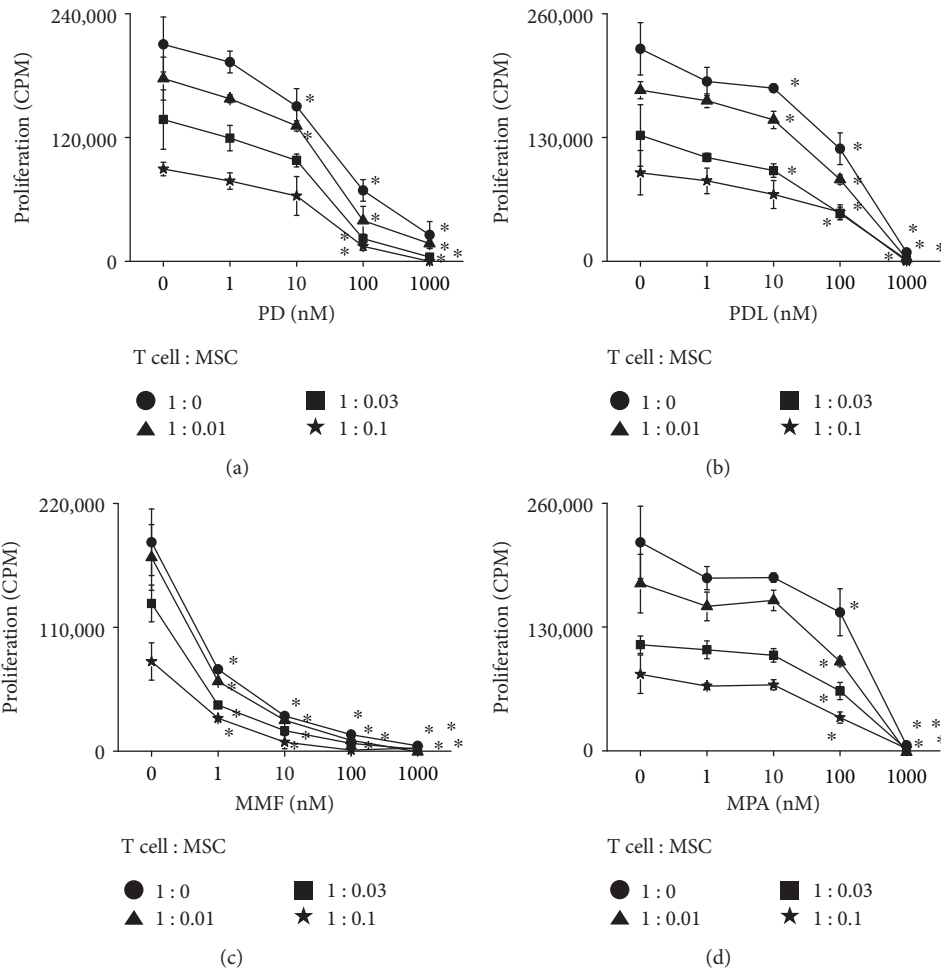
FIGURE 5: Combination effect of immunosuppressants and MSCs *in vitro*. T cells were loaded into a 96-well plate at 1×10^5 cells/well. MSCs were loaded at 0.01, 0.03, or 0.1×10^4 cells/well, or were omitted. Cells were treated with PD (a), PDL (b), MMF (c), or MPA (d). Concanavalin A was added at 1 μg/ml and T cell proliferation was measured 72 h later. $^*p < 0.01$ versus control.

(Figure 7(a)). Immunosuppressant-treated MSCs similarly inhibited the proliferation of (Figure 7(b)) and IFN-γ production (Figure 7(c)) by ConA-activated T cells. Overall, these data suggest that none of the immunosuppressants interfered with MSC functions.

4. Discussion

Immunosuppressive drugs are widely used to treat SLE, but their clinical use is often limited by harmful side effects. The combined application of immunosuppressants and MSCs offers a promising alternative approach, which will decrease the doses of immunosuppressants with maintaining the outcome of therapy. Here, we show that a combination of a low dose of PD or MMF and MSCs ameliorates lupus symptoms in MRL.*Fas*[lpr] mice to the same extent as a high dose of PD or MMF and that this combination also inhibits T cell proliferation in a synergistic manner. Potentially, a critical drawback of this combination therapy might be unwanted effects of PD or MMF on MSCs. In the combination approach, MSCs are exposed to diverse immunosuppressants. Although the molecular targets of these drugs are expressed in both lymphocytes and MSCs, they responded differently: PD or

MMF strongly inhibited lymphocyte functions, but not MSC viability and functions, such as TGF-β1 and PGE$_2$ production, migration, and immunosuppressive capacity. These data suggest that combination therapy of MSCs and a low dose of PD or MMF is a good strategy to attenuate SLE progression.

Our data extend previous studies that have examined the effects of combinations of MSCs and the calcineurin inhibitor cyclosporine A, FK506-binding protein inhibitor tacrolimus, mTOR inhibitor rapamycin, and IMPDH inhibitor MMF [17–19]. Most studies showed that these compounds did not affect the viability and immunosuppressive capacity of MSCs [17, 18]. However, several studies showed inconsistent results: tacrolimus increased MSC inhibitory capacity [17], cyclosporine A increased the inhibition of lymphocyte proliferation by MSCs [17] and enhanced MSC viability [20], and MMF promoted the inhibitory activity of MSCs, whereas cyclosporine A, tacrolimus, and rapamycin antagonized it [21]. Glucocorticoids, such as dexamethasone and PD, are widely used in SLE patients because of their potent anti-inflammatory properties, although they have severe side effects [18]. Dexamethasone enhances human growth factor production by MSCs [18]. PD increases indoleamine 2,3-
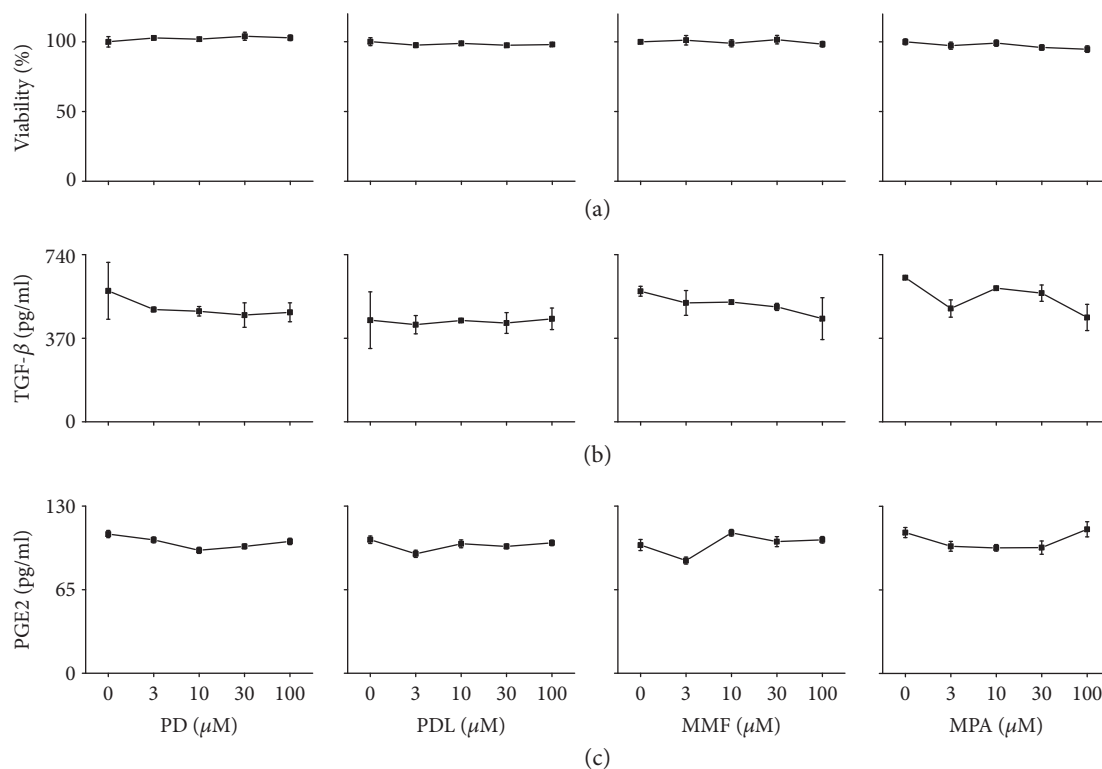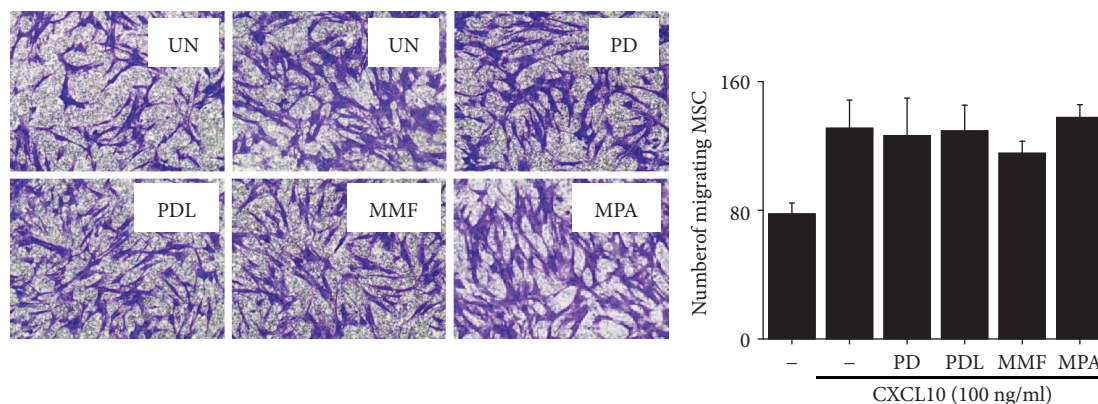
Figure 6: Direct effect of immunosuppressants on MSC functions *in vitro*. MSCs were loaded into a 96-well plate at 1×10^4 cells/well and treated with immunosuppressants for 24 h. Viability was measured by XTT assay (a) and the levels of TGF-β1 (b) and PGE$_2$ (c) in culture medium were measured by ELISA.

dioxygenase production by MSCs without affecting other immunosuppressive capacities [18]. Several studies also showed the efficacy of combinations of immunosuppressants and MSCs [19, 22, 23]. Cotreatment with one of the immunosuppressants and MSCs strongly inhibited Th1 and Th17 cell functions (proliferation, inflammatory cytokine production, and differentiation) but promoted Th2 and Treg cell functions [19]. A combination of MMF and MSCs prolonged allograft survival [22, 23]. In the present study, we observed that PD or MMF in combination with MSCs synergistically inhibited T cell functions without affecting MSC functions. Some discrepancies between our data and those from several previous studies might be due to the diversity of MSC sources, human donor conditions, culture conditions, or experimental conditions, and further studies are required.

A critical question is why PD or MMF does not affect MSC functions. Because MMF inhibits lymphocyte proliferation by inhibiting IMPDH, which is also expressed in MSCs; MMF could be expected to affect MSC functions [2, 5]. The absence of the effect of MMF on MSC viability or functions might be due to the slow proliferation of MSCs: the reported mean doubling time of bone marrow-derived MSCs is 40–60 h and that of adipose tissue-derived MSCs is 24–45 h [24]. The mean doubling time of our BM-derived MSCs was 50 h (data not shown), suggesting that treatment with MMF for 24–48 h was not sufficient to affect MSC proliferation. Glucocorticoids including PD play an essential role in inducing MSC differentiation to adipocytes [25]. PD binds

to the glucocorticoid receptor in the cytosol and forms a regulatory complex on response elements in the target gene encoding myostatin [26]. Myostatin is sufficient to elicit the adipocyte fate decision [27]. However, nothing is known about the effect of glucocorticoids including PD on MSC functions. Our data show that PD does not affect MSC viability or functions, when the cells are treated for 24–48 h. In the future, we will intensively study whether long-term and repeated exposure to immunosuppressants will affect MSC functions, since SLE patients need long-term and repeated treatment with immunosuppressants [19].

Further study will be required to examine the expression levels of inflammatory cytokines in the kidney of mice treated with a combination of MSCs and immunosuppressants. The deposit of immune complex in the kidney activates mesangial and endothelial cells, which produce various types of cytokines, such as IL-1, IL-6, IL-12, IFN-γ, and TNF-α [28]. Single-cell analysis on mesangial cells, endothelial cells, and podocytes will give valuable information to understand the therapeutic mechanism of MSCs for lupus nephritis. It will be also interesting to examine the chemokine expression levels in nephritic kidneys. The chemokines CCL2, CCL3, CCL5, CXCL10, CXCL12, CXCL13, and CX3CL1 are expressed in the nephritic kidney of lupus-prone mice and SLE patients and increase inflammatory cell infiltration into the kidney [29]. Further clinical studies will be also required to address whether PD or MMF affects MSC functions in patients. In the present study, we transplant human MSCs and inject immunosuppressants to MRL.*Fas*$^{\text{lpr}}$ mice, which

(a)
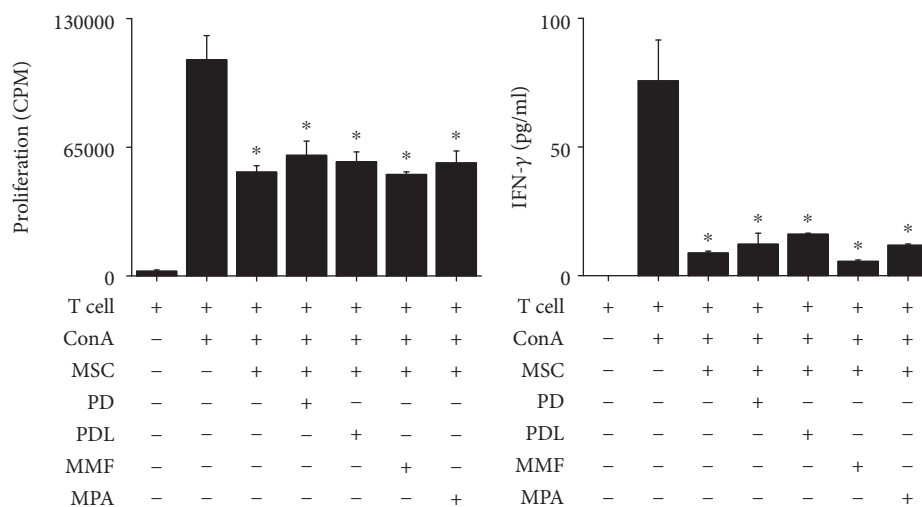
(b)

(c)

FIGURE 7: Effect of immunosuppressants on MSC functions *in vitro*. MSCs were pretreated with 100 μM of PD, PDL, MMF, or MPA for 24 h. MSCs (2×10^4 cells/well) were added to the upper chamber and allowed to migrate to the lower chamber containing CXCL-10 (100 ng/ml). MSCs that migrated to the lower side of inserts were stained with crystal violet (a). Immunosuppressant-pretreated MSCs (0.1×10^4 cells/well) were mixed with T cells (1×10^5 cells/well) in a 96-well plate. Concanavalin A (ConA) was added at 1 μg/ml, and the proliferation of (b) and IFN-γ production (c) by T cells were measured 72 h later. $^*p < 0.01$ versus control.

lack *Fas* and spontaneously develop a lupus-like disease [11]. Although these mice have been widely used in efficacy evaluation of human MSCs in the preclinical studies, xenogeneic human MSCs may induce rejection and adverse inflammation, which will affect lupus progression and therapeutic activity of MSCs. Although xenogeneic human MSCs may escape immune recognition and clearance in mice due to the low expression of MHC-I and no expression of MHC-II, a mouse model does not accurately reflect human condition [11].

The current immunosuppressive protocols for SLE are based on the administration of several immunosuppressants, each with a different mechanism. When combining immunosuppressants and MSCs, two points are needed to be considered. First, it is desirable to decrease the dose of steroids and immunosuppressants, since they have severe side effects. Second, maintaining the cell number and immunosuppressive capacity of MSCs should be taken into account, since enough MSCs should be used to achieve high therapeutic efficacy. Our data demonstrate that the dose of PD or MMF can

be lowered by combining it with MSCs for the treatment of SLE and PD or MMF does not affect MSC functions, providing an important insight on the application of this combination therapy for SLE patients.

Data Availability

The data used to support the findings of this study are available from the corresponding author upon request.

Conflicts of Interest

No potential conflicts of interest were disclosed.

Authors' Contributions

Hong Kyung Lee and Ki Hun Kim contributed equally to this work.

Acknowledgments

References

[1] D. Deng, P. Zhang, Y. Guo, and T. O. Lim, "A randomised double-blind, placebo-controlled trial of allogeneic umbilical cord-derived mesenchymal stem cell for lupus nephritis," *Annals of the Rheumatic Diseases*, vol. 76, no. 8, pp. 1436–1439, 2017.

[2] G. Ruiz-Irastorza, A. Danza, and M. Khamashta, "Glucocorticoid use and abuse in SLE," *Rheumatology*, vol. 51, no. 7, pp. 1145–1153, 2012.

[3] T. Rhen and J. A. Cidlowski, "Antiinflammatory action of glucocorticoids — new mechanisms for old drugs," *The New England Journal of Medicine*, vol. 353, no. 16, pp. 1711–1723, 2005.

[4] F. Buttgereit and A. Scheffold, "Rapid glucocorticoid effects on immune cells," *Steroids*, vol. 67, no. 6, pp. 529–534, 2002.

[5] A. C. Allison and E. M. Eugui, "Mycophenolate mofetil and its mechanisms of action," *Immunopharmacology*, vol. 47, no. 2-3, pp. 85–118, 2000.

[6] L. Sun, K. Akiyama, H. Zhang et al., "Mesenchymal stem cell transplantation reverses multiorgan dysfunction in systemic lupus erythematosus mice and humans," *Stem Cells*, vol. 27, no. 6, pp. 1421–1432, 2009.

[7] D. G. Phinney and D. J. Prockop, "Concise review: mesenchymal stem/multipotent stromal cells: the state of transdifferentiation and modes of tissue repair—current views," *Stem Cells*, vol. 25, no. 11, pp. 2896–2902, 2007.

[8] S. Ma, N. Xie, W. Li, B. Yuan, Y. Shi, and Y. Wang, "Immunobiology of mesenchymal stem cells," *Cell Death and Differentiation*, vol. 21, no. 2, pp. 216–225, 2014.

[9] M. Dominici, K. le Blanc, I. Mueller et al., "Minimal criteria for defining multipotent mesenchymal stromal cells. The International Society for Cellular Therapy position statement," *Cytotherapy*, vol. 8, no. 4, pp. 315–317, 2006.

[10] J. Liang, H. Zhang, B. Hua et al., "Allogenic mesenchymal stem cells transplantation in refractory systemic lupus erythematosus: a pilot clinical study," *Annals of the Rheumatic Diseases*, vol. 69, no. 8, pp. 1423–1429, 2010.

[11] H. K. Lee, H. S. Kim, J. S. Kim et al., "CCL2 deficient mesenchymal stem cells fail to establish long-lasting contact with T cells and no longer ameliorate lupus symptoms," *Scientific Reports*, vol. 7, article 41258, 2017.

[12] J. Y. Kim, Y. J. Kim, J. S. Kim et al., "Adjuvant effect of a natural TLR4 ligand on dendritic cell-based cancer immunotherapy," *Cancer Letters*, vol. 313, no. 2, pp. 226–234, 2011.

[13] S. C. Weng, K. H. Shu, M. J. Wu et al., "Expression of decoy receptor 3 in kidneys is associated with allograft survival after kidney transplant rejection," *Scientific Reports*, vol. 5, no. 1, p. 12769, 2015.

[14] M. Wang, J. Cai, F. Huang et al., "Pre-treatment of human umbilical cord-derived mesenchymal stem cells with interleukin-6 abolishes their growth-promoting effect on gastric cancer cells," *International Journal of Molecular Medicine*, vol. 35, no. 2, pp. 367–375, 2015.

[15] H. K. Lee, H. S. Kim, Y. J. Kim et al., "Sophoricoside isolated from Sophora japonica ameliorates contact dermatitis by inhibiting NF-κB signaling in B cells," *International Immunopharmacology*, vol. 15, no. 3, pp. 467–473, 2013.

[16] V. R. Moulton and G. C. Tsokos, "Abnormalities of T cell signaling in systemic lupus erythematosus," *Arthritis Research & Therapy*, vol. 13, no. 2, p. 207, 2011.

[17] M. J. Hoogduijn, M. J. Crop, S. S. Korevaar et al., "Susceptibility of human mesenchymal stem cells to tacrolimus, mycophenolic acid, and rapamycin," *Transplantation*, vol. 86, no. 9, pp. 1283–1291, 2008.

[18] E. Javorkova, J. Vackova, M. Hajkova et al., "The effect of clinically relevant doses of immunosuppressive drugs on human mesenchymal stem cells," *Biomedicine & Pharmacotherapy*, vol. 97, pp. 402–411, 2018.

[19] M. Hajkova, B. Hermankova, E. Javorkova et al., "Mesenchymal stem cells attenuate the adverse effects of immunosuppressive drugs on distinct T cell subpopulations," *Stem Cell Reviews*, vol. 13, no. 1, pp. 104–115, 2017.

[20] T. L. Chen, J. A. Wang, H. Shi et al., "Cyclosporin A pre-incubation attenuates hypoxia/reoxygenation-induced apoptosis in mesenchymal stem cells," *Scandinavian Journal of Clinical and Laboratory Investigation*, vol. 68, no. 7, pp. 585–593, 2008.

[21] F. Buron, H. Perrin, C. Malcus et al., "Human mesenchymal stem cells and immunosuppressive drug interactions in allogeneic responses: an in vitro study using human cells," *Transplantation Proceedings*, vol. 41, no. 8, pp. 3347–3352, 2009.

[22] E. Eggenhofer, P. Renner, Y. Soeder et al., "Features of synergism between mesenchymal stem cells and immunosuppressive drugs in a murine heart transplantation model," *Transplant Immunology*, vol. 25, no. 2-3, pp. 141–147, 2011.

[23] H. Wang, F. Qi, X. Dai et al., "Requirement of B7-H1 in mesenchymal stem cells for immune tolerance to cardiac allografts in combination therapy with rapamycin," *Transplant Immunology*, vol. 31, no. 2, pp. 65–74, 2014.

[24] R. Hass, C. Kasper, S. Bohm, and R. Jacobs, "Different populations and sources of human mesenchymal stem cells (MSC): a comparison of adult and neonatal tissue-derived MSC," *Cell Communication and Signaling*, vol. 9, no. 1, p. 12, 2011.

[25] B. J. Feldman, "Glucocorticoids influence on mesenchymal stem cells and implications for metabolic disease," *Pediatric Research*, vol. 65, no. 2, pp. 249–251, 2009.

[26] K. R. Yamamoto, "Steroid receptor regulated transcription of specific genes and gene networks," *Annual Review of Genetics*, vol. 19, no. 1, pp. 209–252, 1985.

[27] B. J. Feldman, R. S. Streeper, R. V. Farese, and K. R. Yamamoto, "Myostatin modulates adipogenesis to generate adipocytes with favorable metabolic effects," *Proceedings of the National Academy of Sciences of the United States of America*, vol. 103, no. 42, pp. 15675–15680, 2006.

[28] Y. Iwata, K. Furuichi, S. Kaneko, and T. Wada, "The role of cytokine in the lupus nephritis," *Journal of Biomedicine & Biotechnology*, vol. 2011, Article ID 594809, 7 pages, 2011.

[29] X. Liao, T. Pirapakaran, and X. M. Luo, "Chemokines and chemokine receptors in the development of lupus nephritis," *Mediators of Inflammation*, vol. 2016, Article ID 6012715, 15 pages, 2016.

Research Article

Chronic Inflammation May Enhance Leiomyoma Development by the Involvement of Progenitor Cells

Monia Orciani [ID],[1] **Miriam Caffarini** [ID],[1] **Alessandra Biagini** [ID],[2] **Guendalina Lucarini** [ID],[1] **Giovanni Delli Carpini** [ID],[2] **Antonella Berretta** [ID],[3] **Roberto Di Primio** [ID],[1] **and Andrea Ciavattini** [ID][2]

[1]*Department of Clinical and Molecular Sciences and Histology, Università Politecnica delle Marche, 60126 Ancona, Italy*
[2]*Department of Clinical Science, Università Politecnica delle Marche, 60126 Ancona, Italy*
[3]*Clinic of Immunology, Azienda Ospedali Riuniti di Ancona, 60126 Ancona, Italy*

Correspondence should be addressed to Roberto Di Primio; r.diprimio@univpm.it

Although the etiology of leiomyoma is unclear, a progenitor/undifferentiated cell population has been described whose dysregulation may be involved in the onset of uterine conditions. Moreover, inflammation is involved in the development of several tumors. The aim of this work was to understand if progenitor cells sustain a chronic inflammatory microenvironment that enhances leiomyoma development. Cells from 12 human leiomyoma and 12 normal myometrium samples of the same patients were in vitro isolated and exhaustively characterized (morphology, proliferation, cytofluorometry, differentiation, RT-PCR, immunofluorescence, immunohistochemistry, and Western blotting assays). Selected cytokines (ELISA) and inflammation-related genes (RT-PCR) were analyzed to identify healthy myometrium progenitor cells (MPCs) and leiomyoma progenitor cells (LPCs). Results show that (i) MPCs and LPCs share stemness features, such as immunophenotype and multidifferentiation assay, (ii) LPCs have a significantly shorter doubling time and a significantly higher expression of stemness genes ($p < 0.05$), and (iii) LPCs secreted significantly higher levels ($p < 0.05$) of cytokines related to chronic inflammation and significantly lower amounts ($p < 0.05$) of cytokines related to acute inflammation. Despite the limited sample size, comparisons between leiomyoma and normal myometrium tissue from each patient allowed normalization of patient-specific differences. The evidenced cytokine expression pattern related to chronic inflammation in LPCs may play a role in the increased risk of adverse obstetric outcomes (infertility, spontaneous miscarriage, and preterm birth) in women affected by leiomyomas. These women should be recognized as "high risk" and subjected to specialized management both before and during pregnancy.

1. Introduction

Uterine leiomyomas (fibroids) are benign tumors originating from the myometrium and the most common neoplasms of the female reproductive system [1, 2]. They cause prolonged bleeding, pelvic pain, recurrent abortions, and adverse obstetric outcomes and are a significant cause of infertility [3–5]. Their origin and pathophysiology are unclear. A wide range of factors, from genetic aberrations [6] to an undifferentiated cell population that could give rise to them [7, 8], has been investigated. The latter hypothesis is supported by the uterine tissue remodeling that occurs during life in physiological [9] and pathological conditions [10].

One possible explanation for the development of leiomyomas is the dysregulation of mesenchymal stem cell activity [9]. Previous studies [11, 12] have proposed that undifferentiated cells are involved in myometrial pathologies, and also leiomyoma onset may be the result of impaired function, proliferation, and differentiation of undifferentiated cells inside the myometrium that are under the effect of ovarian hormones [13, 14]. Moreover, the clonality of leiomyomas that originate from a single altered cell strongly enforces this hypothesis [1, 15, 16]. Undifferentiated cells have been sought in normal myometrium and leiomyoma tissue by a variety of techniques to address different questions [17–20]. A role for the microenvironment has been suggested

TABLE 1: Primer sequences.

Gene	Primers
GAPDH	Forward 5$'$-CCCTTCATTGACCTCAACTACATG-3$'$ Reverse 5$'$-TGGGATTTCCATTGATGACAAGC-3$'$
RPLP0	Forward 5$'$-CCATTCTATCATCAACGGGTACAA-3$'$ Reverse 5$'$-TCAGCAAGTGGGAAGGTGTAATC-3$'$
NANOG	Forward 5$'$-TGAACCTCAGCTACAAACAG-3$'$ Reverse 5$'$-CTGGATGTTCTGGGTCTGGT-3$'$
SOX2	Forward 5$'$-ACACCAATCCCATCCACACT-3$'$ Reverse 5$'$-GCAAACTTCCTGCAAAGCTC-3$'$
OCT4	Forward 5$'$-AGCGAACCAGTATCGAGAAC-3$'$ Reverse 5-$'$TTACAGAACCACACTCGGAC-3$'$
KLF4	Forward 5$'$-CCCACACAGGTGAGAAACCT-3$'$ Reverse 5$'$-ATGTGTAAGGCGAGGTGGTC-3$'$
IL-17A	Forward 5$'$-GGTCAACCTCAAAGTCTTTAACTC-3$'$ Reverse 5$'$-TTAAAAATGCAAGTAAGTTTGCTG-3$'$
IL2	Forward 5$'$-TCACCAGGATGCTCACATTTAAGT-3$'$ Reverse 5$'$-GAGGTTTGAGTTCTTCTTCTAGACAC TGA-3$'$
IL4	Forward 5$'$-GAAGAGAGGTGCTGATTG-3$'$ Reverse 5$'$-GGAAGAACAGAGGGGGAAG-3$'$
IL5	Forward 5$'$-TAGCTCTTGGAGCTGCCTACGTGT AT-3$'$ Reverse 5$'$-AAGCAGTGCCAAGGTCTCTTTCAC-3$'$
IL6	Forward 5$'$-ATTCTGCGCAGCTTTAAGGA-3$'$ Reverse 5$'$-AACAACAATCTGAGGTGCCC-3$'$
IL10	Forward 5$'$-CAAGGACTCCTTTAACAACAAGTT-3$'$ Reverse 5$'$-GAGATGCCTTCAGCAGAGTG-3$'$
IL12	Forward 5$'$-GGAGTACCCTGACACCTG-3$'$ Reverse 5$'$-AGATGACCGTGGCTGAGG-3$'$
IL13	Forward 5$'$-CCAGAAGGCTCCGCTCTGCAA-3$'$ Reverse 5$'$-GTGCGGGCAGAATCCGCTCA-3$'$
IL17A	Forward 5$'$-TCACAATCCCACGAAATCCAG-3$'$ Reverse 5$'$-GTGAGGTGGATCGGTTGTAG-3$'$
TGF-β	Forward 5$'$-GGCCAGATCCTGTCCAAGC-3$'$ Reverse 5$'$-GTGGGTTTCCACCATTAGCAC-3$'$
TNF-α	Forward 5$'$-CGAGTCTGGGCAGGTCTACTTT-3$'$ Reverse 5$'$-AAGCTGTAGGCCCCAGTGAGTT-3$'$
IFN-γ	Forward 5$'$-ATGAAATATACAAGTTATATCTTGG-3$'$ Reverse 5$'$-TTACTGGGATGCTCTTCGAC-3$'$
G-CSF	Forward 5$'$-GAGCAAGTGAGGAAGATCCAG-3$'$ Reverse 5$'$-CAGCTTGTAGGTGGCACACTC-3$'$
IL-17RA	Forward 5$'$-CCCAGTAATCTCAAATACCACAGTTC-3$'$ Reverse 5$'$-CGATGAGTGTGATGAGGCCATA-3$'$
IL22	Forward 5$'$-TTGAGGTGTCCAACTTCCAGCA-3$'$ Reverse 5$'$-AGCCGGACGTCTGTGTTGTTA-3$'$

TABLE 1: Continued.

Gene	Primers
IL23	Forward 5$'$-CGTCTCCTTCTCCGCTTCAA-3$'$ Reverse 5$'$-ACCCGGGCGGCTACAG-3$'$
NFKB	Forward 5$'$-CACTGCTCAGGTCCACTGTC-3$'$ Reverse 5$'$-CTGTCACTATCCCGGAGTTCA-3$'$
STAT3	Forward 5$'$-GAGGACTGAGCATCGAGCA-3$'$ Reverse5$'$-CATGTGATCTGACACCCTGAA-3$'$
CCR5	Forward 5$'$-CAAAAAGAAGGTCTTCATTACACC-3$'$ Reverse 5$'$-CCTGTGCCTCTTCTTCTCATTTCG-3$'$
CX3CL1	Forward 5$'$-GGATGCAGCCTCACAGTCCTTAC-3$'$ Reverse 5$'$-GGCCTCAGGGTCCAAAGACA-3$'$
CXCL5	Forward 5$'$-TGGACGGTGGAAACAAGG-3$'$ Reverse 5$'$-CTTCCCTGGGTTCAGAGAC-3$'$
CXCL12	Forward 5$'$-TCAGCCTGAGCTACAGATGC-3$'$ Reverse 5$'$-CTTTAGCTTCGGGTCAATGC-3$'$

for many tumor types, including leiomyoma [21–24], with inflammation appearing to exert a major effect. If the condition causing acute inflammation is not resolved, the inflammation may become chronic, favoring tumor onset and development. Chronic inflammation is maintained by cytokines secreted by the immune system as well as undifferentiated cells [25–29], which are involved in a complex crosstalk with neoplastic cells. These cytokines influence proliferation, fibrosis, and angiogenesis, which in turn sustain fibroid formation and growth [30–32]. Considering that (i) the existence of undifferentiated cells may correlate with leiomyoma onset, (ii) inflammation may sustain leiomyomas, and (iii) cytokines secreted by undifferentiated cells create an inflammatory microenvironment, this study was performed to isolate and characterize undifferentiated cells from myometrium (myometrial progenitor cells, MPCs) and from leiomyoma tissue (leiomyoma progenitor cells, LPCs) and to evaluate the expression of selected inflammation-related cytokines. In addition, the expression of MDR1 (a member of ABC family recognized as a stem cell marker) and of α-SMA, collagen type 1, and fibronectin (primary component of the extracellular matrix involved in fibroid development) was tested.

2. Materials and Methods

2.1. Ethics Statement. All patients provided their written informed consent to participate in the study, which was approved by the institutional ethics committees and was conducted in accordance with the Declaration of Helsinki.

2.2. Human Tissue Collection. Leiomyoma and normal myometrium samples were collected from 12 women of childbearing age (range 30–35 years) undergoing hysterectomy for symptomatic fibroids from February to November 2016 at "Salesi Hospital," Ancona. We investigated normal myometrium and leiomyoma tissue from the same 12 patients with a histologically confirmed diagnosis of leiomyoma. All

(a)

(b)
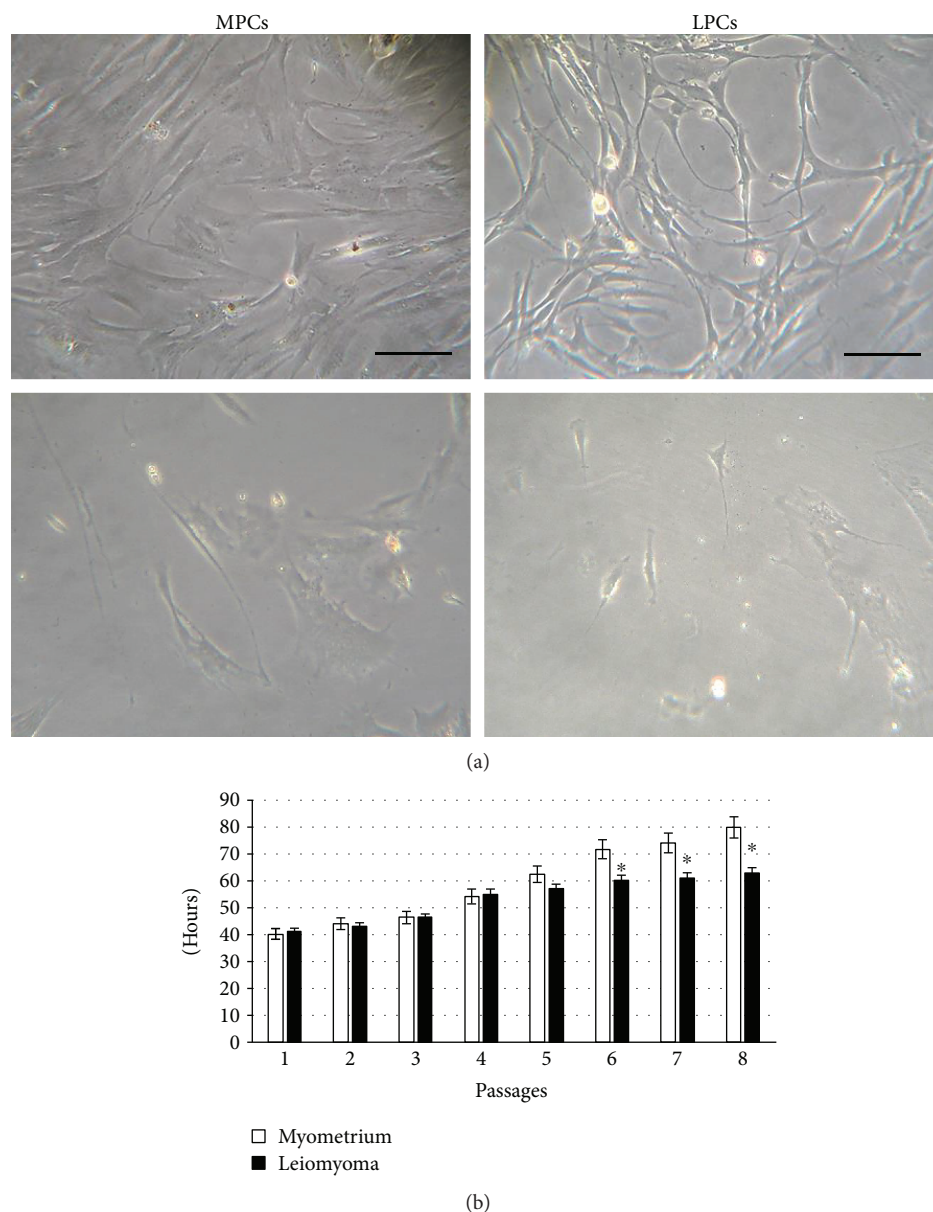
FIGURE 1: Cell morphology and doubling time. (a) Phase-contrast images of myometrium progenitor cells (MPCs, left) and leiomyoma progenitor cells (LPCs, right) at 2nd (top) and 4th (bottom) passage of culture. Scale bar = 100 μm. (b) Doubling time was calculated over 21 days (8th passage). Data are mean ± SD of experiments performed on 12 samples. $^*p < 0.05$ LPCs versus MPCs.

tissue samples were collected in the operating room under surgical conditions from a trained operator. After removal of the uterus, one small fragment (3–5 mm) from the largest leiomyoma and one (3–5 mm) from normal myometrium was removed by a cold-blade scalpel. The samples were placed in MSCGM medium (Mesenchymal Stem Cell Growth Medium, Lonza, Basel, Switzerland) and sent to our laboratory for processing. We reported the size (in cm), topographic site (anterior, posterior, left lateral, right lateral, and fundal), and location (subserosal, intramural or submucosal) of fibroids from where the samples were obtained. The removal of the sample did not alter the histopathological analysis in any case. All patients displayed good general condition; none of them had a history of myomectomy or uterine surgery, had

received medical therapy or oral contraceptives in the previous three months, or had evidence of genital tract infection, endometriosis, or ovarian disease. All had a negative cervical vaginal swab collected prior to surgery, which was performed in the proliferative phase of the cycle. Adenomyosis or other uterine disorders demonstrated on histopathological examination were exclusion criteria.

2.3. Cell Culture. Tissue fragments (2-3 mm^3) were firstly subjected to mechanical digestion then to enzymatic digestion with 0.2% type II collagenase (Sigma-Aldrich, Milan, Italy) at 37°C for 4 hours; subsequently, partially digested solution was placed into 6-well plates containing MSCGM medium which enhances the growth of undifferentiated cells

and maintained in culture using same media at 37°C in 95% air and 5% CO_2. The growth medium was changed after 24 hours to remove unattached cells and then twice a week. Cell morphology was evaluated by phase-contrast microscopy (Leica DM IL; Leica Microsystems GmbH, Wetzlar, Germany) and viability by an automated cell counter (Invitrogen, Milano, Italy). All further analyses involved separate assays of the specimens from each participant up to the first five passages.

2.4. Doubling Time. To assess doubling time, 8×10^4 cells/well were plated using an algorithm available online (http://www.doubling-time.com): $DT = t \times \lg 2 / (\lg Nt - \lg N0)$ where N0 is the number of plated cells, Nt is the number of harvested cells, and t is culture time in hours [33].

2.5. Characterization of Leiomyoma Progenitor Cells and Myometrium Progenitor Cells. Cells were characterized by testing plastic adherence [34]. Immunophenotype and multipotency were evaluated as previously described [27]. Briefly, for immunophenotyping, 2.5×10^5 cells were stained for 45 min with fluorescein isothiocyanate- (FITC-) conjugated antibodies (Becton Dickinson) against HLA-DR, CD14, CD19, CD34, CD45, CD73, CD90, CD105 OCT4, SOX2, NANOG, and KLF4. Since it is reported [35] that many of the mesenchymal markers are also found in fibroblasts, we analyzed the level of CD9 (Becton Dickinson), which is differently expressed by the two cellular subsets.

For differentiation assay, cells were induced towards osteocytes, chondrocytes, and adipocytes using STEMPRO® Osteogenesis and Chondrogenesis and Adipogenesis Kits (GIBCO, Invitrogen), respectively. Osteogenic differentiation was assessed by von Kossa and alkaline phosphatase (ALP) stainings; adipogenic differentiation was tested by Oil Red staining; for chondrogenesis, cells were cultured in pellet culture system and the sections were exposed to a solution of Safranin-O. Cells cultured in MSCGM alone were used as negative controls.

The expression of stemness genes *(OCT4, SOX2, NANOG,* and *KLF4)* was analyzed by real-time PCR (RT-PCR) and cytofluorometry as above reported; total RNA was isolated from 1×10^6 cells at passage 4th by using 5 PRIME PerfectPure RNA Purification (5 PRIME, Hamburg, Germany) and retrotranscribed in cDNA (GoScript™ Reverse Transcription System, Promega, Italy). All samples were tested in triplicate with the housekeeping genes RPLP0 and GAPDH for data normalization. Of the two, GAPDH was the most stable and was used for subsequent normalization. After amplification, melting curves were acquired. Direct detection of PCR products was monitored by measuring the fluorescence produced by SYBR Green I dye (EVA Green PCR Master Mix, Bio-Rad) binding to double strand DNA after every cycle. These measurements were then plotted against cycle numbers. The parameter threshold (Ct) was defined as the number of cycles it took to detect a real signal above background fluorescence.

The amount of mRNA detected in LPCs was calculated as X-fold respect to MPCs (expressed as 1) by the $2^{-\Delta\Delta Ct}$ method [33], where $\Delta Ct = Ct$ (gene of interest) $- Ct$

Table 2: Flow cytometry results of progenitor cells.

	Myometrium	Leiomyoma
HLA-DR	−	−
CD14	−	−
CD19	−	−
CD34	−	−
CD45	−	−
CD73	+	+
CD90	+	+
CD105	+	+
CD9	−	−

Positive immunolabelling (+) was defined as a level of fluorescence > 90% of the corresponding isotype-matched control antibodies. Percentages < 2% were considered negative (−). No statistically significant differences were found among the twelve cultures.

(housekeeping gene) and Δ $(\Delta Ct) = \Delta Ct$ (LPCs) $- \Delta Ct$ (MPCs). X-fold was calculated for the selected genes in all the twelve samples of LPCs and twelve samples of MPCs. Subsequently, mean ± SD from three independent experiments in triplicates was calculated and displayed. All the primer sequences are reported in Table 1.

2.6. Analysis of MDR1 Expression by Western Blotting. MDR1, a member of the large family of ABC transporters, which confer multidrug resistance on human stem cells, was investigated in the two cell types by Western blotting. Briefly, RIPA buffer (150 mM NaCl, 10 mM Tris, pH 7.2, 0.1% SDS, 1.0% Triton X-100, 5 mM EDTA, pH 8.0) containing protease inhibitor cocktail (Roche Applied Science, Indianapolis, IN, USA) was used for protein extraction from 1×10^6 cells at passage 4th. Protein concentration was determined using Bradford reagent (Sigma-Aldrich, Milan, Italy). Total protein extracts (40 μg) were reduced in DTT (0.5 M) for 10 min at 70°C and samples run on a 4–12% gradient precast NuPAGE Bis-Tris polyacrylamide gel for 1 h at 200 V. Electroblotting was performed using iBlot® Dry Blotting System (Invitrogen). Membranes were incubated overnight with primary anti-MRD1 antibody (Santa Cruz Biotechnology, Heidelberg, Germany, 1 : 400) followed by incubation with a secondary antibody conjugated to horseradish peroxidase. Immunoreactive proteins were visualized using a chemiluminescent substrate (Santa Cruz Biotechnology). Anti-β-actin (Santa Cruz Biotechnology) was the endogenous control and normal human lung fibroblasts (NHLFs) were the negative control.

2.7. Expression of α-SMA, Collagen Type 1, and Fibronectin. It is known that even if all mesenchymal stem cells exhibit the original MSC features as defined by the ISCT minimum criteria (spindle-shape, multilineage differentiation, and surface marker expression), the tissue of origin leaves a sort of imprinting in the isolated cells that will express some specific proteins that best characterized their histological source [36–38]. For this reason and to better characterized isolated cells, the expression of α-SMA, collagen type 1, and
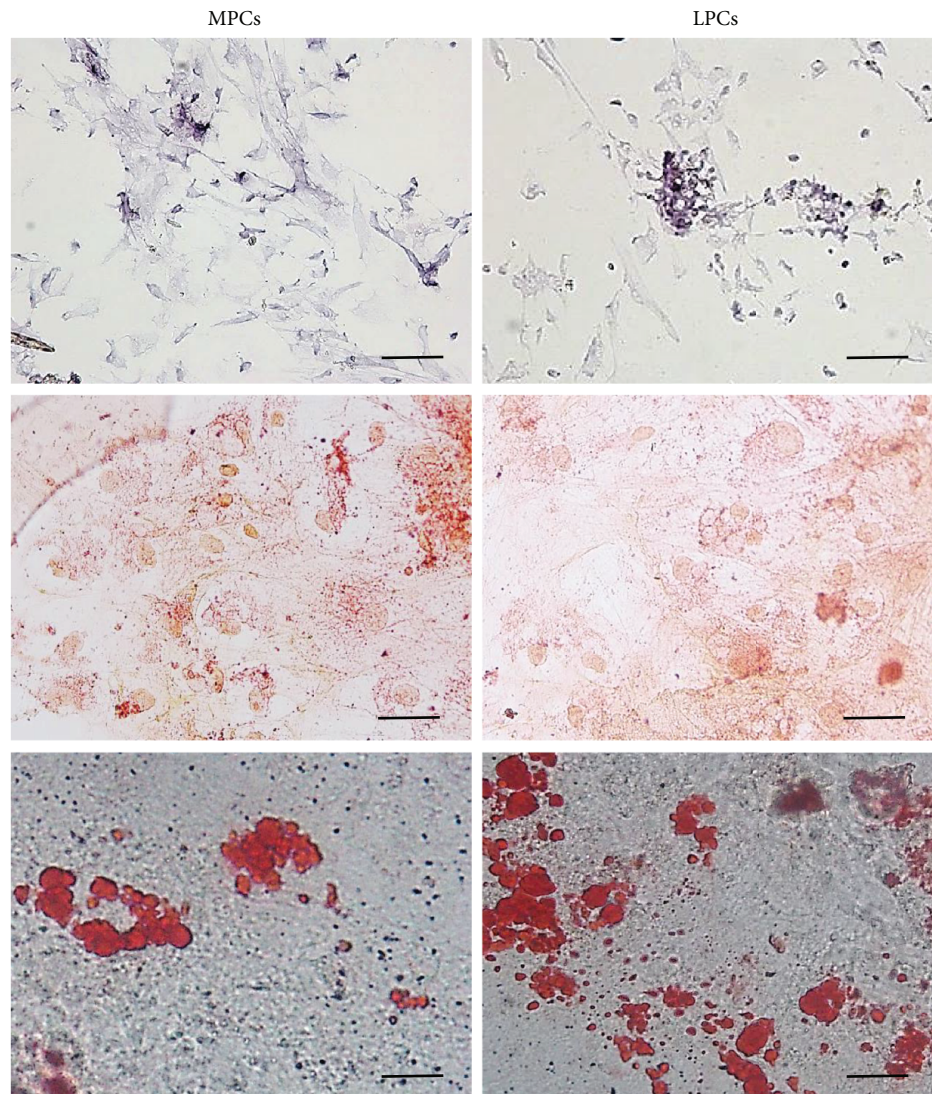
MPCs LPCs

FIGURE 2: Multilineage differentiation of MPCs and LPCs. Representative images of differentiation experiments. Osteogenic differentiation: ALP staining (top); chondrogenic differentiation: acid mucopolysaccharide coloration with Safranin-O (center); adipocyte differentiation: Oil Red staining (bottom). No differences were noted among different leiomyoma and myometrium samples. Scale bar $= 100\,\mu$m. MPCs: myometrium progenitor cells; LPCs: leiomyoma progenitor cells.

fibronectin expression has been tested by indirect immuno-fluorescence (IIF) and immunocytochemistry (ICC).

For IIF, 1.5×10^4 cells at passage 3rd were plated, fixed, permeabilized, and treated overnight with mouse anti-human primary antibodies: anti-collagen type I (1 : 1000), anti-cellular fibronectin (1 : 400), and anti-α-SMA (1 : 400, all from Sigma-Aldrich, Milano, Italy). Goat anti-mouse FITC-conjugated antibody (Sigma-Aldrich) was the secondary antibody.

Nuclei were visualized using Hoechst 33342 (Sigma-Aldrich, 1 : 1000) under a Zeiss Axiovert 200 M inverted microscope (Carl Zeiss, Jena, Germany).

For ICC, 1.5×10^4 cells from 1×10^6 cells at passage 3rd were plated, fixed, permeabilized, and incubated overnight at 4°C with anti-collagen type I (1 : 1000), anti-cellular fibronectin (1 : 400), and anti-α-SMA (1 : 400) monoclonal antibodies. Cells were immunostained using the streptavidin-biotin-peroxidase technique (LSAB universal peroxidase kit, Dako Cytomation, Milano, Italy) and incubated with 3,3-diaminobenzidine. Slides were counterstained with Mayer's hematoxylin.

2.8. ELISA and RT-PCR Analysis of the Expression of Inflammation-Related Cytokines. Selected cytokines related to acute and chronic inflammation, IL6, IL12, IFN-γ, TNF-α, IL2, IL4, IL5, IL13, IL10, TGF-β11, IL17A, and G-CSF, were investigated by RT-PCR (as above reported) and by ELISA (Multi-Analyte ELISArray kit, Qiagen, Milan, Italy) as previously described [39]. Briefly, medium conditioned for 72 hours by each sample of MPCs (1×10^5 cells at passage 5th) and LPCs (1×10^5 cells at passage 5th) was used for the test. Samples were dispensed into a 96-well microtiter plate and incubated for 2 hours at room temperature. After washing, avidin-HRP-conjugated antibody was added to
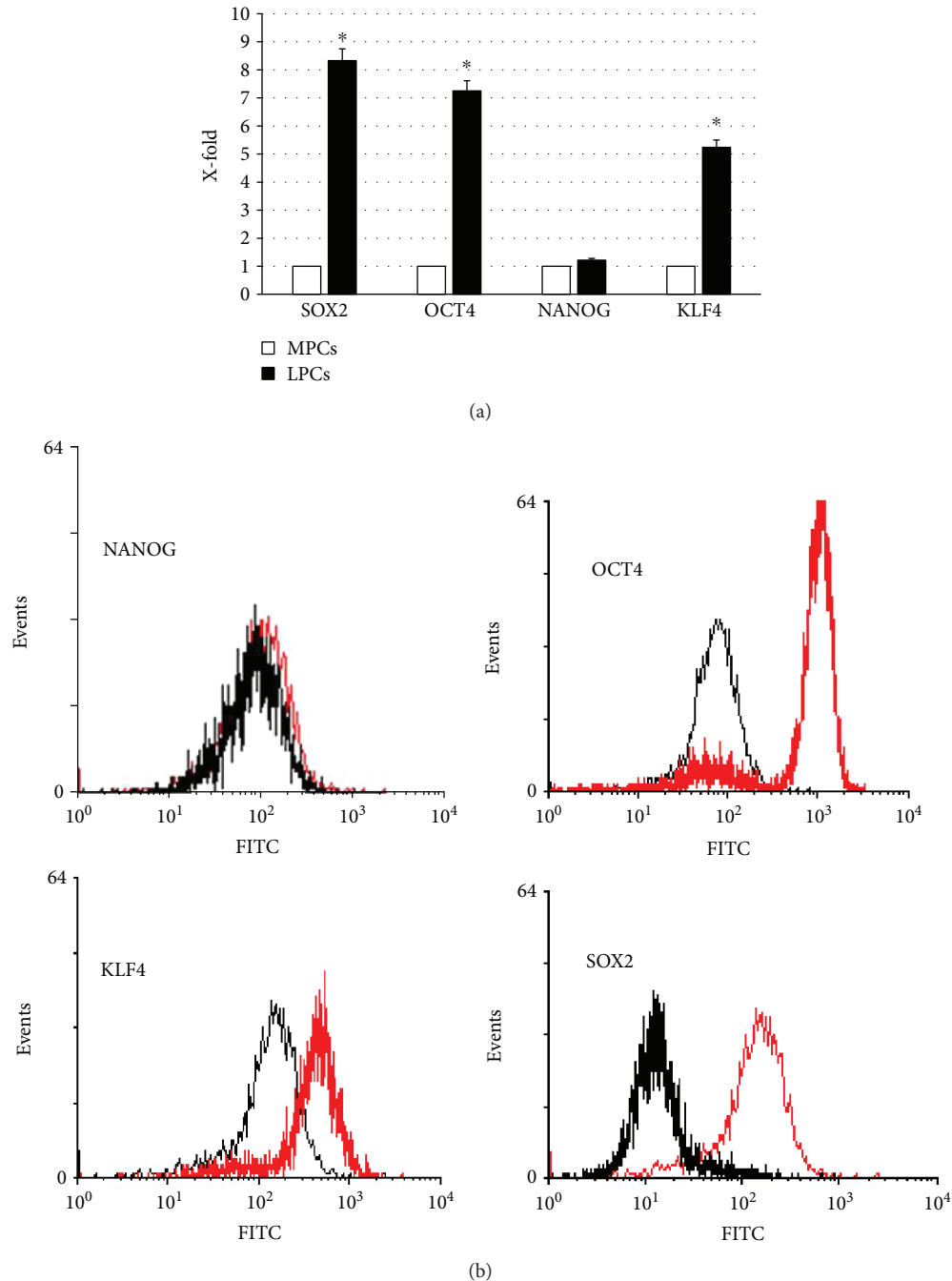
(a)

(b)

FIGURE 3: OCT4, SOX2, NANOG, and KLF4 expression. Selected markers of self-renewal and differentiation potential (OCT4, SOX2, NANOG, and KLF4) were evaluated by RT-PCR (a) and cytofluorometry (b). For PCR analysis, the expression levels measured in LPCs are considered as X-fold with respect to MPCs (considered as 1). Data are mean ± SD of analyses performed in 12 different MPC and LPC cultures, upon three independent experiments in triplicates. $^*p < 0.05$ LPCs versus MPCs. For cytofluorometric analysis, representative FACScan analyses of cell-surface antigen expression, as indicated. Black histograms refer to the MPCs and red histograms refer to LPCs.

the plate and incubated for 30 minutes. Finally, captured cytokines were detected by addition of substrate solution. The OD at 450 nm was determined using a microtiter plate reader (Multiskan GO Microplate Reader, Thermo Scientific).

The levels of the cytokines secreted by leiomyoma cells are reported as a percentage of the levels measured in the corresponding myometrial sample. After, mean ± SD from three independent experiments in triplicates was calculated

and displayed. Quantification of mRNA expression in MPCs and LPCs was calculated with the $2^{-\Delta Ct}$ method, where $\Delta Ct = Ct$ (gene of interest) − Ct (housekeeping gene). ΔCt was calculated for the selected genes in all the twelve samples of MSCs. Subsequently, mean ± SD from three independent experiments in triplicates was calculated and displayed.

The expression of other Th1/Th17-related soluble factors (IL22, NFKB1, IL23A, STAT3, CCR5, IL17RA, CX3CL1,

CXCL12, and CXCL5) was also assessed by RT-PCR, and the amount of mRNA calculated as above described. All the primer sequences are reported in Table 1.

2.9. Statistical Analysis. Statistical analysis of data from at least 3 independent experiments was performed using SPSS 19.0 software (SPSS Inc., Chicago, IL, USA). All data are mean ± SD. For two-sample comparisons, significance was calculated by Student's *t*-test using SPSS 17.0 software. p values ≤ 0.05 were considered significant.

3. Results

3.1. Sample Collection. Twelve 3–5 mm samples of leiomyoma and 12 samples of normal myometrium were collected. The median size of leiomyomas was 5 cm (range 3–8 cm); 3 of them were anterior, 4 posterior, 2 left lateral, 1 right lateral, and 2 were fundal. The location was subserousal in 2 cases, intramural in 4, and submucosal in the remaining six.

3.2. Cell Isolation and Characterization. Leiomyoma and normal myometrium samples from the same 12 patients were used to establish cell cultures. Up to the second passage, the cell population was heterogeneous (Figure 1(a), top panels), probably because it was composed by differentiated and undifferentiated cells; cells displayed different morphologies, from rounded to spindle-like and different sizes. After, cells appeared homogeneous, with a fibroblastoid morphology, (Figure 1(a), bottom panels) and also the cytofluorometric analysis revealed the presence of just one cell population. All subsequent experiments were performed separately on each cell sample. Since no differences were detected among the samples from the two tissue groups, no pairwise analysis was necessary and values are the average of 12 samples.

Doubling time was stable up to the 5th passage and almost identical in the two cell groups; it then increased, the increment being greater in myometrium cells (Figure 1(b)).

Evaluation of the stemness criteria identified by Dominici et al. demonstrated that cells adhered to plastic and that they were strongly positive for CD73, CD90, and CD105 and negative for HLA-DR, CD14, CD19, CD34, CD45, and for the key marker CD9 (Table 2).

Cells were also capable of differentiating to osteogenic, chondrogenic, and adipogenic lineages (Figure 2).

Both cell types expressed NANGO, OCT4, SOX2, and KLF4, tested by RT-PCR and cytofluorometry, with a higher expression in leiomyoma cells (Figure 3).

Since all experiments confirmed their undifferentiated status, the two cell types were designated, respectively, as myometrium progenitor cells (MPCs) and leiomyoma progenitor cells (LPCs).

3.3. MDR1, α-SMA, Collagen Type 1, and Fibronectin Expression. Western blotting demonstrated a reactive band (molecular weight 170 kDa, corresponding to MDR1) in the MPC and LPC lanes. Densitometric analysis revealed that MDR1expression was higher in LPCs (Figure 4), whereas no signal was detected in NHLFs (negative control).
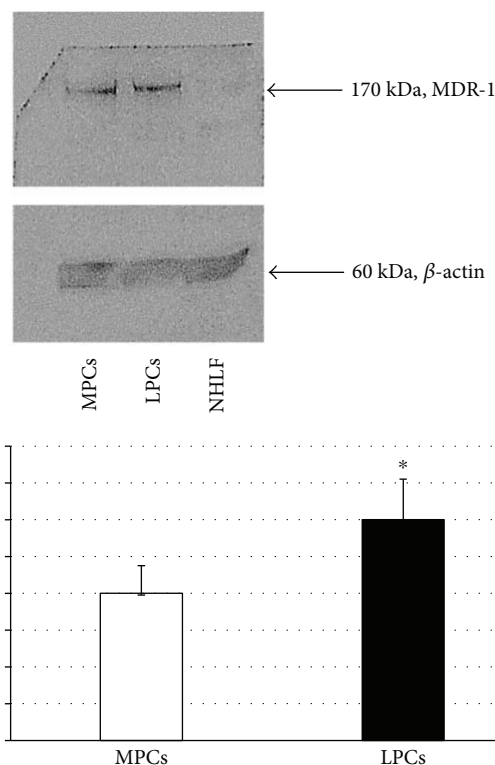

FIGURE 4: Western blots and densitometric analyses of MDR1 expression. (Top) representative Western blot gels showing the bands of MDR1 and of the endogenous control β-actin. (Bottom) densitometric analyses of the immunoreactive bands (quantified as MDR1/β-actin bands in corresponding samples and expressed as arbitrary units, A.U.). Data are mean ± SD of analyses performed in MPCs and LPCs from the 12 patients. *$p < 0.05$ LPCs versus MPCs. MPCs: myometrium progenitor cells; LPCs: leiomyoma progenitor cells.

MPCs and LPCs were positive for α-SMA, collagen type 1, and fibronectin on IIF (Figure 5) and IIC (Figure 6), without significant differences between the two cell types. Although more than 90% of MPCs and LPCs were strongly positive for all three proteins, the staining for collagen type 1 was fainter than the other two.

3.4. Expression Profile of Inflammatory Cytokines. The expression and secretion of inflammation-related cytokines were, respectively, evaluated by RT-PCR (Figure 7(a)) and ELISA (Figure 7(b)).

Compared to MPCs, LPCs exhibited significantly ($p < 0.05$) higher levels of Th2 pathway cytokines (IL4, IL5, IL10, and IL13), with IL10 showing a 40% increase, and significantly ($p < 0.05$) lower levels of Th1/Th17 cytokines (IL6, IL12, IL17A, IFN-γ, G-CSF, and TGF-β1).

Finally, IL2 and TNF-α expression was not significantly different between MPCs and LPCs. Since both mRNA levels and ELISA revealed a strong downregulation of Th1/Th17 pathway cytokines in leiomyoma, the expression of other soluble factors belonging to these pathways was assessed by RT-PCR and found to be lower in LPCs (Figure 7(c)).
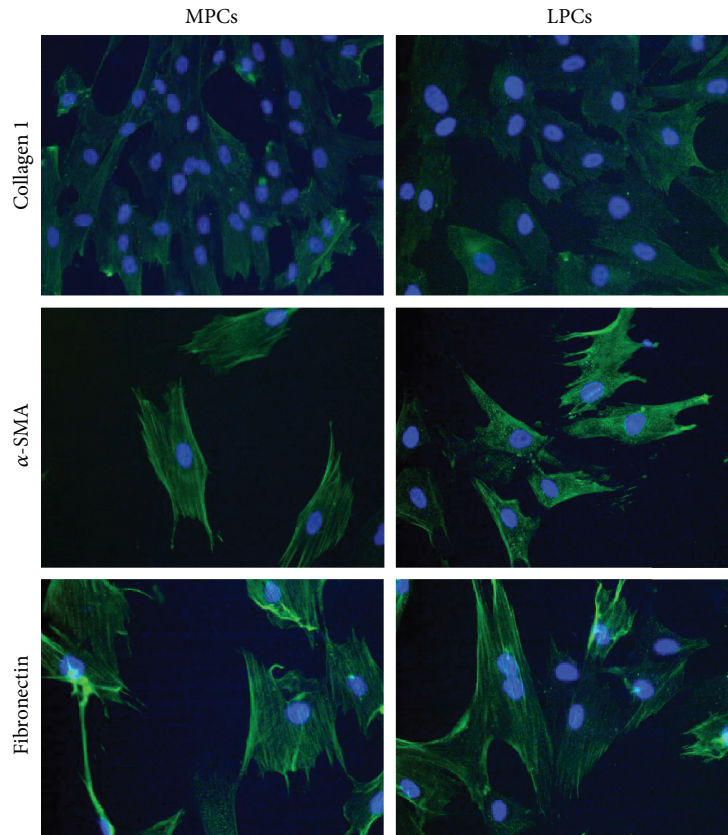
MPCs   LPCs

FIGURE 5: Indirect immunofluorescence analysis of α-SMA, collagen type 1, and fibronectin. A secondary FITC-conjugated antibody was used after incubation with the primary antibodies. Nuclei were counterstained with Hoechst 33342. Myometrium progenitor cells (MPCs) and leiomyoma progenitor cells (LPCs) showed a similarly strong positivity for α-SMA and fibronectin, whereas collagen type 1 expression was fainter. Differences between MPCs and LPCs were not significant (×200 original magnification).

4. Discussion

Uterine leiomyomas are highly common lesions of unclear etiology. Several hypotheses have been formulated and predisposing factors have been described [40]. Investigation of the factors responsible for the significant plasticity of the uterus has led to the identification of a progenitor/ undifferentiated cell population, prompting the hypothesis that its dysregulation may be implicated in the development of uterine pathologies [8, 41, 42]. Various approaches have been applied to identify and characterize progenitor cells [17–20, 43].

Since inflammation is a recognized mechanism underlying the onset of several tumors, the role of an inflammatory microenvironment has also been explored in leiomyoma development. The overall hypothesis is that leiomyomas are caused in part by an immune milieu that is chronically inflammatory [28]. In addition, the chronic inflammatory state increases estrogen which in turn may increase leiomyoma growth [44]. Chronic inflammation is sustained by specific cytokines secreted by immune, undifferentiated, and tumor cells [25, 26] and seems to be exploited by tumor cells to escape the host immune system [25]. Undifferentiated cells play a central role in the microenvironment and modulate the cellular functions of a variety of immune cells

including B and T lymphocytes, natural killer cells, monocytes, and dendritic cells [45–50]. Presumably, this role is operated by a complex interplay of short- and long-range signaling that may entail a wide spectrum of molecular mediators, including soluble cytokines and growth factors [51].

However, a correlation between undifferentiated cells and inflammation in leiomyoma onset has never been explored. In the present work, the issue was investigated through isolation and extensive characterization of undifferentiated progenitor cells from 12 specimens of normal myometrium and 12 leiomyoma samples. Demonstration of a stem-like immunophenotype and of the ability to differentiate into osteoblasts, chondrocytes, and adipocytes enabled their designation as MPCs and LPCs. For the first 5 passages, MPCs and LPCs showed a stable and comparable DT; subsequently, the doubling time increased. This increment was higher in MPCs than in LPCs (75.36 ± 4.19 versus 61.55 ± 1.32 hours, resp.). The DT increase corresponded with a reduction in proliferation, which in cultured cells is a sign of senescence; since senescence is greater in more differentiated cells, LPCs seemed to be less differentiated than MPCs. Although this finding disagrees with those of Chang et al. [16], it is consistent with the higher expression by LPCs of stemness genes (SOX2, OCT4, and KLF4) and of MDR1 (as demonstrated by Western blot and densitometric analysis).
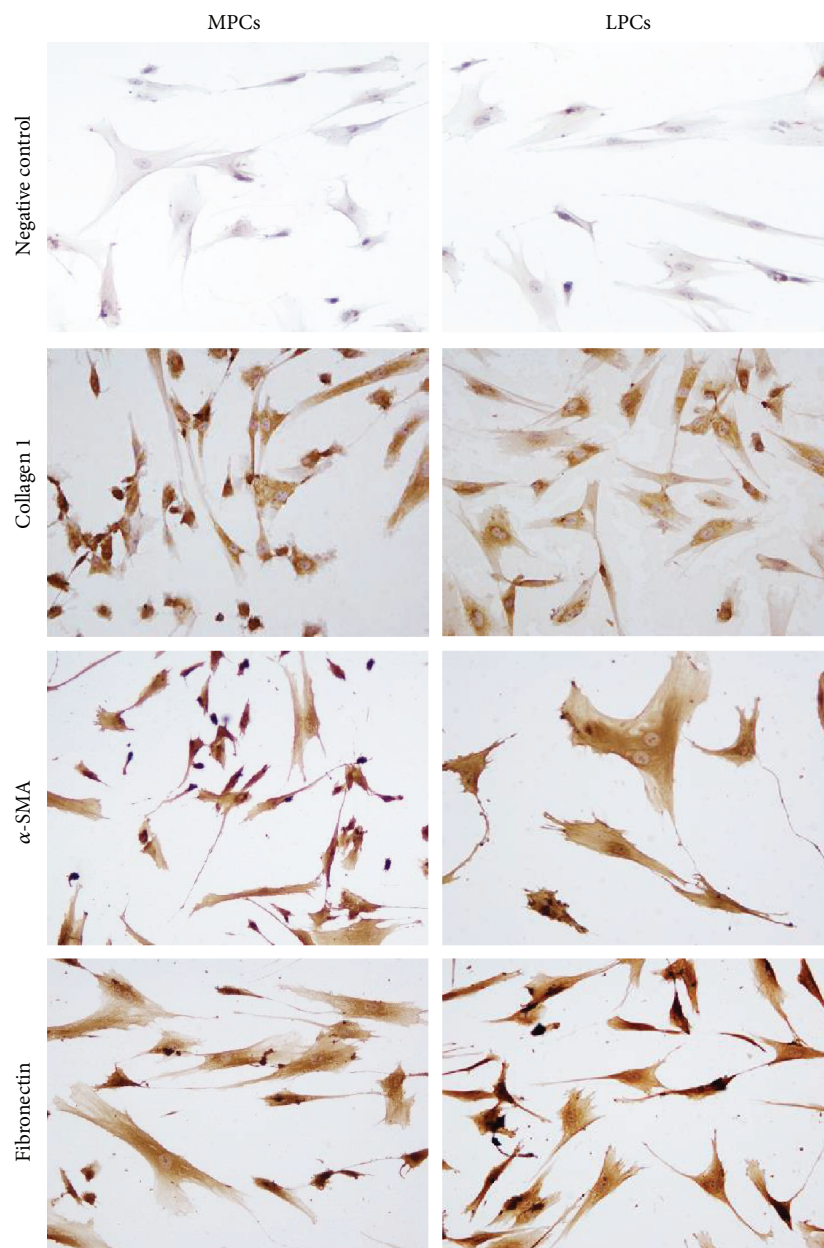
MPCs LPCs

FIGURE 6: Immunocytochemical analysis of α-SMA, collagen type 1, and fibronectin. Compared to the negative control (secondary antibody alone), the primary antibodies induce brownish staining in myometrium progenitor cells (MPCs) and leiomyoma progenitor cells (LPCs). The reaction was weaker for collagen type 1 than for α-SMA and fibronectin. Differences between MPCs and LPCs were not significant (immunoperoxidase, $\times$400 original magnification).

MDR1 is a member of the ABC transporter family, which is believed to protect stem cells from genetic damage by naturally occurring xenobiotics [52, 53]. ABC family members are considered as stem cell markers and may be used for stem cell purification; treating cells with specific dyes (Rhodamine123 or Hoechst 33342), stem cells show a reduced retention by the presence of this transmembrane proteins capable of pumping these dyes out of the cell [54]. Different roles have been attributed to MDR1, such as drug efflux and protection of cells against apoptotic cell death induced by a variety of causes, and to modulate signal transduction pathways enhancing cell survival [54].

Progenitor cells were further characterized by IIF and ICC through the expression of α-SMA, collagen type 1, and fibronectin. Their expression was strong and similar in MPCs and LPCs, although staining for collagen type 1 was weaker. It is now well accepted that progenitor/mesenchymal cells are a very heterogeneous reservoir of cells; even if cells satisfied all the three essential criteria identified by Dominici, progenitor displays biologic properties that may differ according to the tissue of derivation. Specific molecules, receptors that characterized a particular tissue, may be expressed by undifferentiated cells derived from it. In this case, myometrium is characterized by abundant amounts of
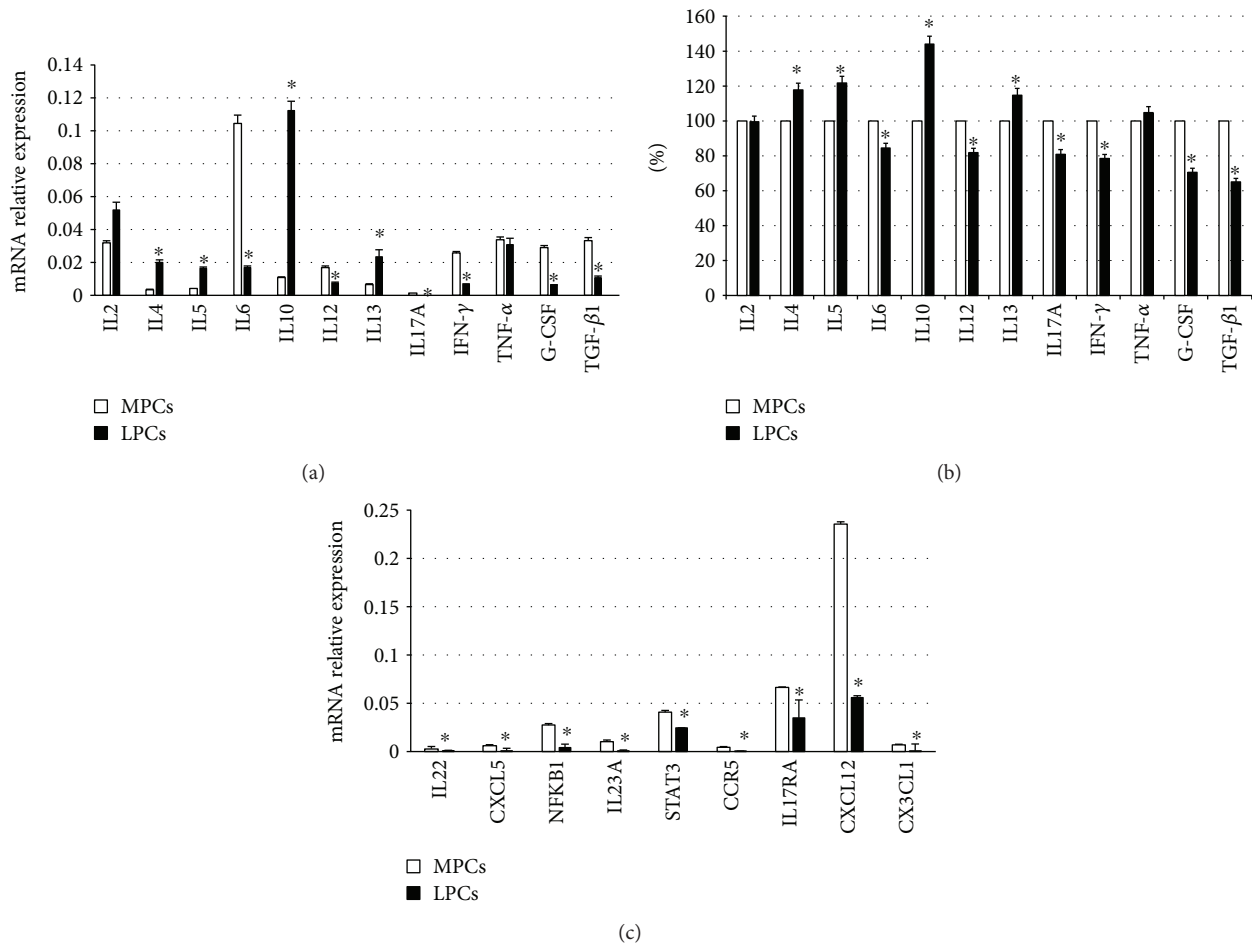
(a)

(b)

(c)

Figure 7: Expression of selected cytokines in myometrium progenitor cells (MPCs) and leiomyoma progenitor cells (LPCs). (a) Quantification of mRNA expression in MPCs and LPCs was calculated with the $2^{-\Delta Ct}$ method, where $\Delta Ct = Ct$ (gene of interest) $- Ct$ (housekeeping gene). ΔCt was calculated for the selected genes on 12 different cultures. Subsequently, mean $\pm$ SD from three independent experiments in triplicates was calculated for LPCs and displayed. $^*p < 0.05$ LPCs versus MPCs. (b) ELISA test; the levels measured in MPCs were considered as 100% and those detected in LPCs accordingly calculated; $^*p < 0.05$ LPCs versus MPCs. (c) Selected Th1/Th17 pathway molecules evaluated by RT-PCR. Quantification of mRNA expression in MPCs and LPCs was calculated with the $2^{-\Delta Ct}$ method, where $\Delta Ct = Ct$ (gene of interest) $- Ct$ (housekeeping gene). ΔCt was calculated for the selected genes on 12 different cultures. Subsequently, mean $\pm$ SD from three independent experiments in triplicates was calculated for LPCs and displayed. $^*p < 0.05$.

α-SMA, collagen type 1, and fibronectin. We found a detectable expression of these three molecules at mRNA level; interestingly, progenitors from leiomyoma do not hyperexpress these factors compared to cells from myometrium even if it is known their involvement in fibroid development. This apparent contradiction may reside in the fact that accumulation of extracellular matrix (ECM) in leiomyoma may be the result of a dysregulated proliferation of cells; in fibroids, ECM is more abundant because of a more elevated number of producing cells. In vitro experiments were performed using the same amount of cells derived from myometrium and leiomyoma [55]. The expression of collagen type 1 was weaker than the other two molecules; it may depend by the low secretion of TGF-β1 observed by ELISA test. TGF-β1 is in fact known as a great promoter of collagen type 1 production [56, 57].

As regards the role of inflammation, it is well accepted that leiomyoma onset may correlate with active inflammation

[21] and that undifferentiated cells participate in microenvironment formation. For this reason, a panel of 12 cytokines related to acute and chronic inflammation was evaluated in LPCs and MPCs as mRNA expression and secretion.

Although IL6, TNF-α, IFN-γ, G-CSF, and TGF-β1, which have been implicated in leiomyoma development [58, 59], were expressed in both cell types, the most notable finding was the significantly different expression of Th2 and Th1/Th17 pathways in LPCs and MPCs. Indeed, LPCs exhibited a significantly greater expression of IL4, IL5, IL10, and IL13 (Th2 pathway) and a significantly lower expression of Th1/Th17 pathway cytokines. In particular, they secreted less TGF-β1 which, alone or combined with IL6, is involved in the differentiation of naive T-cells to Treg T-cells and Th17 T-cells, which in turn secrete TGF-β1 and IL17. Treg T-cells are actively involved in inhibiting tissue inflammation, and their suppression may enhance the maintenance of the inflammatory microenvironment that favors leiomyoma

development. IL12 and IFN-γ, which allow differentiation of naive cells to Th1 T-cells, were lower in LPCs, whereas secretion of IL4, IL5, and IL13, which drive the differentiation to Th2 T-cells, was lower in MPCs; this also applied to IL10, which is subsequently produced.

To lend support to the downregulation of Th1/Th17 pathway cytokines in LPCs, other soluble factors of the same subgroups (IL22, NFKB, IL23A, STAT3, CCR5, IL17A, IL17RA, CXCL12, CX3CL1, and CXCL5) were evaluated by RT-PCR. This panel of molecules with different functions (chemokines, cytokines, transcription factors, and signaling pathway molecules) provided a general picture of the involvement of Th1/Th17 pathways. All molecules were downregulated in LPCs, confirming the upregulation of the Th2 profile. Th2 cells and cytokines are associated with chronic inflammation, whereas the Th1/Th17 pathways are related to acute inflammation. The upregulation of the Th2 pathway in LPCs may reflect a protracted inflammatory state that is maintained by paracrine effect exerted also by undifferentiated cells, which create a stroma favoring leiomyoma development.

These observations suggest a relationship between chronic myometrial inflammation and uterine leiomyomatosis, infertility, and adverse obstetric outcomes [60]. Indeed, a chronic inflammatory reaction induced by fibroids and altered myometrium contractility may hinder embryo implantation, affecting fertility [61–63]. Among the mechanisms invoked to explain the increased myometrial contractility are an excess of cytokines, growth factors, neurotensin, neuropeptides, enkephalin, oxytocin modulators, and chronic inflammation of the fibroid capsule [64–66].

Alterations in the endometrial-myometrial junction (EMJ) seem to play a key role in implantation failure and recurrent miscarriage. The EMJ, the inner third of the myometrium adjacent to the endometrium, provides macrophages and uterine natural killer cells, which are essential for endometrial decidualization in the midluteal window of implantation [67]. It is conceivable that intramural/submucosal fibroids not only physically disrupt the EMJ [68–70] but also cause chronic inflammation, steroid receptor alterations, and ultimately implantation failure. A chronic proinflammatory effect exerted by leiomyoma progenitor cells may explain why even small myomas or early-stage diffuse leiomyomatosis hamper embryo implantation. Inflammatory stimuli also seem to alter progesterone receptor activation; hence, transrepressive activity in myometrial cells, providing support for the hypothesis that tissue inflammation, may be involved in miscarriage and preterm delivery [71].

In conclusion, the present data suggest that (i) progenitor cells are found both in leiomyomas and normal myometrium, (ii) these progenitors show a differential expression of cytokines related to acute and chronic inflammation, and (iii) the upregulation of cytokines related to chronic inflammation in leiomyoma progenitors may favor the formation of a microenvironment suitable for leiomyoma onset and development.

Conflicts of Interest

The authors declare that there is no conflict of interest regarding the publication of this article.

References

[1] C. L. Walker and E. A. Stewart, "Uterine fibroids: the elephant in the room," *Science*, vol. 308, no. 5728, pp. 1589–1592, 2005.

[2] S. Okolo, "Incidence, aetiology and epidemiology of uterine fibroids," *Best Practice & Research Clinical Obstetrics & Gynaecology*, vol. 22, no. 4, pp. 571–588, 2008.

[3] E. A. Stewart, "Uterine fibroids," *The Lancet*, vol. 357, no. 9252, pp. 293–298, 2001.

[4] W. H. Parker, "Etiology, symptomatology, and diagnosis of uterine myomas," *Fertility and Sterility*, vol. 87, no. 4, pp. 725–736, 2007.

[5] A. Ciavattini, N. Clemente, G. Delli Carpini, J. Di Giuseppe, S. R. Giannubilo, and A. L. Tranquilli, "Number and size of uterine fibroids and obstetric outcomes," *The Journal of Maternal-Fetal & Neonatal Medicine*, vol. 28, no. 4, pp. 484–488, 2015.

[6] S. E. Bulun, "Uterine fibroids," *The New England Journal of Medicine*, vol. 369, no. 14, pp. 1344–1355, 2013.

[7] P. Zhang, C. Zhang, J. Hao et al., "Use of X-chromosome inactivation pattern to determine the clonal origins of uterine leiomyoma and leiomyosarcoma," *Human Pathology*, vol. 37, no. 10, pp. 1350–1356, 2006.

[8] R. A. Canevari, A. Pontes, F. E. Rosa, C. A. Rainho, and S. R. Rogatto, "Independent clonal origin of multiple uterine leiomyomas that was determined by X chromosome inactivation and microsatellite analysis," *American Journal of Obstetrics & Gynecology*, vol. 193, no. 4, pp. 1395–1403, 2005.

[9] M. M. Carneiro, "Stem cells and uterine leiomyomas: what is the evidence?," *JBRA Assisted Reproduction*, vol. 20, no. 1, pp. 33–37, 2016.

[10] R. E. Blake, "Leiomyomata uteri: hormonal and molecular determinants of growth," *Journal of the National Medical Association*, vol. 99, no. 10, pp. 1170–1184, 2007.

[11] A. Mas, I. Cervello, C. Gil-Sanchis, and C. Simón, "Current understanding of somatic stem cells in leiomyoma formation," *Fertility and Sterility*, vol. 102, no. 3, pp. 613–620, 2014.

[12] A. Mas, I. Cervelló, A. Fernández-Álvarez et al., "Overexpression of the truncated form of high mobility group a proteins (HMGA2) in human myometrial cells induces leiomyoma-like tissue formation," *MHR: Basic Science of Reproductive Medicine*, vol. 21, no. 4, pp. 330–338, 2015.

[13] T. Kurita, P. S. Cooke, and G. R. Cunha, "Epithelial–stromal tissue interaction in paramesonephric (müllerian) epithelial differentiation," *Developmental Biology*, vol. 240, no. 1, pp. 194–211, 2001.

[14] G. P. Flake, J. Andersen, and D. Dixon, "Etiology and pathogenesis of uterine leiomyomas: a review," *Environmental Health Perspectives*, vol. 111, no. 8, pp. 1037–1054, 2003.

[15] T. Maruyama, K. Miyazaki, H. Masuda, M. Ono, H. Uchida, and Y. Yoshimura, "Review: human uterine stem/progenitor cells: implications for uterine physiology and pathology," *Placenta*, vol. 34, pp. S68–S72, 2013.

[16] H. L. Chang, T. N. Senaratne, L. Zhang et al., "Uterine leiomyomas exhibit fewer stem/progenitor cell characteristics when compared with corresponding normal myometrium," *Reproductive Sciences*, vol. 17, no. 2, pp. 158–167, 2010.

[17] M. Ono, W. Qiang, V. A. Serna et al., "Role of stem cells in human uterine leiomyoma growth," *PLoS One*, vol. 7, no. 5, article e36935, 2012.

[18] M. Ono, P. Yin, A. Navarro et al., "Paracrine activation of WNT/β-catenin pathway in uterine leiomyoma stem cells

promotes tumor growth," *Proceedings of the National Academy of Sciences of the United States of America*, vol. 110, no. 42, pp. 17053–17058, 2013.

[19] M. Ono, P. Yin, A. Navarro et al., "Inhibition of canonical WNT signaling attenuates human leiomyoma cell growth," *Fertility and Sterility*, vol. 101, no. 5, pp. 1441–1449.e1, 2014.

[20] P. Yin, M. Ono, M. B. Moravek et al., "Human uterine leiomyoma stem/progenitor cells expressing CD34 and CD49b initiate tumors in vivo," *The Journal of Clinical Endocrinology & Metabolism*, vol. 100, no. 4, pp. E601–E606, 2015.

[21] G. Wegienka, "Are uterine leiomyoma a consequence of a chronically inflammatory immune system?," *Medical Hypotheses*, vol. 79, no. 2, pp. 226–231, 2012.

[22] O. Protic, P. Toti, M. S. Islam et al., "Possible involvement of inflammatory/reparative processes in the development of uterine fibroids," *Cell and Tissue Research*, vol. 364, no. 2, pp. 415–427, 2016.

[23] M. S. Islam, M. M. Akhtar, A. Ciavattini et al., "Use of dietary phytochemicals to target inflammation, fibrosis, proliferation, and angiogenesis in uterine tissues: promising options for prevention and treatment of uterine fibroids?," *Molecular Nutrition & Food Research*, vol. 58, no. 8, pp. 1667–1684, 2014.

[24] G. Weiss, L. T. Goldsmith, R. N. Taylor, D. Bellet, and H. S. Taylor, "Inflammation in reproductive disorders," *Reproductive Sciences*, vol. 16, no. 2, pp. 216–229, 2009.

[25] E. Elinav, R. Nowarski, C. A. Thaiss, B. Hu, C. Jin, and R. A. Flavell, "Inflammation-induced cancer: crosstalk between tumours, immune cells and microorganisms," *Nature Reviews Cancer*, vol. 13, no. 11, pp. 759–771, 2013.

[26] S. Ma, N. Xie, W. Li, B. Yuan, Y. Shi, and Y. Wang, "Immunobiology of mesenchymal stem cells," *Cell Death & Differentiation*, vol. 21, no. 2, pp. 216–225, 2014.

[27] M. Orciani, R. Lazzarini, M. Scartozzi et al., "The response of breast cancer cells to mesenchymal stem cells: a possible role of inflammation by breast implants," *Plastic and Reconstructive Surgery*, vol. 132, no. 6, pp. 899e–910e, 2013.

[28] M. Orciani, G. Sorgentoni, M. Torresetti, R. Di Primio, and G. Di Benedetto, "MSCs and inflammation: new insights into the potential association between ALCL and breast implants," *Breast Cancer Research and Treatment*, vol. 156, no. 1, pp. 65–72, 2016.

[29] M. Orciani, G. Sorgentoni, F. Olivieri, M. Mattioli-Belmonte, G. Di Benedetto, and R. Di Primio, "Inflammation by breast implants and adenocarcinoma: not always a bad company," *Clinical Breast Cancer*, vol. 17, no. 4, pp. 286–292, 2017.

[30] P. Ciarmela, M. S. Islam, F. M. Reis et al., "Growth factors and myometrium: biological effects in uterine fibroid and possible clinical implications," *Human Reproduction Update*, vol. 17, no. 6, pp. 772–790, 2011.

[31] N. Chegini, "Proinflammatory and profibrotic mediators: principal effectors of leiomyoma development as a fibrotic disorder," *Seminars in Reproductive Medicine*, vol. 28, no. 3, pp. 180–203, 2010.

[32] M. S. Islam, O. Protic, P. Stortoni et al., "Complex networks of multiple factors in the pathogenesis of uterine leiomyoma," *Fertility and Sterility*, vol. 100, no. 1, pp. 178–193, 2013.

[33] C. Mariotti, R. Lazzarini, M. Nicolai et al., "Comparative study between amniotic-fluid mesenchymal stem cells and retinal pigmented epithelium (RPE) stem cells ability to differentiate towards RPE cells," *Cell and Tissue Research*, vol. 362, no. 1, pp. 21–31, 2015.

[34] M. Dominici, K. le Blanc, I. Mueller et al., "Minimal criteria for defining multipotent mesenchymal stromal cells. The International Society for Cellular Therapy position statement," *Cytotherapy*, vol. 8, no. 4, pp. 315–317, 2006.

[35] S. Halfon, N. Abramov, B. Grinblat, and I. Ginis, "Markers distinguishing mesenchymal stem cells from fibroblasts are downregulated with passaging," *Stem Cells and Development*, vol. 20, no. 1, pp. 53–66, 2011.

[36] S. Barlow, G. Brooke, K. Chatterjee et al., "Comparison of human placenta- and bone marrow–derived multipotent mesenchymal stem cells," *Stem Cells and Development*, vol. 17, no. 6, pp. 1095–1108, 2008.

[37] R. Izadpanah, C. Trygg, B. Patel et al., "Biologic properties of mesenchymal stem cells derived from bone marrow and adipose tissue," *Journal of Cellular Biochemistry*, vol. 99, no. 5, pp. 1285–1297, 2006.

[38] R. A. Panepucci, J. L. C. Siufi, W. A. Silva Jr. et al., "Comparison of gene expression of umbilical cord vein and bone marrow–derived mesenchymal stem cells," *Stem Cells*, vol. 22, no. 7, pp. 1263–1278, 2004.

[39] M. Orciani, A. Campanati, M. Caffarini et al., "T helper (Th)1, Th17 and Th2 imbalance in mesenchymal stem cells of adult patients with atopic dermatitis: at the origin of the problem," *British Journal of Dermatology*, vol. 176, no. 6, pp. 1569–1576, 2017.

[40] M. M. McWilliams and V. M. Chennathukuzhi, "Recent Advances in Uterine Fibroid Etiology," *Seminars in Reproductive Medicine*, vol. 35, no. 2, pp. 181–189, 2017.

[41] C. E. Gargett, H. P. T. Nguyen, and L. Ye, "Endometrial regeneration and endometrial stem/progenitor cells," *Reviews in Endocrine and Metabolic Disorders*, vol. 13, no. 4, pp. 235–251, 2012.

[42] S. A. Hubbard, A. M. Friel, B. Kumar, L. Zhang, B. R. Rueda, and C. E. Gargett, "Evidence for cancer stem cells in human endometrial carcinoma," *Cancer Research*, vol. 69, no. 21, pp. 8241–8248, 2009.

[43] I. Cervelló, C. Gil-Sanchis, A. Mas et al., "Human endometrial side population cells exhibit genotypic, phenotypic and functional features of somatic stem cells," *PLoS One*, vol. 5, no. 6, article e10964, 2010.

[44] F. Modugno, R. B. Ness, C. Chen, and N. S. Weiss, "Inflammation and endometrial cancer: a hypothesis," *Cancer Epidemiology Biomarkers & Prevention*, vol. 14, no. 12, pp. 2840–2847, 2005.

[45] A. Corcione, F. Benvenuto, E. Ferretti et al., "Human mesenchymal stem cells modulate B-cell functions," *Blood*, vol. 107, no. 1, pp. 367–372, 2006.

[46] J. Plumas, L. Chaperot, M. J. Richard, J. P. Molens, J. C. Bensa, and M. C. Favrot, "Mesenchymal stem cells induce apoptosis of activated T cells," *Leukemia*, vol. 19, no. 9, pp. 1597–1604, 2005.

[47] P. A. Sotiropoulou, S. A. Perez, A. D. Gritzapis, C. N. Baxevanis, and M. Papamichail, "Interactions between human mesenchymal stem cells and natural killer cells," *Stem Cells*, vol. 24, no. 1, pp. 74–85, 2006.

[48] G. M. Spaggiari, A. Capobianco, S. Becchetti, M. C. Mingari, and L. Moretta, "Mesenchymal stem cell-natural killer cell interactions: evidence that activated NK cells are capable of killing MSCs, whereas MSCs can inhibit IL-2-induced NK-cell proliferation," *Blood*, vol. 107, no. 4, pp. 1484–1490, 2006.

[49] S. Beyth, Z. Borovsky, D. Mevorach et al., "Human mesenchymal stem cells alter antigen-presenting cell maturation and induce T-cell unresponsiveness," *Blood*, vol. 105, no. 5, pp. 2214–2219, 2005.

[50] X. X. Jiang, Y. Zhang, B. Liu et al., "Human mesenchymal stem cells inhibit differentiation and function of monocyte-derived dendritic cells," *Blood*, vol. 105, no. 10, pp. 4120–4126, 2005.

[51] C. W. Park, K. S. Kim, S. Bae et al., "Cytokine secretion profiling of human mesenchymal stem cells by antibody array," *International Journal of Stem Cells*, vol. 2, no. 1, pp. 59–68, 2009.

[52] E. P. L. M. de Grouw, M. H. G. P. Raaijmakers, J. B. Boezeman et al., "Preferential expression of a high number of ATP binding cassette transporters in both normal and leukemic CD34+CD38− cells," *Leukemia*, vol. 20, no. 4, pp. 750–754, 2006.

[53] A. Shervington and C. Lu, "Expression of multidrug resistance genes in normal and cancer stem cells," *Cancer Investigation*, vol. 26, no. 5, pp. 535–542, 2008.

[54] K. D. Bunting, "ABC transporters as phenotypic markers and functional regulators of stem cells," *Stem Cells*, vol. 20, no. 1, pp. 11–20, 2002.

[55] M. Iwahashi, Y. Muragaki, M. Ikoma et al., "Immunohistochemical analysis of collagen expression in uterine leiomyomata during the menstrual cycle," *Experimental and Therapeutic Medicine*, vol. 2, no. 2, pp. 287–290, 2011.

[56] X. M. Tang, Q. Dou, Y. Zhao, F. McLean, J. Davis, and N. Chegini, "The expression of transforming growth factor-beta s and TGF-beta receptor mRNA and protein and the effect of TGF-beta s on human myometrial smooth muscle cells in vitro," *MHR: Basic Science of Reproductive Medicine*, vol. 3, no. 3, pp. 233–240, 1997.

[57] I. Sozen and A. Arici, "Interactions of cytokines, growth factors, and the extracellular matrix in the cellular biology of uterine leiomyomata," *Fertility and Sterility*, vol. 78, no. 1, pp. 1–12, 2002.

[58] P. Hatthachote and J. I. Gillespie, "Complex interactions between sex steroids and cytokines in the human pregnant myometrium: evidence for an autocrine signaling system at term," *Endocrinology*, vol. 140, no. 6, pp. 2533–2540, 1999.

[59] O. Kurachi, H. Matsuo, T. Samoto, and T. Maruo, "Tumor necrosis factor-α expression in human uterine leiomyoma and its down-regulation by progesterone," *The Journal of Clinical Endocrinology & Metabolism*, vol. 86, no. 5, pp. 2275–2280, 2001.

[60] Practice Committee of the American Society for Reproductive Medicine, "Myomas and reproductive function," *Fertility and Sterility*, vol. 86, no. 5, Supplement 1, pp. S194–S199, 2006.

[61] B. W. Rackow and H. S. Taylor, "Submucosal uterine leiomyomas have a global effect on molecular determinants of endometrial receptivity," *Fertility and Sterility*, vol. 93, no. 6, pp. 2027–2034, 2010.

[62] A. Kido, S. M. Ascher, W. Hahn et al., "3 T MRI uterine peristalsis: comparison of symptomatic fibroid patients versus controls," *Clinical Radiology*, vol. 69, no. 5, pp. 468–472, 2014.

[63] O. Yoshino, O. Nishii, Y. Osuga et al., "Myomectomy decreases abnormal uterine peristalsis and increases pregnancy rate," *The Journal of Minimally Invasive Gynecology*, vol. 19, no. 1, pp. 63–67, 2012.

[64] A. Malvasi, C. Cavallotti, G. Nicolardi et al., "NT, NPY and PGP 9.5 presence in myomeytrium and in fibroid pseudocapsule and their possible impact on muscular physiology," *Gynecological Endocrinology*, vol. 29, no. 2, pp. 177–181, 2013.

[65] J. Ben-Nagi, J. Miell, D. Mavrelos, J. Naftalin, C. Lee, and D. Jurkovic, "Endometrial implantation factors in women with submucous uterine fibroids," *Reproductive BioMedicine Online*, vol. 21, no. 5, pp. 610–615, 2010.

[66] H. Cakmak and H. S. Taylor, "Implantation failure: molecular mechanisms and clinical treatment," *Human Reproduction Update*, vol. 17, no. 2, pp. 242–253, 2011.

[67] D. C. Sinclair, A. Mastroyannis, and H. S. Taylor, "Leiomyoma simultaneously impair endometrial BMP-2-mediated decidualization and anticoagulant expression through secretion of TGF-β3," *The Journal of Clinical Endocrinology & Metabolism*, vol. 96, no. 2, pp. 412–421, 2011.

[68] K. Kitaya and T. Yasuo, "Leukocyte density and composition in human cycling endometrium with uterine fibroids," *Human Immunology*, vol. 71, no. 2, pp. 158–163, 2010.

[69] A. Tocci, E. Greco, and F. M. Ubaldi, "Adenomyosis and 'endometrial–subendometrial myometrium unit disruption disease' are two different entities," *Reproductive BioMedicine Online*, vol. 17, no. 2, pp. 281–291, 2008.

[70] P. Purohit and K. Vigneswaran, "Fibroids and infertility," *Current Obstetrics and Gynecology Reports*, vol. 5, no. 2, pp. 81–88, 2016.

[71] G. A. Peters, L. Yi, Y. Skomorovska-Prokvolit et al., "Inflammatory stimuli increase progesterone receptor-a stability and transrepressive activity in myometrial cells," *Endocrinology*, vol. 158, no. 1, pp. 158–169, 2017.